Effects of protein kinase inhibitors on hair bundle structure

Thesis submitted in accordance with the requirements of the University of Sussex for the degree of Doctor of Philosophy

Helen Sum Kay Ratnayaka

December 2009

Declaration

I declare that this thesis has not been, and will not be, submitted in whole or in part to another university for the award of any other degree.

Signature,

Helen Sum Kay Ratnayaka

Acknowledgements

With thanks to Professor Guy Richardson and Dr Richard Goodyear who made this work possible through their generous time and effort. I'd also like to thank the other members of the lab, namely Dr Kevin Legan and Dr Hilary Pollard (registered lethal weapon), for their kindness and support, as well as Dr Luz Leticia Olavarrieta-Scappini for making her year in the lab such an enjoyable one. To Gowri Nayak, I'm grateful to have had you as a fellow traveller on this winding, and occasionally tortuous, road! To mum and dad, whose courage and stoicism in doing what had to be done has been a constant source of inspiration, and finally, to Arjuna and Joshua: "alis grave nil", so thank you for being mine.

University of Sussex

Submitted for the degree of Doctor of Philosophy

Title: Effects of protein kinase inhibitors on hair bundle structure

Abstract

The sensory hair bundles of the cochlea are complex structures that are vital for hearing. Phosphorylation plays an important role in regulating actin in many cell types, but the role it plays in regulating the development and maintenance of the hair bundle has yet to be fully elucidated. Furthermore, the extent to which damaged hair bundles can be repaired in the mammalian cochlea remains to be determined. The aims of this study were twofold: 1) to assess the role of phosphorylation in hair bundle development and 2) to ascertain whether hair bundles could recover from any damage caused by protein kinase inhibition or the aminoglycoside neomycin. Post-natal mouse cochlear cultures were treated with a range of protein kinase inhibitors. Of those tested, the broad-spectrum protein kinase inhibitor staurosporine was found to cause hair bundle collapse and detachment of the apical cell membrane from the cuticular plate without causing cell death. Further investigation suggests that staurosporine may have its effects through inhibiting the function of the Ezrin-Radixin-Moesin proteins, an important family of proteins that cross link actin to the plasma membrane. An inhibitor of c-Jun NH_2-terminal kinase, JNK inhibitor I, was also found to cause the loss of hair bundles, but in contrast to staurosporine, also caused hair cell death. This was unexpected, as previous studies have shown that inhibition of c-Jun NH_2-terminal kinase confers protection on hair cells from noise and aminoglycoside damage. Recovery of hair bundles was not observed following brief treatment with either staurosporine or neomycin. The current study shows that protein phosphorylation is vital for the proper maintenance of the hair bundle, and hair that bundles show little sign of recovery from limited damage in vitro.

Table of Contents

Chapter 1 Introduction

Chapter 2 Methods and Materials

Chapter 3 Results

Chapter 4 Discussion and conclusions

List of Tables

List of Figures

Chapter 1

Chapter 3

List of abbreviations

ABD actin-binding domains

ADF actin depolymerisation factor

Akt protein kinase B

ARP 2/3 actin-related protein 2/3

bFGF basic fibroblast growth factor

bHLH basic helix-loop-helix transcription factor

BCIP 5-bromo-4 chloro-3-indolyl phosphate

BIM I Bisindolylmaleimide I

CaM kinase II Ca^{2+}/calmodulin-dependent protein kinase II

CDH23 cadherin 23

Cdkn1B cyclin-dependent kinase inhibitor 1B

CH calponin homology domain

DDSA dodecenyl succinic anhydride

DMEM Dulbecco's Modified Eagle's Medium

DMP-30 2,4,6- Tri (Dimethylaminomethyl) phenol

DMSO dimethyl sulfoxide

DTT dithiothreitol

E 19, E21 embryonic day 19, Embryonic day 21

ERM ezrin, radixin, and moesin

ERMAD ezrin, radixin, and moesin association domains

EVH enabled/vasodilator-stimulated phosphoprotein homology domain

F-actin filamentous actin

FM1-43 Fie Mao1-43

GSK 3-inhibitor glycogen synthase kinase-3 inhibitor

H-89, Dihydrochloride N-[2-((p-Bromocinnamyl)amino)ethyl]-5-isoquinolinesulfonamide, 2HCl

HBHBSS Hepes buffered Hank's balanced salt solution

Hepes 4-(2-hydroxyethyl)-1-piperazineethanesulfonic acid

IC_{50} concentration required to produce 50% inhibition

IHCs inner hair cells

JNK c-Jun NH_2-terminal kinase

K_i inhibitor concentration at which 50% inhibition is observed

KN-93 2-[N-(2-hydroxyethyl)-N-(4-methoxybenzenesulfonyl)]amino-N-(4-chlorocinnamyl)-N-methylbenzylamine

KT5823 protein kinase G inhibitor

LIMK Lin11, Isl-1 & Mec-3 kinases

LOK lymphocyte-oriented kinase

MLK mixed lineage kinase

mAb monoclonal antibody

MAPK mitogen-activated protein kinases

MAPKK mitogen-activated protein kinase kinase

$MgCl_2$ magnesium chloride

ML-7, Hydrochloride 1-(5-Iodonaphthalene-1-sulfonyl)homopiperazine, HCl

MLCK myosin light chain kinase

MNA methyl nadic anhydride

MRCK myotonic dystrophy kinase-related Cdc42-binding kinase

NBT nitro-blue tetrazolium chloride

NGF nerve growth factor

OHCs outer hair cells

P1, P2 Postnatal day 1, postnatal day 2

$p27^{Kip1}$ a cyclin-dependent kinase inhibitor

PBS phosphate buffered saline

PCDH15 protocadherin 15

PDZ postsynaptic density 95, **P**SD-95; discs large, **D**lg; zonula occludens-1, **Z**O-1

phos-ERM phospho-ezrin (Thr567)/radixin (Thr564)/moesin (Thr 558)

PIP_2 phosphatidylinositol 4,5-bisphosphate

PKA/B/C/G protein kinase A/B/C/G

Ptprq protein tyrosine phosphatase receptor Q

PVDF polyvinylidene difluoride

ROS reactive oxygen species

SAPK stress-activated protein kinases

SEM scanning electron microscopy

SDS sodium dodecyl sulfate

SDS PAGE Sodium Dodecyl Sulphate Polyacrylamide Gel Electrophoresis

TBS tris buffered saline

TEM transmission electron microscopy

TEMED N,N,N',N'-Tetramethylethylenediamine

Tris tris(hydroxymethyl)aminomethane

Tween-20 Polysorbate 20

VEGF vascular endothelial growth factor

Vlgr1 very large G-protein-coupled receptor 1

WASP Wiskott-Aldrich syndrome protein

WH2 Wiskott-Aldrich syndrome protein homology 2

Chapter 1

Introduction

1.1 The inner ear and its sensory organs

The mammalian inner ear provides the sensory perceptions of balance and hearing. It consists of six sensory organs: the maculae, comprising of the utricle and saccule which detect gravity in the horizontal and vertical planes, the three cristae of the semicircular canals, which detect angular head movement, and the organ of Corti, which is responsible for hearing (Figure 1.1). All six of these organs are formed from an ordered arrangement of sensory hair cells and their non-sensory supporting cells which reside on a basal lamina. As the supporting cells surround the hair cells, hair cells are effectively isolated from each other as well as the basal lamina. Overlying the hair cells are different extracellular matrices depending on the sensory organ: the otolithic membrane in the maculae, the gelatinous cupula in the cristae and the tectorial membrane of the cochlea (Figure 1.2).

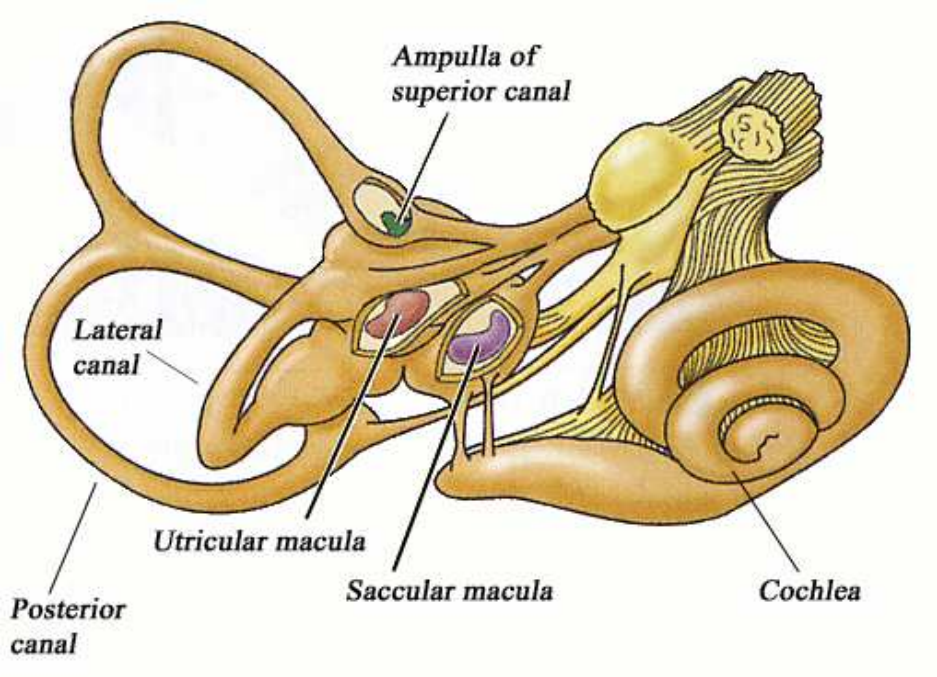

Figure 1.1 The six sensory organs of the mammalian inner ear (adapted from Purves et al, 2007).

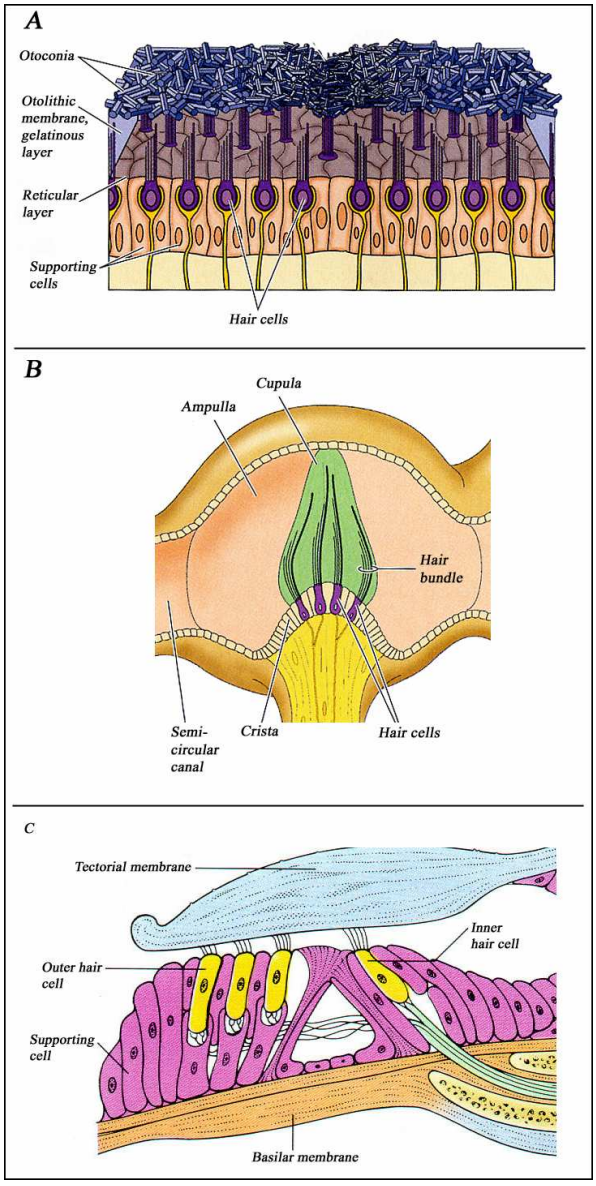

Figure 1.2 Inner ear extracellular matrices: otolithic membrane of the maculae (A), gelatinous cupula of the cristae (B) and the tectorial membrane of the cochlea (C). Panel A and B adapted from Purves et al (2007), panel C adapted from "Index of//Fisiologia/neurofisiologia/Objetivo _4/Clayman89c.jpeg".

1.2 Hair cell function

The sensory hair cells on which the functions of the inner ear are based are polarised epithelial cells that possess a tuft of stereocilia (the hair bundle) on their apical surfaces. It is this tuft that gives the hair cells their name, and within the inner ear, movement of

the hair cell relative to its overlying matrix causes hair bundle deflection. Deflection away from the tallest part of the hair bundle results in hyper-polarisation of the hair cell, but deflection towards the tallest part of the hair bundle leads to an influx of potassium ions into the hair cells via the mechanotransduction channels situated at the tips of all but the tallest stereocilia (Beurg et al, 2009). This leads to hair cell depolarisation and neurotransmitter release from the basal pole of the cell (Figure 1.3) with subsequent excitation of the primary afferent nerve connected to the hair cell (Khan et al, 1982). The neurotransmitter used by hair cells is thought to be glutamate (Cochran and Correia, 1995: Kataoka and Ohmori, 1996: Glowatzki et al, 2006).

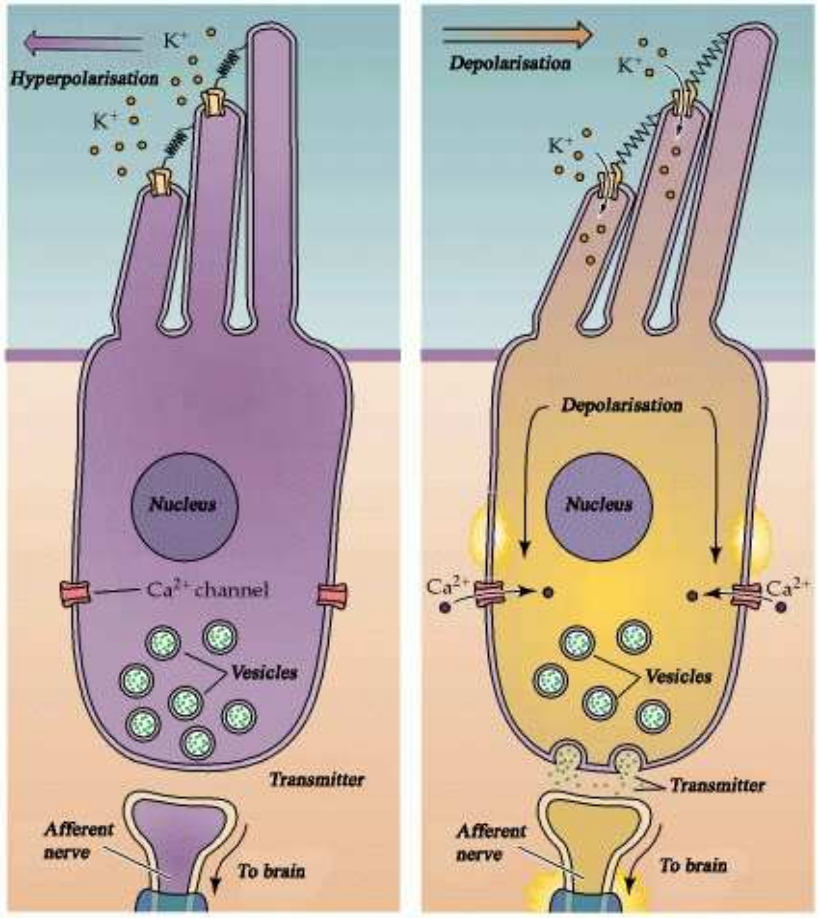

Figure 1.3 Hair bundle movement leading to hair cell hyperpolarisation and depolarisation (adapted from Purves et al, 2007).

1.3 The hair bundle

The stereocilia that make up the hair bundle are rigid, actin-filled protrusions which are arranged in rows in a height dependent manner (Figure 1.4 A, B, C). Within the organ of Corti, this height dependent arrangement of the stereocilia is extremely regular, resulting in the distinctive staircase morphology of hair bundles in the inner hair cells (IHCs) and outer hair cells (OHCs) (Furness et al, 1989) (Figure 1.4 B, C). The shape of the IHC and OHC hair bundles also differ, with the IHC hair bundles tending towards a wide shallow "W" shape and comprising of approximately three rows of stereocilia, while OHC hair bundles have a "V" shape and have approximately three to five rows of stereocilia (Furness et al, 1989: Shim, 2006) (Figure 1.4 B, C). The exact shape, height and number of stereocilia in an inner or outer hair cell hair bundle also depend on its location along the organ of Corti, of the three rows of OHCs on the basilar membrane, hair bundles on the most laterally located OHCs (third row) are taller than those situated on the more medially located first row, while stereocilia at the high frequency basal end of the cochlea are shorter, have a greater diameter and are more numerous than those at the low frequency apical end (Lim, 1980: Tilney and Saunders, 1983). Regardless of their location, both inner and outer hair cell bundles are strictly orientated with the tallest stereocilia lying on the opposite side to the modiolus (Tilney et al, 1986).

In order for the entire hair bundle to move as a single unit in response to mechanical stimulation, each stereocilium within the hair bundle is connected to its immediate neighbours within its row, as well as to the taller and shorter stereocilia in front or behind it, by filamentous links (Osborne et al, 1984: Pickles et al, 1984: Takumida, 2001). These links are highly organised, and occur in specific locations along the stereocilia. In the mouse cochlea, a mature collection of different link types consisting

of tectorial membrane attachment crowns, tip links, and horizontal top connectors is present by postnatal day 19 (P19) on OHC hair bundles (Goodyear et al, 2005).

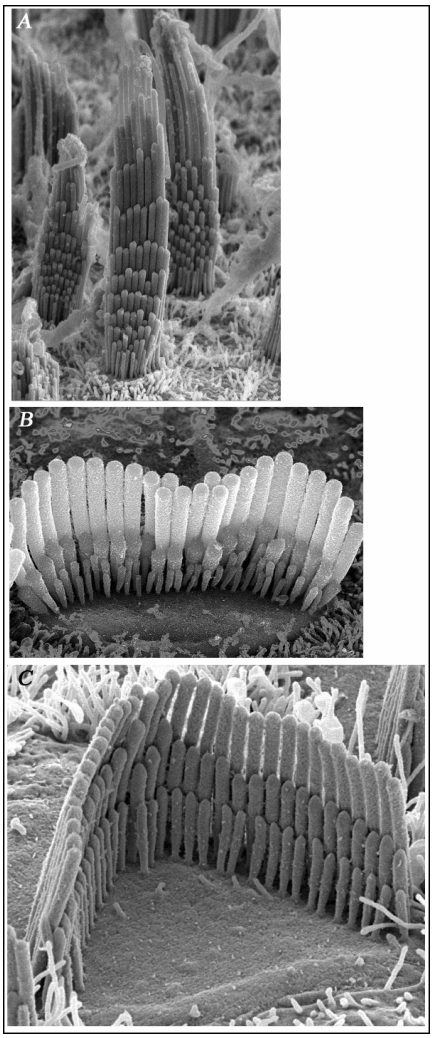

Figure 1.4 Hair bundles of the inner ear: vestibular hair bundles (A), IHC hair bundle (B) and OHC hair bundle (C) (adapted from Wellcome Images: B0006268, B0004625 and B0000111).

1.3.1 Attachment crowns, tip links, and horizontal top connectors

At the top of the tallest row of OHC stereocilia are the tectorial membrane attachment crowns, which consist of a number of particles attached by filaments to the top of the stereocilium (Tsuprun and Santi, 1998: Goodyear et al, 2005) (Figure 1.5).

Tip links connect the tip of shorter stereocilia to the side of taller stereocilia in the next row (Figure 1.5) (Osborne et al, 1984: Comis et al, 1985). This particular type of link has generated much interest due to the possibility that it can gate the opening and closing of the mechanotransduction channel. Indeed, experimental removal of tip links abolished transducer currents (Assad et al, 1991: Preyer et al, 1995), although whether the tip link gates the mechanotransducer channel directly or as part of another mechanism is unknown (Meyer et al, 1998: Meyer et al, 2005). Currently, tip links are known to comprise of two members of the cadherin superfamily of cell adhesion molecules, cadherin 23 (CDH23) and protocadherin 15 (PCDH15) (Siemens et al, 2004: Söllner et al, 2004: Ahmed et al, 2006: Kazmierczak et al, 2007), both of which contain a transmembrane domain and a C-terminal cytoplasmic domain (El-Amraoui and Petit, 2005). However, they differ from classical cadherins by containing many more ectodomain repeats, up to 11 in PCDH15 (Ahmed et al, 2006: Ahmed et al, 2008) and 27 in CDH23 (Di Palma et al, 2001).

Below the tip links are the horizontal top connectors that link stereocilia both intra- and inter-row (Tsuprun and Santi, 2002: Verpy et al, 2008) (Figure 1.5). Horizontal top connectors consist of the protein stereocilin. At the onset of audition in mice at approximately P14, stereocilin-null mice show no horizontal top connectors, but demonstrate normal hearing. These mice however, go on to show progressive hearing loss (Verpy et al, 2008).

1.3.2 Transient links: ankle link, shaft connectors and kinocilial links

Before hair bundle links reach their mature complement, other transient link types exist (Goodyear et al, 2005). The kinocilium of the mammalian hair bundle degenerates as

the hair bundle matures. During development however, kinocilial links connect the kinocilium to the tallest stereocilia (Müller, 2008) (Figure 1.5).

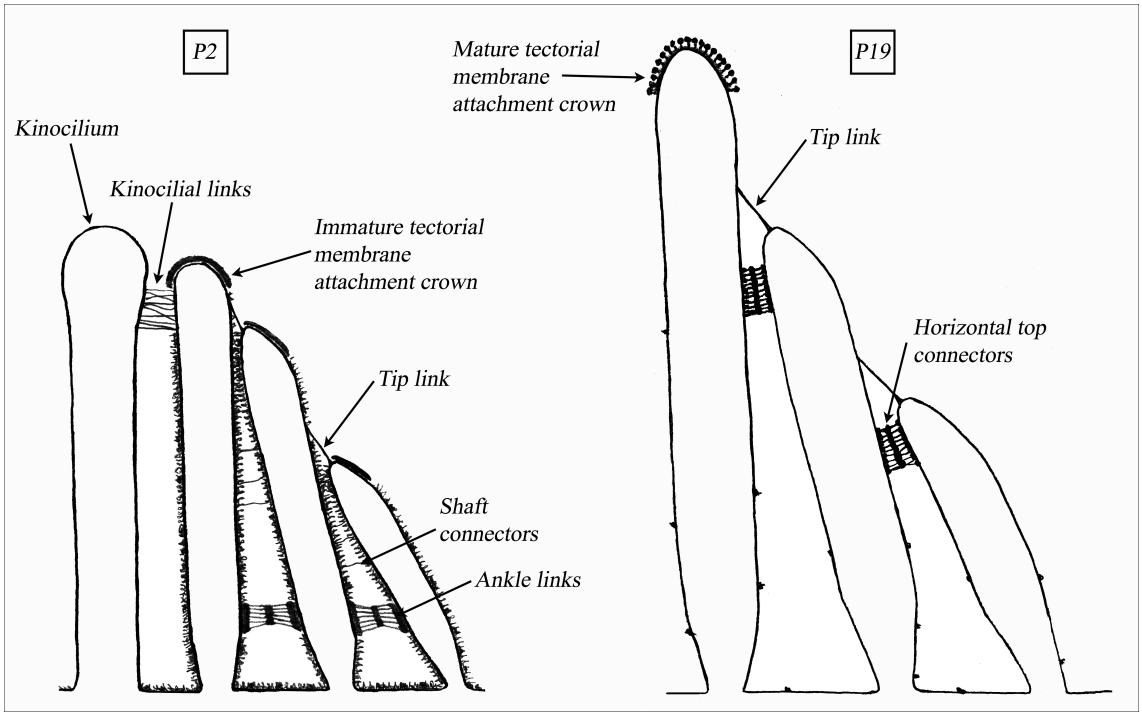

Figure 1.5 OHC hair bundle links in the mouse at postnatal day 2 (P2) and postnatal day 19 (P19) (courtesy of Dr RJ Goodyear).

The kinocilial links may comprise of the proteins that form tip links: CDH23 and PCDH15 (Michel et al, 2005: Ahmed et al, 2006). Transient stereocilia shaft connectors consisting of protein tyrosine phosphatase receptor Q (Ptprq) are important for the maturation of hair bundles, and the absence of Ptprq during development results in hair bundle disorganisation and hair cell loss (Goodyear et al, 2003: Sakaguchi et al, 2008). Ankle links appear transiently at the base of mice hair bundles at approximately P2 and disappear by P12 (Goodyear et al, 2005). Despite its brief existence, the ankle link complex, comprising of the very large G-protein-coupled receptor 1 (Vlgr1), the transmembrane proteins usherin and vezatin, as well as the triple PDZ (postsynaptic

density 95, **P**SD-95; discs large, **D**lg; zonula occludens-1, **Z**O-1) domain-containing submembrane protein whirlin, plays an important part in the organizational integrity of the hair bundle. Where the formation of ankle links has been compromised as in Vlgr1$^{-/-}$ mice, there is hair bundle disorganisation and mechanotransduction impairment resulting in early postnatal hearing loss and eventual hair cell loss (Adato et al, 2005: McGee et al, 2006).

1.3.3 Actin-bundling proteins within the stereocilia

Each individual stereocilium of the hair bundle consists of densely packed, highly cross-linked and highly organised actin filaments (F-actin) (Flock and Cheung, 1977: Tilney et al, 1980), which are polarised such that their plus ends (site of net polymerisation) are situated at the tip of the stereocilium, while their minus ends (site of net de-polymerisation) are positioned at the base of the stereocilium (Tilney et al, 1992a). These F-actin filaments are cross-linked by two proteins, espin and fimbrin (I-plastin). Espin is a ~ 110 kDa actin binding protein, with F-actin binding sites at both the N-terminus and C-terminus (Chen et al, 1999). There are 4 known espin isoforms that arise from different transcription sites of the same gene (Sekerková, 2004), and all 4 isoforms contain the 116-amino acid C-terminal actin-bundling module, as well as the actin-monomer-binding WASP homology 2 (WH2) domain (Bartles et al, 1996: Loomis et al, 2003: Sekerková, 2006b). Espin 1 to 3 also contain proline rich regions, while Espin 1 and 2 have additional F-actin binding sites. Espin 1 also has multiple ankyrin-like repeats (Sekerková, 2006b).

In rats, espin can be detected in immature hair bundles as soon as the hair bundle appears on hair cells at around E16 (Sekerková, 2006a), rat espin 1 is restricted to the vestibular hair cells, while espin 2 is expressed during development but levels decrease

before birth. Espin 3 is transiently expressed during development, and espin 4 remains present in mature hair bundles (Sekerková, 2006a). In addition to their role as highly efficient actin bundling proteins (Chen et al, 1999), espins may have a role in the regulation of stereocilia height, before their eventual degeneration, OHC stereocilia of espin null mice (jerker mice) show both reduced height and width, and the vestibular stereocilia of jerker mice also show shortening in comparison to heterozygous controls (Zheng et al, 2000: Rzadzinska et al, 2005). Further support for the role of espin in stereocilia height regulation stems from a recent study showing over-expression of espin 1 and myosin IIIa in rat hair cells causes stereocilia elongation compared to over-expression of either espin 1 or myosin IIIa alone (Salles et al, 2009). It is thought that the WH2 domain of espin 1 interacts with the plus-end-directed motor myosin IIIa, resulting in the transportation of espin 1 to the tips of stereocilia in rat hair cells (Salles et al, 2009). In humans, a novel espin mutation has recently been identified, resulting in the loss of both the WH2 and the C-terminal actin binding domains and causing severe to profound hearing loss with no apparent vestibular dysfunction (Boulouiz et al, 2008).

Fimbrin is a ~ 64 kDa actin bundling protein, with two EF-hands at the N-terminal and two actin binding domains (ABD1, ABD 2), each divided into two calponin homology (CH) domains (Delanote et al, 2005). There are 3 isoforms of fimbrin/plastin: I, T and L, with the I and T isoforms expressed in stereocilia (Shepherd et al, 1989: de Arruda et al, 1990: Drenckhahn et al, 1991). I-plastin is present in rat IHCs from at least embryonic day 18, and is present in the adult hair bundle (Zine et al, 1995). In contrast, the levels of T-plastin peak at P7 in rat stereocilia, but T-plastin is not detectable at all in hair cell stereocilia by P60 (Daudet and Lebart, 2002).

As a result of the tight packing and cross-linking of F-actin by espin and fimbrin, under normal physiological conditions a stereocilium is stiff, and does not tend to bend along its length.

1.3.4 Anchoring the stereocilia: rootlets and the cuticular plate

The rigidity of the stereocilia means that the deflection of the hair bundle during mechanical stimulation occurs at the ankle of the stereocilia, where the F-actin enters the hair cell as the rootlet (Flock and Cheung, 1977: Slepecky and Chamberlain, 1982). Due to the tapering that occurs at the stereocilium ankle, only a small number of the total actin filaments that are present in the stereocilium make up the rootlet (Itoh, 1982). The rootlet itself can be seen as an electron dense column that starts two-thirds of the way down within the stereocilia, becoming wider as it nears the apical surface of the cell, then extending into and anchoring itself within the cuticular plate of the hair cell (Figure 1.6) (Furness et al, 2008). Inside the hair cell, numerous fibrils extend from the rootlet and are attached to the network of actin filaments that makes up the cuticular plate (Itoh, 1982: Arima et al, 1987). Rootlets damaged either by experimental means such as a water jet, or by noise, can contribute to the loss of cochlear sensitivity even where there is no obvious hair bundle injury (Liberman and Dodds, 1987: Duncan and Saunders, 2000).

Within the cuticular plate, the randomly orientated actin filaments form a gel-like mesh due to linkage by spectrin (alpha-fodrin) (Demêmes and Scarfone, 1992: Mahendrasingam, 1998), a protein that exists as an α- (molecular mass 240 kDa) and β- (220 kDa) heterotetramer (Chakrabarti et al, 2006: Prasain and Stevens, 2009). In addition to being localised in the cuticular plate, the αII-βV spectrin isoform has also been localised to the cortical lattice of the OHC, where it contributes to OHC motility

by providing structural integrity (Legendre et al, 2008). Other constituents of the cuticular plate have not been unequivocally agreed upon: different studies have shown either tropomyosin or α-actinin are present or absent, or present but in different locations within the cuticular plate (Sans et al, 1989: Slepecky and Chamberlain, 1985: Drenckhahn et al, 1991: Furness et al, 2008).

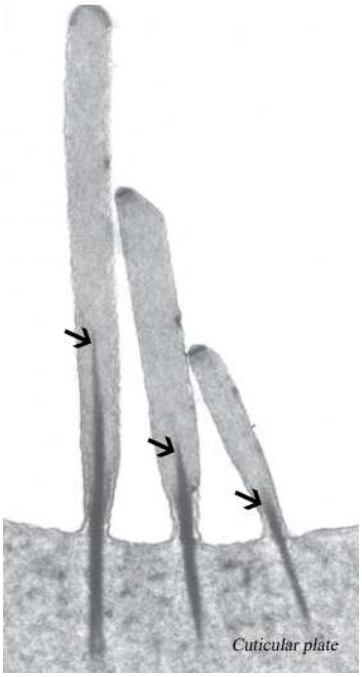

Figure 1.6 Transverse section through three rows of stereocilia showing rootlets, with arrows indicating the beginning of the rootlet (adapted from Fettiplace and Hackney, 2006).

1.3.5 Actin treadmilling within the stereocilia

A distinctive feature of mammalian hair bundles is that they are intended to function over the entire lifespan of the organism (Corwin, 1992), and as a consequence, stereocilia of the hair bundle have been viewed as extremely stable structures. Yet like F-actin in the cell cytoplasm, the F-actin cores of stereocilia have been shown to undergo “head-to-tail polymerisation” (treadmilling) (Schneider et al, 2002: Rzadzinska et al, 2004), where the rate of actin polymerisation at the plus end equals the rate of

depolymerisation at the minus end, resulting in a filament of constant length (Figure 1.7) (Wegner, 1976: Neuhaus et al, 1983).

The rate of treadmilling in each individual stereocilium is dependent upon its height, the taller the stereocilia, the faster the treadmilling (Rzadzinska et al, 2004). Hence in the mature rat hair bundle, actin monomers are polymerised at the plus end of the filaments, along with espin, and over a 48-hour period, the entire bundle is turned over as one unit (Schneider et al, 2002: Rzadzinska et al, 2004).

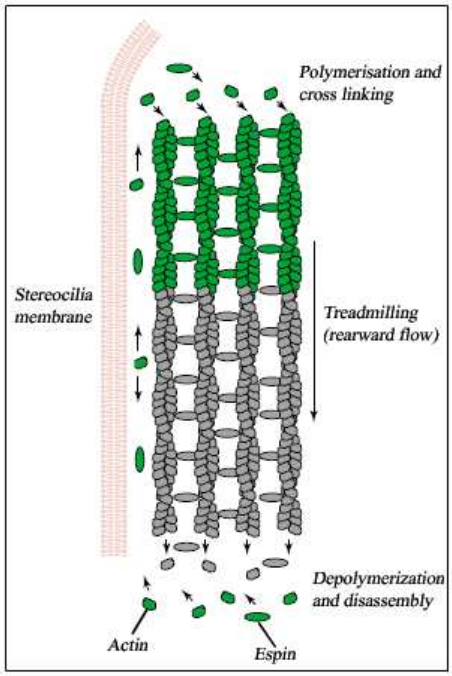

Figure 1.7 Actin molecular treadmill model (adapted from Lin et al, 2005).

1.4 Hair bundle development

1.4.1 Chick hair bundle development

Much of the work on the highly coordinated and organised development of the hair bundle has been carried out in chicks, where hair cells can be first distinguished from supporting cells at embryonic day 6 (E6) by the concentric arrangement of the microvilli on their apical surfaces (Cotanche, 1987a). A single microtubular kinocilium

is also present at the centre of hair cells, but between E9-11, this will have moved so that the kinocilium of each developing hair bundle is roughly in the same peripheral area of the circular hair bundle (Tilney et al 1992b). Over this same time period, the hitherto variable widths of the stereocilia become more standardised, possibly due to cross-linking by actin-bundling proteins such as espin (Li et al, 2004).

Formation of the characteristic hair bundle staircase begins from E10-12 by sequential elongation, where the row of stereocilia nearest the kinocilium begins to elongate first, followed by the next row and so on (Tilney et al, 1988). As a row of stereocilia becomes incorporated into the staircase, tip links appear, and transducer currents can be detected from E11 (Tilney et al, 1992a: Si et al, 2003). The circular shape of the hair bundle also changes as the side with the tallest stereocilia straightens out, creating a semi-circle (Tilney et al 1992b), and the final rectangular shape of the chick hair bundle is eventually achieved by the reabsorbing of superfluous stereocilia (Tilney et al, 1992b).

From E13-16, the hair bundle temporarily pauses elongation to increase the diameters of the stereocilia by incorporating new actin filaments onto the cross-linked “cores” (Tilney and DeRosier, 1986), and the number of filaments added can be high, increasing from 100 filaments at E11 to 400 at E16 (Tilney and DeRosier, 1986). Although the height of the hair bundle is not increasing at this time, stereocilia are in fact extending downwards into the developing cuticular plate by way of newly formed rootlets (Cotanche, 1987a). The tapered morphology of mature stereocilia also develops at this time as the base of the stereocilia becomes pinched in (Tilney and DeRosier, 1986).

From E17, elongation of the entire hair bundle recommences until the mature height is reached, but this stage is also used to reinforce the staircase pattern, with the shortest row completing elongation first and the tallest row completing last (Tilney et al, 1986).

1.4.2 Mammalian hair bundle development

A similar process of hair bundle development has been reported in mammals, although there does not appear to be the temporal separation of stereocilia thickening and elongation (Zine and Romand, 1996: Mu et al, 1997: Forge, 1997). In addition, the hair bundle staircase morphology that is generated in the chick by the sequential elongation of stereocilia, in mammalian hair bundles, may be the result of different stereocilia growth rates (Kaltenbach et al, 1994).

For both chick and mammals, the hair bundle development process is highly organised and must necessarily involve the close regulation of actin polymerisation, depolymerisation, and cross-linking, although very little is known about how these processes are regulated. Certain aspects are gradually being elucidated however, actin treadmilling within stereocilia has been proposed to provide a method of transporting cargo such as myosins and other proteins to the appropriate sites along the stereocilia (Naoz et al, 2008). Currently though, most of what is known about hair bundle development and actin regulation within the stereocilia stems from studying proteins directly associated with the stereocilia, as mutations in these proteins causes hair bundle defects and many of these proteins derive from known deafness loci.

1.4.3 Usher's syndrome

Mutations of the proteins that cause hair bundle defects are often, but not exclusively, associated with Usher's syndrome, the most common form of deaf-blindness, caused by progressive retinal degeneration (retinitis pigmentosa) coupled with varying degrees of hearing loss (Kloepfer et al, 1966: Fishman et al, 1979: Rosenberg et al, 1997: Spandau and Rohrschneider, 2002). Mutations in Usher's syndrome genes can also result in non-syndromic hearing loss (Saihan et al, 2009).

Clinically, Usher's syndrome is categorised into 3 types: Usher type 1 is characterized by severe to profound congenital sensorineural loss and continuous balance deficiency (vestibular dysfunction). Hearing loss in Usher type 2 varies from mild to severe, with no vestibular dysfunction, while Usher type 3 shows progressive hearing loss and variable vestibular dysfunction. All 3 types present with retinitis pigmentosa and possible cataract (Petit, 2001: Williams, 2008). Table 1.1 summarises the Usher's syndrome loci and their affected proteins (Gibson et al, 1995: Weil et al, 1995: Verpy et al, 2000: Alagramam et al, 2001: Ahmed et al, 2001: Bork et al, 2001: Adato et al, 2002: Weil et al, 2003: Weston et al, 2004: van Wijk et al, 2006: Ebermann et al, 2007). Although Usher's syndrome genes represent a number of different protein classes, there is evidence that many of the proteins interact, forming an Usher protein network (Saihan et al, 2009).

1.4.3.1 The Usher protein network

Mutations of the individual proteins that make up Usher type 1 produce characteristic small individual clumps of randomly distributed hair bundles (Lefèvre et al, 2008). As a group, the Usher type I proteins consist of myosin VIIa, SANS, harmonin b, CDH23 and PCDH15 (Chen et al, 1996: Verpy et al, 2000: Udovichenko et al, 2002: Kikkawa et al, 2003: Weil et al, 2003: Adato et al, 2005: Pan et al, 2009) (Figure 1.8). During hair bundle development, the myosin VIIa tail interacts with the harmonin b PDZ 1 domain, thereby transporting harmonin b to the top of the stereocilia where its PDZ 2 domain anchors the CDH23 part of the tip link (Boëda et al, 2002: Lefèvre et al, 2008). Although it has been shown that SANS interacts directly with harmonin b via its PDZ 1 and PDZ 2 domains, and that SANS is critical for the cohesion of the developing hair bundle (Weil et al, 2003), its mechanism of function is still unclear.

Figure 1.9 illustrates the domains of Usher type I proteins. The complexity of the Usher protein interactome continues to increase as shown by the interaction of harmonin b with members of the USH 2 family usherin and Vlgr1 via its PDZ 1 domain (Reiners et al, 2005) (Figure 1.8). Furthermore, a new USH1 locus (designated USH1H) has recently been reported in two large Pakistani consanguineous families (Ahmed et al, 2009).

Usher Type	**Usher syndrome locus**	**Gene symbol**	**Protein name and class**
USH1	USH1B	MYO7A	myosin VIIa - motor protein
USH1	USH1C	USH1C	harmonin b – scaffold protein
USH1	USH1D	CDH23	cadherin 23 – cell to cell adhesion protein
USH1	USH1F	PCDH15	protocadherin15 - cell to cell adhesion protein
USH1	USH1G	USH1G	SANS - scaffold protein
USH2	USH2A	USH2A	usherin – transmembrane protein
USH2	USH2C	VLGR1	Mass1 – transmembrane receptor protein
USH2	USH2D	WHRN	whirlin - scaffold protein
USH3	USH3A	USH3A	clarin1 - transmembrane protein

Table 1.1 Usher's syndrome type, loci, gene symbol, protein names and class.

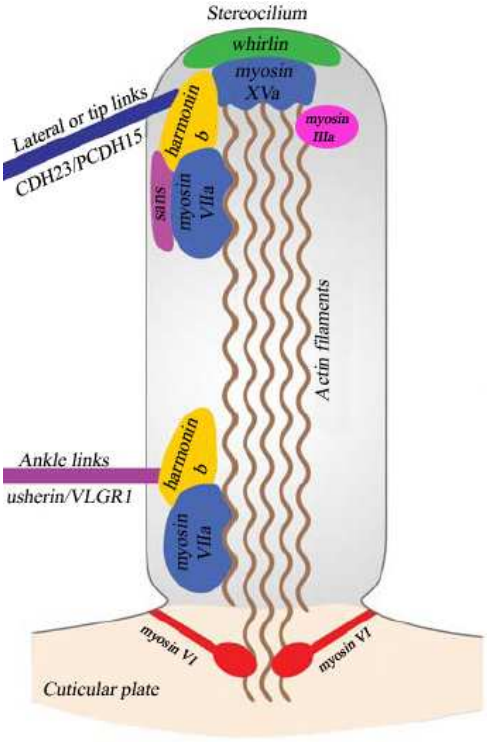

Figure 1.8 Illustration of the interaction of Usher type 1 and type 2 proteins (adapted from Friedman et al, 2007). Non-Usher proteins (myosin XVa and myosin VI) have been included for completeness.

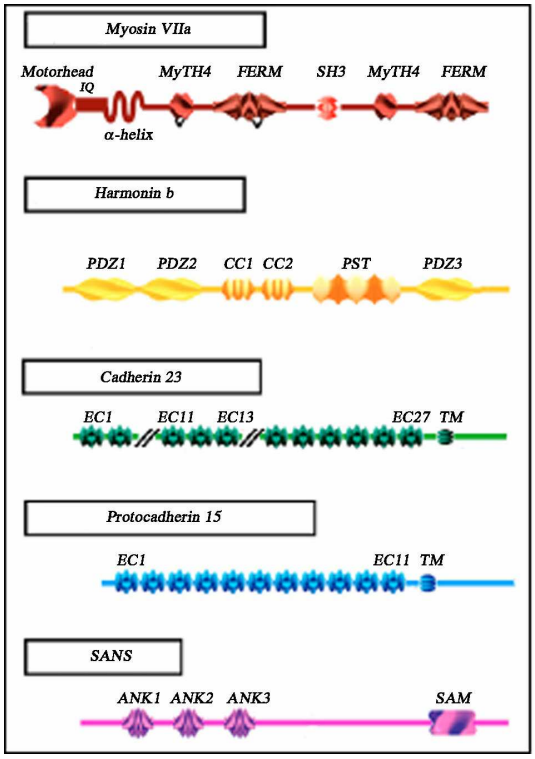

Figure 1.9
Domains of Usher type 1 proteins. MyTH4 (Myosin tail homology 4), IQ (isoleucine-glutamine motifs), FERM (band 4.1, ezrin, radixin, moesin), SH3 (Src homology 3), PDZ (postsynaptic density 95, PSD-95; discs large, Dlg; zonula occludens-1, ZO-1), CC (coiled-coil), PST (proline, serine and threonine rich sequence), EC (extracellular cadherin repeat), ANK (ankryn-like repeats), SAM (sterile alpha motif). Adapted from Lefèvre et al (2008).

1.4.4 Non-Usher syndrome related myosins

In addition to myosin VIIa, which forms a part of the Usher type I network, a number of other myosins are now known to play a role in hair bundle development. These include myosin XVa, myosin VI and myosin IIIa.

In the hair bundle, myosin XVa (Figure 1.10) is concentrated at the tip of the stereocilia in a height dependent manner, hence the taller the stereocilia, the larger the amount of myosin XVa (Rzadzinska et al, 2004). Indeed, myosin XVa is essential for the creation of the hair bundle staircase, as the hair bundles of myosin XVa mutants lack a defined staircase, and additionally are much shorter than their wild type counterparts, resulting in hearing loss in shaker 2 mice (Anderson et al, 2000: Gong et al, 2006).

Figure 1.10 Myosin XVa domains: MyTH4 (myosin tail homology 4), IQ (isoleucine-glutamine motifs), FERM (band 4.1, ezrin, radixin, moesin), SH3 (Src homology 3). Adapted from Belyantseva et al (2005).

Even though it is not an Usher's syndrome protein, the shortened hair bundle phenotype seen in myosin XVa mutants is similar to that of the deaf mouse strain "whirler", which lacks the USH2D scaffold protein whirlin (Delprat et al, 2005: Mogensen et al, 2007). Whirlin exists as two isoforms, short and long: the long isoform consists of three PDZ domains and a proline rich region, while the short isoform contains the proline rich region and PDZ 3 domain only (Delprat et al, 2005: van Wijk et al, 2006) (Figure 1.11). Along with myosin XVa, whirlin is known to have an important role in stereocilia elongation and it has been demonstrated that myosin XVa can interact with the short

whirlin isoform with its SH3-MyTH4 region, or with the PDZ 1 and PDZ 2 domains of the long whirlin isoform with its MyTH4-FERM region (Delprat et al, 2005). Thus myosin XVa interacts with and is thought to transport whirlin to the tips of the stereocilia (Belyantseva et al, 2005, Kikkawa et al, 2005), although it is possible that myosin XVa also interacts with proteins other than whirlin that are important in hair bundle development (Mustapha et al, 2007).

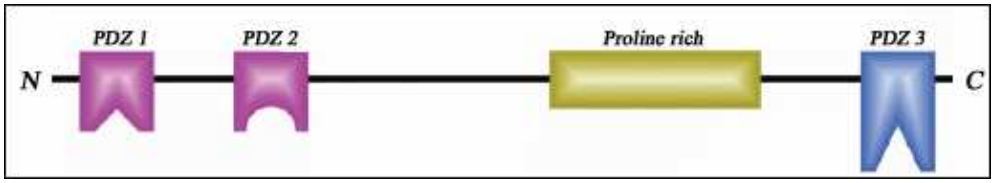

Figure 1.11 Whirlin domains: PDZ (PDZ (postsynaptic density 95, PSD-95; discs large, Dlg; zonula occludens-1, ZO-1). Adapted from Belyantseva et al (2005).

Myosin VI (Figure 1.12) is unusual for being the only myosin to move towards the minus end of actin filaments (Wells et al, 1999). In Snell's waltzer mice, which have a null mutation for myosin VI (Friedman et al, 1999), and Tailchaser mice, in which a missense mutation disrupts myosin VI function (Hertzano et al, 2008), there is membrane fusion at the base of the stereocilia as well as the formation of giant stereocilia (Friedman et al, 1999: Self et al, 1999: Hertzano et al, 2008). This has led to the proposal that myosin VI acts as an anchor, tethering the hair cell apical membrane to the cuticular plate via its head domain.

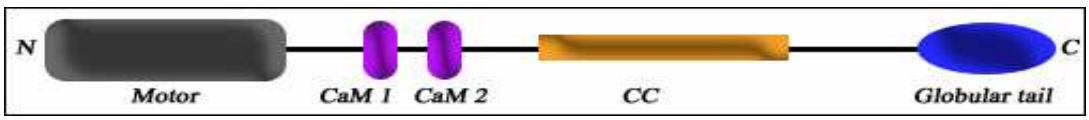

Figure 1.12 Myosin VI domains: CaM (calmodulin binding motif), CC (coiled-coil). Adapted from Sweeney and Houdusse (2007).

The link between myosin IIIa (Figure 1.13) and hearing loss was first established by Walsh et al (2002), and since then, myosin IIIa has demonstrated motor domain dependent localisation to the tip of the hair bundle (Schneider et al, 2006). It is possible that myosin IIIa has a role in regulating stereocilia height as deletion of the kinase domain results in abnormally elongated stereocilia as well as bulging of the stereocilia tip (Schneider et al, 2006). In contrast, another study has shown that over-expression of myosin IIIa, in conjunction with espin over-expression, also causes stereocilia elongation (Salles et al, 2009).

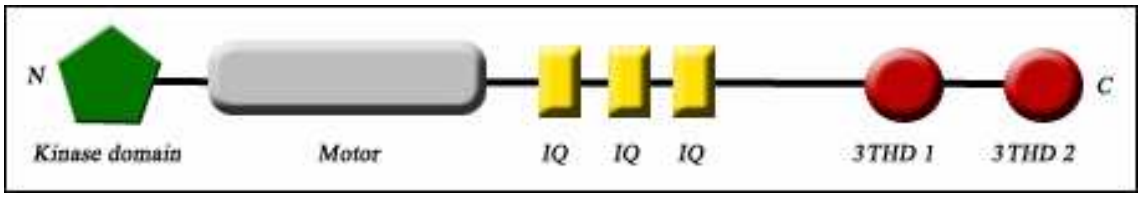

Figure 1.13 Myosin IIIa domains: IQ (isoleucine-glutamine motifs), 3THD (class 3 tail homology domains). Adapted from Salles et al (2009).

1.5 Regeneration of hair bundles

Whether, and to what extent, hair cells recover from damage due to noise or drugs (such as aminoglycosides) is species dependent. In zebrafish, hair cells and hair bundles recover to pre-treatment numbers 14 days after ablation of saccular hair cells by noise (Schuck and Smith, 2009), although a hair-cell like phenotype has been documented as early as 24-36 hours after copper sulphate or neomycin treatment (Harris et al, 2003: Hernández et al, 2007). It appears that zebrafish can generate new hair cells from supporting cells that re-enter the cell cycle and create daughter cells, which then differentiate into hair cells (proliferative regeneration). Creation of new hair cells in zebrafish can also occur by transdifferentiation, where existing supporting cells transform into hair cells without mitosis, less severe damage may induce

transdifferentiation while more severe damage may need proliferative regeneration for complete hair cell recovery (Hernández et al, 2007). Furthermore, by looking at cell morphology and by using non-mitotic hair-cell markers as well as markers for mitosis such as bromodeoxyuridine (Li and Forge, 1997: Steyger et al, 1997: Zheng and Gao, 1997: Avallone et al, 2008: Kaiser et al, 2009), it has been shown that both proliferative regeneration and transdifferentiation are used to regenerate hair cells in amphibians (Jones and Corwin, 1996: Balak et al, 1990: Baird et al, 2000: Taylor and Forge, 2005), birds (Duncan et al, 2006: Cafaro et al, 2007) and the mammalian vestibular organs (Warchol et al, 1993: Forge et al, 1993: Li and Forge, 1997: Kawamoto et al, 2009). Behavioural studies using birds have shown that these new hair cells are functional, the quality of birdsong was found to degenerate with ototoxic treatment, but recovers commensurately with hair cell recovery, although hair cell recovery can lag behind birdsong recovery (Dooling et al, 1997: Marean et al, 1998: Woolley and Rubel, 2002). However, function does not always appear to fully recover to pre-hair cell damage levels, with electrophysiological testing showing a residue of ~ 15-20 dB hearing loss at all frequencies in aminoglycoside treated birds (Müller and Smolders, 1998), while another study shows a residual loss in the high frequencies only (Irvine et al, 2009). In mammals, transducer currents from vestibular hair cells are abolished by gentamicin treatment, but return with hair bundle recovery over the following 13-17 days (Taura et al, 2006), indicating that damaged vestibular hair cells show functional, as well as morphological, recovery.

The regulatory mechanisms of proliferative regeneration and transdifferentiation have yet to be elucidated. However, there is evidence to show that in zebrafish, the Notch signalling pathway, which plays a role in embryonic hair cell differentiation, may have

a role in regulating the number of hair cells regenerated after neomycin exposure (Haddon et al, 1998: Ma et al, 2008). In addition, over-expression of the basic helix-loop-helix (bHLH) transcription factor *Hath1* (also known as *Atoh1* or *Math1*) in the gentamicin treated rat utricle results in the generation of new hair cells via transdifferentiation (Shou et al, 2003).

The presence of growth factors is essential for normal inner ear development (Represa et al, 1988: Després et al, 1991). This observation has led to suggestions that growth factors may also promote hair cell regeneration (Zheng et al, 1997: Doetzlhofer et al, 2004), and heregulin, a member of the epidermal growth factor family, has been shown to promote proliferative regeneration in gentamicin treated rat utricles (Zheng et al, 1999). In the chick, both basic fibroblast growth factor (bFGF) and nerve growth factor (NGF) show up-regulation in response to noise-induced hair cell loss. However, the relationship between growth factor up-regulation and hair cell loss may not be straight forward, with 8 hours daily exposure to 120 dB SPL for 5 days (total of 40 hours noise exposure) causing greater bFGF and NGF up-regulation than continuous exposure to 120 dB SPL for 72 hours (Sliwinska-Kowalska et al, 2005).

1.5.1 Regeneration of mammalian auditory hair cells

The ability of hair cells to repair and regenerate, especially in the avian auditory and mammalian vestibular systems, has led to hopes that this could be repeated in mammalian auditory hair and supporting cells. It has been shown that hair cells, which survive even severe mechanical trauma, can self-repair to a certain extent (Sobkowicz et al, 1992), although where hair cells are entirely missing, no regeneration occurs (Quint et al, 1998: Lenoir et al, 1999: Yamasoba and Kondo, 2006).

Nevertheless, growth factors may well support the survival of any remaining cells in an aminoglycoside-damaged organ of Corti (Romand and Chardin, 1999: Daudet et al, 2002).

The transcription factor *Atoh1* is crucial for normal mammalian hair cell development (Gubbels et al, 2008), and has been reported to induce the transdifferentiation of supporting cells into hair cells (Kawamoto et al, 2003). Where cochlear hair cells were removed by a combination of aminoglycoside and diuretic drugs, both inner and outer hair cells were apparently regenerated by supporting cells over-expressing *Atoh1*, although OHCs were often mis-orientated and incompletely differentiated (Izumikawa et al, 2005). Moreover, these new hair cells were found to be functional on electrophysiological testing, although as the authors of the study point out, the condition of the OHCs may not fully restore their function as the active cochlea amplifier (Izumikawa et al, 2005).

The Notch pathway is one of the major signalling pathways involved in almost all developmental decisions in multi-cellular organisms (Abelló and Alsina, 2007) and in the developing inner ear, Notch suppresses *Atoh1* expression by regulation of *Hes1* and *Hes5*, bHLH transcription regulators which antagonize *Atoh1* expression (Zheng et al, 2000). Due to the potential of *Atoh1*/*Math1*/*Hath1* to induce cochlear hair cell regeneration, the Notch pathway is being investigated for a possible role in this process. The results have been paradoxical so far. Some workers have found increased *Hes1* and *Hes5* labelling in the cochlea of adult guinea pigs in response to aminoglycoside damage (Batts et al, 2009), suggesting the suppression of potential *Atoh1* expression. In contrast, another study found no such increase in adult *Hes5*-GTP transgenic mice in response to aminoglycoside and diuretic damage (Hartman et al, 2009).

The cyclin-dependent kinase inhibitor $p27^{Kip1}$ (Cdkn1B) is also being investigated as a potential target for modulating hair cell regeneration. In the normal cochlea, $p27^{Kip1}$ is expressed in post-mitotic supporting cells to prevent them from re-entering the cell cycle, hence in $p27^{Kip1}$ deficient mice there is overproduction of inner and outer hair cells as well as supporting cells (Löwenheim et al, 1999a: Kanzaki et al, 2006). Ex vivo post mitotic supporting cells have been shown to down regulate $p27^{Kip1}$ and proliferate in the presence of periotic mesenchymal cells, which normally support embryonic cochlea development, with a resulting portion of the new cells differentiating into hair cells, although transdifferentiation was also observed (White et al, 2006: Ono et al, 2009).

1.5.2 Recovery of mammalian auditory hair cells and hair bundles

Where there is non-fatal injury to the hair cell, but there is enough damage to cause the loss of the hair bundle, hair cell survival is possible. Hair cells from the bullfrog saccule which survive aminoglycoside damage have been shown to exist in a bundle-free state for at least a week (Gale et al, 2002), while bundle-free hair cells from aminoglycoside treated P3 rat utricles can survive for at least 11 days (Zheng et al, 1999).

In the mammalian organ of Corti, mechanically damaged, bundle-free neonatal hair cells can also survive (Sobkowicz et al, 1992: Sobkowicz et al, 1997), and even show signs of hair bundle repair by reforming the kinocilium (Sobkowicz et al, 1995). The ability of the mammalian auditory hair cell to repair itself is further demonstrated by the decrease in cell surface blebs found on cochlear cultures of P1-3 mice after 2 hours of recovery following a short (30 minutes) treatment with neomycin (Goodyear et al, 2008). In the mature mammalian cochlea, studies have shown that both hair bundle tip links and side connectors can be damaged by noise exposure with concomitant hair

bundle disarray, fusion of stereocilia and hearing loss (Pickles et al, 1987: Clark and Pickles, 1996). However, side connectors damaged by noise exposure have been shown to undergo repair, returning the hair bundle to its intact state in 14-28 days, although other ultra-structural damage such as blebs remained (Tsuprun et al, 2003).

The mechanism of this hair bundle recovery has yet to be fully elucidated, but it has been suggested that the continuous turnover of actin filaments may play a part by transporting the required proteins for repair to the necessary location along the stereocilia (Schneider et al, 2002: Rzadzinska et al, 2004).

1.6 The role of phosphorylation in actin cytoskeleton regulation

Hair bundle development, maintenance and regeneration necessarily involve the regulation of actin polymerisation and depolymerisation. However, aside from the possible transportation of proteins within the stereocilium by treadmilling (Naoz et al, 2008), very little else is known about stereocilia actin regulation.

In non-hair cells, actin is known to be closely regulated as it is involved in a myriad of dynamic cellular processes such as cell migration, mitosis, gene expression or the trafficking of intracellular proteins and organelles (Gieni and Hendzel, 2009: Hall, 2009: Kunda and Baum, 2009) The utilization of protein kinases for phosphorylation plays an important role in actin regulation. Currently, there appear to be three major processes that regulate actin within cells, which are nominally independent, but are highly interconnected: the capping and uncapping of actin filaments, actin filament depolymerisation and de novo actin nucleation. Each of these three processes are regulated by different proteins such as the family of small GTPases, Rho, Rac and Cdc42, and by phospholipids such as phosphatidylinositol 4,5-bisphosphate (PIP_2), both

of which depend on both upstream and downstream phosphorylation to exert their effects on the actin cytoskeleton.

1.6.1 Protein kinases and regulation of actin filament un/capping

Two important proteins involved in the capping of existing filaments to prevent spontaneous actin polymerisation are gelsolin (Harris and Weeds, 1984) and capping protein (also known as CapZ or β-actinin) (Casella et al, 1986: Caldwell et al, 1989) (Figure 1.14). Gelsolin is a ~ 90 kDa member of the gelsolin superfamily, and contains six homologous repeats of a domain named gelsolin-like (G) domain, with two actin binding domains situated at the N-terminus and C-terminus respectively (Chaponnier et al, 1986: Silacci et al, 2004). In order to cap an actin filament, gelsolin binds two opposing actin strands with its actin binding domains, and in response to an increase in intracellular Ca^{2+} concentration, undergoes a conformational change which severs the filament, leaving gelsolin attached to the barbed end as a cap (McLaughlin et al, 1993: Silacci et al, 2004). Protein kinase C (PKC) signalling has been shown to be involved in gelsolin expression. As part of its anti-tumour effects, the histone deacetylase inhibitor apicidin induces the production of gelsolin (Han et al, 2000), but when PKCε is inhibited in human cervix cancer cells, apicidin-induced gelsolin expression is completely abrogated (Eun et al, 2007). On the other hand, gelsolin severing of actin filaments and their subsequent capping can be prevented by the action of the phosphoinositides phosphatidylinositol 4-phosphate (PI4P) and PIP_2 (Janmey and Stossel, 1989), with PIP_2 binding to a sequence in the N-terminus that prevents gelsolin binding to an actin filament (Yin et al, 1988: Lin et al, 1997). The protein kinase phosphatidylinositol 4-phosphate 5 kinase (PI5K), which phosphorylates PI4P to

produce PIP_2, is important in this process as PI5K ensures the correct localisation of PIP_2 (El Sayegh et al, 2007).

CapZ is an αβ heterodimer with an α subunit of 32–36 kDa and a β subunit of 28–32 kDa (Wear and Cooper, 2004) which form an unusual tertiary structure consisting of two C-terminal extensions which bind actin and subsequently causes filament capping (Yamashita et al, 2003).

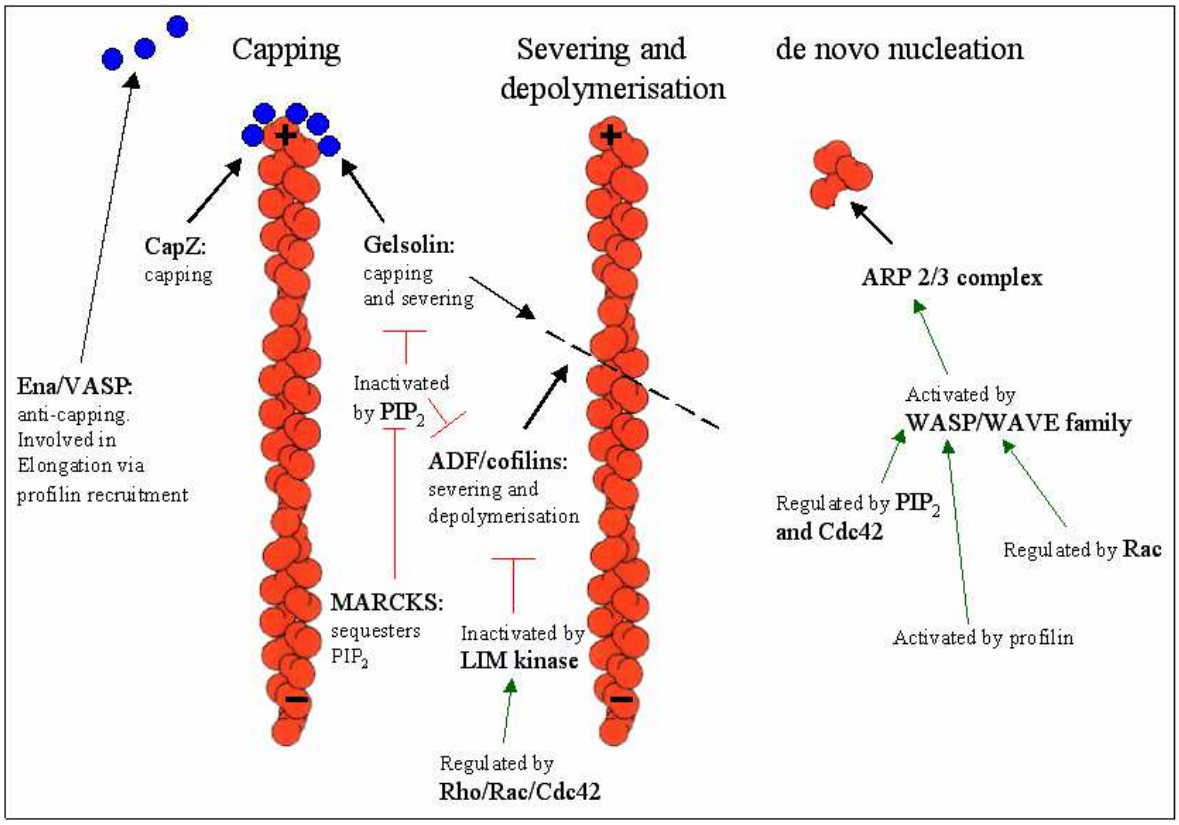

Figure 1.14 Actin filament regulation routes and their major regulatory processes.

Previous studies showed that PIP_2 inhibits the action of CapZ in a concentration dependent manner (Schafer et al, 1996: DiNubile and Huang, 1997), possibly by binding to the C-terminal extension of the α subunit, therefore preventing filament capping (Kim et al, 2007). The level of available PIP_2 is therefore an important factor in actin regulation. Among the many ways in which PKC influences the actin

cytoskeleton, PKC can phosphorylate PIP_2-sequestering proteins such as the myristoylated alanine-rich C-kinase substrate (MARCKS), resulting in an increase of PIP_2, and thereby encouraging actin filament assembly (Glaser et al, 1996).

Actin filament capping can also be prevented by the Ena/VASP family (Figure 1.14), a family of proteins that have an N-terminal Ena/VASP homology 1 (EVH1) domain, a proline-rich domain and a C-terminal EVH2 domain (Bear and Gertler, 2009). One method by which Ena/VASP prevents capping is by increasing the rate of filament elongation, which it accomplishes even in the presence of capping proteins (Barzik et al, 2005), possibly via the recruitment of profilin, a protein which promotes the presence of ATP-actin monomers (Pasic et al, 2008). Activation of the Ena/VASP proteins is dependent on multiple phosphorylation sites that are targets for either cAMP-dependent protein kinase (PKA) or cGMP-dependent protein kinase (PKG) (Lebrand et al, 2004). How the phosphorylation of specific sites affects Ena/VASP function has not been fully elucidated, but it is known that phosphorylation of Ena/VASP by PKA is essential for its correct localisation (Benz et al, 2009).

1.6.2 Protein kinases in actin depolymerisation and de novo actin nucleation

ADF/cofilin is one of a family of important F-actin regulatory proteins. These proteins have highly conserved G-actin and F-actin binding domains, as well as a PIP_2 binding domain (Bamburg, 1999). ADF/cofilin increases actin filament depolymerisation by increasing the rate of disassociation of ADP-actin at the minus end of the actin filament, and once bound to an ADP-actin monomer, ADF/cofilin inhibits nucleotide exchange, thus decreasing the level of ATP-actin monomers ready for incorporation at the plus end of the filament (Chen et al, 2000: Paavilainen et al, 2008). To aid in actin filament depolymerisation, ADF/cofilin can also sever actin filaments by using an unusual

mechanism: ADF/cofilin binding to an actin filament causes the filament to twist, thus weakening the lateral links between actin monomers in the filament, leading to filament fragmentation (McGough and Chiu, 1999: Bobkov et al, 2006). The ultimate polymerisation or depolymerisation action of ADF/cofilin on actin filaments however, may depend on the local concentration within the cell, as high concentrations of ADF/cofilin have been shown to favour creation of new actin filaments (Andrianantoandro and Pollard, 2006). Regulation of ADF/cofilin activity is effected by the serine protein kinases Lim kinase 1 (LIMK1) and Lim kinase 2 (LIMK2) (Figure 1.14), which inactivate ADF/cofilin by phosphorylation of the ADF/cofilin N-terminal serine residue (Maciver and Hussey, 2002). The LIM kinases are themselves downstream effectors of the Rho, Rac and Cdc42 family, with Rac and Cdc42 mediating the phosphorylation of LIMK1 by p21-activated kinase (Pak1) at threonine 508 (Edwards et al, 1999). The threonine 508 residue of LIMK1 is also the target for phosphorylation by Rho-associated kinase (ROCK) (Ohashi et al, 2000), and in addition, ROCK is thought to phosphorylate LIMK2 (Vardouli et al, 2005).

Actin nucleation is the first step in the formation of new actin filaments, and the role of the actin nucleation core is provided by the Arp2/3 complex, which consist of actin related proteins 2 and 3 (Arp2/3) as well as 5 other subunits (Welch et al, 1997). Arp2/3 is activated by the Wiskott-Aldrich syndrome family proteins (WASP), including WASP, N-WASP and WAVE 1-3 (Machesky and Insall, 1998: Yarar et al, 1999). Although WASP and WAVE differ in their N-termini, with WASP containing a WH1 domain and WAVE a novel SHD/WHD domain, both WASP and WAVE contain a highly basic region, a GBD/CRIB motif, a proline-rich region, and the Arp2/3 activating VCA region in the C-terminal (Miki and Takenawa, 2003).

While the VCA region can be masked by WASP auto-inhibition, binding of Cdc42 to the GBD/CRIB motif and PIP_2 to the basic region releases this inhibition, resulting in actin nucleation by Arp2/3 (Kim et al, 2000: Papayannopoulos et al, 2005). Furthermore, profilin has been shown to cause partial/full release of WASP auto-inhibition by binding to the proline-rich domain of WASP by its SH3 domain (Suetsugu et al, 1998). It has recently been suggested that in addition to WASP activation, phosphorylation of the threonine 237 and 238 residues in the Arp2 protein is also necessary for Arp 2/3-induced actin nucleation (LeClaire III et al, 2008).

Different members of the Rho, Rac and CDC42 family are thought to show a degree of selectivity in WASP activation, with Cdc42 more efficient at WASP activation, while Rac shows greater potency for N-WASP activation as well as being the activator for the WAVE proteins (Yamazaki et al, 2007: Tomasevic et al, 2007: Abou-Kheir et al, 2008). As well as regulation by the Rho family, both WASP and WAVE proteins have multiple phosphorylation sites that are important for localisation or for actin binding affinity via their VCA regions (Blundell et al, 2009: Pocha and Cory, 2009).

Rho also has a role in the activation of the Diaphanous-related formins, another group of actin nucleation proteins, which contain a C-terminal formin homology 2 (FH2) domain that mediates their effects on actin, with the N-terminus providing the site for auto-inhibition (Seth et al, 2006). The N-terminus of the Diaphanous-related formins contains the GTPase-binding domain, which on Rho binding releases the auto-inhibition, thereby recruiting the diaphanous-related formins to the plasma membrane (Rose et al, 2005), with further interaction with ROCK initiating nucleation of new actin filaments (Hannemann et al, 2008).

1.6.3 c-Jun NH_2-terminal kinase: a downstream effector of Rho, Rac and Cdc42

As the section above illustrates, there are many effector proteins downstream of Rho, Rac and Cdc42 that have roles in regulating the cytoskeleton. These effector proteins can act by either initiating further downstream phosphorylation, like that carried out by the Pak family of protein kinases (Sells et al, 1997: Parrini et al, 2009), or by direct actin binding, such as for Filamin A (Nunnally et al, 1981: Bustelo et al, 2007). The c-Jun N-terminal kinase (JNK) is a member of the mitogen-activated protein kinase (MAPK) family and among the protein kinases potentially activated downstream of Rho, Rac and Cdc42 signalling, JNK has emerged as an important regulator of actin. Thus in morphogenesis, mouse double mutants for *Jnk1*$^{-/-}$ and *Jnk2*$^{-/-}$ do not survive embryogenesis due to failure of neural tube closure (Kuan et al, 1999), a complex process dependent, among other factors, on the precise actin-generated movements of epithelial cell sheets (Morriss-Kay and Tuckett, 1985: Moephuli et al, 1997: Hildebrand and Soriano, 1999: Xia and Karin, 2004). In inflammation, wound closure is prevented in the presence of JNK inhibitors due to inhibition of lamellipodia formation (Altan and Fenteany, 2008: Nomachi et al, 2008) and in bacterial infection, the mobility and migration of neutrophils enabled by the actin cytoskeleton involves the activation of the JNK pathway (Arndt et al, 2005: Zemans and Arndt, 2009). Three mammalian JNK genes encode for JNK proteins I, II and III, which may vary in their distribution in different tissue types (Yang et al, 1997). As a consequence of splicing, there are at least 10 known JNK isoforms (Gupta et al, 1996), which are activated by phosphorylation of specific threonine and tyrosine residues (Dérijard et al, 1994). Upon activation, JNK phosphorylates the transcription factor c-Jun at Ser-63 and Ser-73 (Dérijard et al, 1994), leading to apoptosis in a wide range of cell types such as neurons (Liu et al, 2009), retinal cells (Guma et al, 2009) and cardiac cells (Izumi et al, 2000).

1.6.3.1 c-Jun NH_2-terminal kinase inhibition and auditory hair cells

In the organ of Corti, activation of the JNK pathway leading to apoptosis has been demonstrated in hair cells subjected to aminoglycoside or noise damage (Pirvola et al, 2000: Ylikoski et al, 2002). In common with JNK-induced apoptosis in other cell types, apoptosis in hair cells is due to JNK-induced mitochondrial release of cytochrome c leading to apoptosis without further gene expression (Tournier et al, 2000: Aoki et al, 2002), although other receptor mediated pathways involving JNK and requiring further gene expression are likely (Yang et al, 1997: Dickens et al, 1997). However, where the hair cells have been treated with JNK inhibitor during or after trauma, studies have shown that there is reduced hair cell loss as well as a reduction in hearing loss (Coleman et al, 2007: Eshraghi et al, 2007: Wang et al, 2007). Nevertheless, JNK inhibition is not always protective, even though the JNK-induced apoptosis pathway is activated in hair cells treated with the chemotherapeutic agent cisplatin, JNK inhibitors were shown to actually potentiate cisplatin oto-toxicity (Wang et al, 2004).

1.7 Aims

To assess the impact of protein kinase inhibitors on the morphology of immature mouse hair bundles by a variety of biochemical and microscopic techniques. All of the protein kinases screened are known to influence actin regulation in vivo, in a variety of cell types. Furthermore, as auditory hair cells have been shown to recover from limited mechanical or drug induced trauma, a second aim of this project is to look for any signs of hair bundle recovery in response to either protein kinase inhibitors or neomycin treatment.

Chapter 2

Materials and Methods

2.1 Dissection and preparation of mouse cochlear cultures

Cochlear cultures were prepared using methods described previously (Russell and Richardson 1987): CD1 (HaM/ICR) mice aged P1 to P2 were killed by cervical dislocation, and sterilised by immersion in 80% ethanol. After being separated from the body, the head was dissected mid-sagitally in Hepes-buffered (10 mM, pH 7.2) Hank's balanced salt solution (HBHBSS) (Invitrogen, Paisley, UK), and the brain removed. The cochlea was pinched off from the vestibular apparatus and placed in fresh HBHBSS, where the cochlear capsule was then removed to reveal the stria vascularis surrounding the cochlear duct. After removal of the stria vascularis, the sensory epithelium was divided into apical and basal coils by cutting at approximately 360° from the apex. Collagen coated coverslips were prepared by pipetting a drop of rat tail collagen Type 1 (BD Biosciences, Oxford, UK) onto 22 mm round coverslips, these were then exposed to ammonia vapour for 10 minutes in a fume cupboard. After 3 washes in autoclaved water, the coverslips were transferred to a Columbia staining jar containing 8 ml HBHBSS and 4 drops of foetal bovine serum (Biosera, Ringmer, UK).

Apical and basal coils were plated onto the coverslips and fed with three drops of medium (93% DMEM/F12 HAM [Sigma-Aldrich, Dorset, UK], 7% foetal bovine serum [Biosera, Ringmer, UK], 10 μg/ml ampicillin). After being sealed into Maximow slide assemblies with wax, coils were grown for 24 hours at 37°C.

2.2 Treating cochlear cultures with protein kinase inhibitors

Coverslips were removed from the Maximow slide assemblies, placed in 35 mm diameter plastic Petri dishes, washed once with HBHBSS and incubated with medium containing the appropriate protein kinase inhibitor at 37°C in a 5% CO_2, 95% air incubator. A list of the protein kinase inhibitors and the concentrations used are

provided in Table 2.1. Compounds were dissolved in dimethyl sulfoxide (DMSO) (Sigma-Aldrich, Dorset, UK) or water as stock concentrations. Equivalent volumes of DMSO or water were added to control culture medium.

Protein kinase inhibitors	**Target**	**Concentrations used**	**Time (hours)**
Akt Inhibitor IV	PKB (IC_{50} 625 nM)	1 μM	24
C3 transferase	Rho A, B, C	2 μg/ml, 4 μg/ml	6, 14
GSK-3 Inhibitor IX	GSK-3α/β (IC_{50} 5 nM)	50 nM, 100 nM	24
JNK Inhibitor I	c-Jun NH_2- terminal kinase (IC_{50} 1 μM)	5 μM	5, 14, 24, 48
JNK Inhibitor I negative control	--	5 μM	14, 24, 48
JNK Inhibitor II	c-Jun NH_2- terminal kinase (IC_{50} 40 nM)	50 μM	10, 24
JNK Inhibitor V	c-Jun NH_2- terminal kinase (IC_{50} 220 nM)	0.2 μM, 1 μM, 2 μM	24, 48
Staurosporine	PKC (IC_{50} 0.7 nM), MLCK (IC_{50} 1.3 nM), PKA (IC_{50} 7 nM), PKG (IC_{50} 8.5 nM). CaM kinase II (IC_{50} 20 nM).	1 nM, 2 nM, 5 nM, 10 nM	2, 2.5, 4, 5, 10, 14, 16, 22, 24, 48
Specific inhibitors of potential staurosporine targets	**Target**	**Concentrations used**	**Time (hours)**
Bisindolylmaleimide I (BIM I)	PKC_{α} (IC_{50} 0.008 μM), $PKC_{\beta I}$ (IC_{50} 0.018 μM), PKC_{δ} (IC_{50} 0.21 μM), PKC_{ε} (IC_{50} 0.132 μM), PKC ξ (IC_{50} 5.8 μM).	10 nM, 1 μM	24

Protein Kinase C_θ pseudosubstrate inhibitor, myristoylated: Myr-HQRRGAIKQ AKV HHVKC-NH_2	PKC_θ	1 μM, 10 μM, 40 μM	24
Rottlerin	PKC_δ (IC_{50} 3-6 μM), PKC_θ	1 μM, 2 μM, 5 μM	16, 24
ML-7	MLCK (K_i 300 nM)	1 μM, 10 μM, 50 μM	24, 48
H-89	PKA (K_i 48 nM)	10 μM, 100 μM	24
KT5823	PKG (K_i 234 nM)	1 μM, 5 μM, 10 μM	24
KN-93	CaM kinase II (K_i 370 nM)	5 μM, 50 μM	24

Table 2.1 Protein kinase inhibitors: cellular targets, $IC_{50,}$ concentrations used and time points. IC_{50} = concentration required to produce 50% inhibition, K_i = inhibitor concentration at which 50% inhibition is observed.

2.3 Treating cochlear cultures with neomycin

Coverslips were removed from the Maximow slide assemblies, placed in 35 mm diameter plastic Petri dishes, washed once with HBHBSS and incubated with medium containing the desired concentration of neomycin at 37°C in a 5% CO_2, 95% air incubator or at room temperature (~ 23°C). For experiments performed at room temperature, Leibovitz's L-15 (Invitrogen, Paisley, UK) medium was used.

2.4 Transfection of cochlear cultures by gene gun

2.4.1 Preparation of plasmid DNA-coated gold particle “bullets”

In order to adhere plasmid DNA to gold particles, spermidine solution was made as follows: fresh spermidine hydrochloride stock was made up with 31.75 mg spermidine hydrochloride (Sigma-Aldrich, Dorset, UK) in 250 µl of sterile water, and 5 µl of this

0.5 M spermidine hydrochloride solution was then added to 45 µl of sterile water to give a final concentration of 0.05 M spermidine hydrochloride. Gold particles (25 mg of 1 µm particles) (Biorad, Hemel Hempstead, UK) were added to 50 µl of the 0.05 M spermidine hydrochloride solution and vortexed, followed by brief sonication. EGFP-$PLC_{\delta 1}PH$ plasmid DNA (100 µg) was then added to the spermidine hydrochloride solution, which was subsequently vortexed for 5 seconds, immediately after which 50 µl of autoclaved 1 M $CaCl_2$ was added, the solution vortexed, and then left to stand for 10 minutes at room temperature. This solution was spun for 15 seconds, the supernatant discarded and the remaining pellet vortexed briefly. 1 ml of 100% ethanol was added to the vortexed pellet and spun for 15 seconds, after which the supernatant was discarded and the remaining suspension gently pipetted. This was repeated three times in total. The pellet was finally re-suspended in 200 µl of polyvinylpyrrolidone (PVP) solution. The PVP solution consisted of 10 mg of PVP (Biorad, Hemel Hempstead, UK) in 500 µl of 100% ethanol, with 35 µl of this solution added to 7 ml of 100% ethanol, giving a final PVP concentration of 0.02 mg/ml.

To create the gene gun bullets, Tefzel tubing (Biorad, Hemel Hempstead, UK) in the tubing preparation station Biolistic PDS-100/HE (Biorad, Hemel Hempstead, UK) was filled with the plasma DNA-coated gold particle solution via a syringe. After rotation of the tubing for 30 seconds, the interior of the tube was dried by N_2 flow for 5 minutes. The tubing was removed from the preparation station, cut into 13 mm lengths and stored at 4°C with silica crystals.

2.4.2 Gene gun transfection

Plasmid DNA bullets were loaded into the cartridge of the Helios gene gun system (Biorad, Hemel Hempstead, UK). Cochlear cultures were removed from Maximow slide

assemblies, placed on the gene gun stand and covered by a high pore-density cell culture insert (BD Biosciences, Oxford, UK). After positioning the cochlear culture beneath the gene gun muzzle, plasmid DNA was fired at the culture at 120 psi, following which the culture was removed to a 35 mm diameter plastic Petri dish with fresh media, examined under light microscopy for distribution of gold particles and then incubated at 37°C.

2.5 Annexin V detection of phosphatidylserine externalization

Coverslips with adherent cultures were transferred from the petri dish to a glass bottomed Perspex viewing chamber containing 0.5 ml HBHBSS. Alexa Fluor 488 annexin V (Invitrogen, Paisley, UK) was added to a dilution of 1:50. Cultures were viewed using a x63 water immersion lens and images were captured 5 minutes after the onset of annexin V labelling.

2.6 FM1-43 dye loading

Coverslips were removed from the petri dish and washed in a Columbia staining jar containing HBHBSS. After dipping in 3 μM FM1-43 (Molecular Probes, Paisley, UK) for 10 seconds, the coverslips were washed 3 times with fresh HBHBSS, placed in a glass bottomed Perspex viewing chamber containing 0.5 ml HBHBSS and examined under a x63 water immersion lens.

2.7 Fixing of cochlear cultures for fluorescent and confocal imaging

Cultures were washed with HBHBSS and fixed in 4% paraformaldehyde (Agar Scientific, Essex, UK) in 0.1 M sodium phosphate buffer (pH 7.3) for 30 minutes, then washed three times in phosphate buffered saline (PBS). Cultures were stained with a

1:1000 dilution of rhodamine conjugated phalloidin (Sigma-Aldrich, Dorset, UK) or a 1:300 dilution of Texas Red phalloidin (Invitrogen, Paisley, UK) in PBS with 10% inactivated horse serum and 0.1% Triton X-100 for 1.5 hours at room temperature. After staining, cultures were rinsed three times in PBS and mounted onto glass slides with Vectashield mounting medium (Vector Laboratories, Peterborough, UK).

2.8 Propidium iodide loading

Cochlear cultures were fixed as above, then incubated in 500 nM propidium iodide for 5 minutes before being mounted and examined under fluorescence microscopy.

2.9 Antibody staining of cochlear cultures

After fixation, the cultures were placed in PBS with 10% heat-inactivated horse serum and 0.1% Triton X-100. Antibody (see below) was added to the required concentration and cultures were incubated overnight at 4 °C with constant rotation. Following 3 washes with PBS, the cultures were then incubated with the secondary antibody (see below) diluted in PBS with 10% heat-inactivated horse serum and 0.1% Triton X-100 containing 1:1000 dilution of rhodamine conjugated phalloidin (Sigma-Aldrich, Dorset, UK) or 1:300 dilution Texas Red phalloidin (Invitrogen, Paisley, UK) for 2 hours at room temperature with rotation. Cultures were mounted as described above.

Primary antibodies were used as follows: rabbit anti-phospho-ezrin (Thr567)/radixin (Thr564)/moesin (Thr 558) (phos-ERM) (Cell Signalling Technologies, Massachusetts, US) at a 1:50 dilution, rabbit anti-radixin (Sigma-Aldrich, Dorset, UK) at a 1:100 dilution. Secondary antibodies were used as follows: Alexa Fluor® 488 F(ab')2 fragment of goat anti-rabbit IgG (H+L) (Invitrogen, Paisley, UK) at a 1:500 dilution, and polyclonal swine anti-rabbit immunoglobulins/FITC (DakoCytomation, Ely, UK) at a 1:100 dilution.

2.10 Scanning electron microscopy

Cultures were washed with HBHBSS and fixed in 2.5% glutaraldehyde (TAAB, Berkshire, UK) in 0.1 M sodium cacodylate buffer (pH 7.2) for 2 hours at room temperature, rinsed three times in 0.1 M sodium cacodylate buffer, and post-fixed with 0.1 M sodium cacodylate-buffered 1% osmium tetroxide (TAAB, Berkshire, UK) for 1 hour. Tissue pieces were finally washed twice in 0.1 M cacodylate buffer, once with water and then dehydrated through a series of ascending concentrations of ethanol (50%, 70%, 80 %, 90%) for a minimum of 10 minutes in each ethanol concentration. Tissue pieces were further dehydrated with three 100% ethanol washes of 20 minutes per wash, and one final 100% dehydration step was carried out overnight at 4 ºC. Samples were critical point dried, mounted on aluminium specimen stubs (TAAB, Berkshire, UK) and sputter coated with gold particles.

2.11 Transmission electron microscopy

Cultures were washed with HBHBSS and fixed with 2.5% glutaraldehyde (TAAB, Berkshire, UK) in 0.1 M sodium cacodylate buffer (pH 7.2) containing 1% tannic acid (TAAB, Berkshire, UK) for 2 hours at room temperature. After washing three times with 0.1 M sodium cacodylate buffer, the cultures were post-fixed with 0.1 M sodium cacodylate-buffered 1% osmium tetroxide (TAAB, Berkshire, UK) for 1 hour. Tissue pieces were finally washed twice in 0.1 M sodium cacodylate buffer and once with water. Dehydration of the tissue was carried out through a series of ascending concentrations of ethanol (50%, 70%, 80 %, 90% 100%), for a minimum of 5 minutes in each ethanol concentration. The tissue was further dehydrated twice in propylene oxide for a minimum of 10 minutes per wash, then transferred to a 1:1 propylene oxide: epoxy resin (TAAB 812 resin, dodecenyl succinic anhydride [DDSA], methyl nadic

anhydride [MNA], [2,4,6- Tri [Dimethylaminomethyl] phenol] [DMP-30]) (TAAB, Berkshire, UK) solution for one hour, before being transferred to a 1:3 propylene oxide: epoxy resin solution overnight. The tissues were then placed in 100% epoxy resin for a further 8 hours, and finally embedded in fresh pure resin in BEEM capsules (TAAB, Berkshire, UK). These resin-embedded samples were cured at 60°C for 24 hours. Ultrathin sections (100 and 150 nm thick) were cut using a Diatome diamond knife (TAAB, Berkshire, UK) on a Reichert Ultracut E microtome (Leica, Milton Keynes, UK) before being mounted on copper grids. Sections were stained with 1% aqueous uranyl acetate for 30 minutes, and then washed 3 times with water. Further staining was carried out according to Reynolds (1963). In brief, lead citrate solution was prepared with 45 μg/ml lead nitrate, 25 μg/ml trisodium citrate and 6 μg/ml sodium hydroxide, and used to stain grids for 8 minutes, after which the grids were washed 4 times with water and allowed to dry.

2.12 Labelling cochlear cultures with cationic ferritin

Coverslips with adherent cultures were removed from Maximow slide assemblies, placed in 35-mm diameter plastic Petri dishes, washed once with HBHBSS, and incubated with 10 nM staurosporine (InSolution™ Staurosporine, Calbiochem) for 4 hours at 37 ºC. The cultures were then chilled on ice before being washed 3 times with 2 ml of cold HEPES (10 mM, pH 7.0) buffered DMEM/F12 (serum free) (Sigma-Aldrich, Dorset, UK). Medium containing 1 mg/ml ferritin (Sigma-Aldrich, Dorset, UK) was then added and cultures were incubated on ice for 1 hour. After 3 further washes with 2 ml HEPES buffered serum-free DMEM/F12, the cultures were further incubated in 10 nM staurosporine for 4 hours, before being prepared for transmission electron microscopy as described above.

2.13 Toluidine blue dye staining

Cochlear cultures embedded in TAAB 812 resin (please see section 2.11 above) were cut at a thickness of 1 μm thin using glass knives on a Reichert Ultracut E microtome (Leica, Milton Keynes, UK). After being transferred to a glass slide, the sections were dried on a hotplate at 80˚C and then stained with Toluidine blue dye for approximately 30 seconds before the glass slide was removed from the hotplate and the sections washed with distilled water. Following further drying, the sections were mounted with Histomount (TAAB, Berkshire, UK).

2.14 Microscopy

A Zeiss Axioplan II microscope with AttoArc HBO 100W (Zeiss, Hertfordshire, UK) was used for light and fluorescence microscopy. Confocal images were obtained with a Zeiss LSM 510 confocal microscope (Zeiss, Hertfordshire, UK). Scanning electron microscopy was carried out with a Leica Leo S240 scanning electron microscope (Leica, Nussloch, Germany), and tissue prepared for transmission electron microscopy was viewed with a Hitachi 7100 transmission electron microscope (Hitachi, Tokyo, Japan). Images were routinely taken from the mid-point of the apical and basal coils.

2.15 Westerns blotting

2.15.1 Sodium Dodecyl Sulphate Polyacrylamide Gel Electrophoresis (SDS PAGE)

The resolving and stacking gels (Table 2.2 and Table 2.3) were prepared using the BioRad mini gel system (BioRad, Hertfordshire, UK). Protein samples were then mixed with an equal volume of 2x reducing sample buffer (10% glycerol, 3% SDS, 12.5% 4x stacking Tris buffer, 0.1 M DTT), boiled at 100°C for 5 minutes, spun to pellet any insoluble protein and loaded into the wells. Electrophoreses was carried out at 40 mA

(for two gels) for approximately 40 minutes and coloured markers were run alongside the samples in at least one lane in each gel.

2.15.2 Semi-dry Western Blotting and detection of proteins

The proteins separated by SDS-PAGE were subsequently transferred onto Amersham Hybond-P polyvinylidene difluoride (PVDF) protein transfer membranes (GE Healthcare, Bucks, UK) by the semi-dry blotting method. In brief, 3 sheets of Whatman 3MM filter paper (Whatman International Ltd, Kent, UK) were soaked in anode buffer 1 (300 mM Tris, 20% methanol, pH 10.4) and placed on the anode plate. On top of this were placed 2 sheets of filter paper soaked in anode buffer 2 (25 mM Tris, 20% methanol, pH 10.4). After wetting with methanol, a sheet of PVDF was added to the top of the filter papers. The resolving gel was placed on the PVDF and finally, 5 sheets of filter paper soaked in cathode buffer (25 mM Tris base, 40 mM 6-amino-n-hexanoic acid, 20% methanol, pH 9.4) were placed on top of the resolving gel. The transfer was carried out at 40 mA per gel for 45 minutes. After the transfer, the blot was placed in blocking buffer (tris buffered saline [TBS] with 3% skimmed milk powder and 0.05% polysorbate 20 [Tween-20]) with gentle shaking for one hour at room temperature. Primary antibodies were then added and left overnight on a shaker at room temperature. The primary antibody rabbit anti-phospho-ezrin (Thr567)/radixin (Thr564)/moesin (Thr558) (phos-ERM) (Cell Signalling Technologies, Massachusetts, US) was used at a dilution of 1:50 while rabbit anti-radixin (Sigma-Aldrich, Dorset, UK) was used at a dilution of 1:100. After washing with TBS buffer and TBS buffer containing 0.05% Tween-20, the probed membrane was incubated in alkaline phosphatase conjugated secondary antibody at 1:1000 dilution for one hour at room temperature. Following further washes with TBS buffer and TBS buffer containing 0.05% Tween-20, the

membrane was washed in alkaline phosphatase buffer (0.2 M $MgCl_2$, 0.1 M Tris pH 9.5 and 0.1 M NaCl) for 5 minutes. Finally the membrane was incubated in 20 ml of alkaline phosphatase buffer containing 20 µl of 5-bromo-4 chloro-3-indolyl phosphate (BCIP) and 20 µl of nitro-blue tetrazolium chloride (NBT) until the colour developed (~ 10 minutes). Washing the membrane several times with deionised water stopped the reaction and the membrane was dried on paper towels.

Reagent	*10% gel (2 gels)*	*7.5% gel (2 gels)*
Acrylamide (30% acrylamide, 0.8% bis-acrylamide)	2.66 ml	2 ml
4x Resolving gel buffer (18.2 g Trizma base, 400 mg SDS, pH 8.6)	2 ml	2 ml
Ammonium persulphate (5 mg/ml)	0.8 ml	0.8 ml
Distilled water	2.54 ml	3.2 ml
TEMED	10 µl	10 µl

Table 2.2 Resolving gel composition

Reagent	*For 2 gels*
Acrylamide	0.4 ml
Distilled water	2.2 ml
Ammonium persulphate (5 mg/ml)	0.4 ml
4x stacking Tris buffer (6.65 g Trizma base, 400 mg SDS, pH 8.6)	1 ml
TEMED	10 µl

Table 2.3 Stacking gel composition

2.15.3 Gel densitometry

PVDF membranes were scanned using an Epson 1600 Pro scanner, and the grey-scale values were measured using ImageJ software. SPSS 16.0 software was used to check normality of distribution using the Kolmogorov-Smirnov test, and Excel software was used to calculate p values using independent t-tests with equal variances not assumed. Excel software was also used to generate histograms from the grey-scale values and to calculate mean and standard deviation.

Chapter 3

Results

3.1 Inhibitors of c-Jun N-terminal kinase have different effects on hair bundle structure.

c-Jun N-terminal kinase (JNK) is a member of the mitogen-activated protein kinase (MAPK) family, and is activated by stimuli that cause cell stress, such as ischemia (Rincón and Davis, 2009). One result of JNK activation is apoptotic cell death. The three JNK inhibitors (JNK inhibitor I, JNK inhibitor II, JNK inhibitor V) used in the screen inhibit all known isoforms of JNK.

Application of 5 μM JNK inhibitor I (IC_{50} 1 μM) for 24 hours caused the elongation and collapse of inner hair cell (IHC) stereocilia (Figure 3.1 A) and disrupted a number of outer hair cell (OHC) hair bundles (Figure 3.1 A, arrows) in apical coils. In the basal coils, damage was more severe, with hair bundles being lost from both the IHCs and OHCs, and remaining stereocilia showing elongation and collapse (Figure 3.1 B). JNK inhibitor II (IC_{50} 40 nM) at a concentration of 50 μM and JNK inhibitor V (IC_{50} 220 nM) at a concentration of 2 μM had no effect on hair bundle morphology when applied for a 24-hour period under the same conditions (Figure 3.1 C, D, E, F).

3.1.1 The effects of other protein kinase inhibitors range from no effect to hair cell death.

Glycogen synthase kinase-3 (GSK-3) is an enzyme involved in a large number of diverse signalling pathways, notably the Wnt signalling pathway that determines cell fate in embryonic development, the insulin signalling pathway and the neurotrophic pathways (Gould and Manji, 2005). At a concentration of 100 nM, GSK-3 inhibitor (IC_{50} 5 nM) had no effect on hair bundle morphology in either apical or basal coils (Figure 3.2 A, B) when applied for a 24-hour period.

Akt (PKB) is another signalling protein that responds to a wide variety of signals and, as a consequence, is involved in many processes such as the regulation of metabolism, cell motility and cell-cycle progression (Fayard et al, 2005). A PKB inhibitor, Akt inhibitor IV (IC_{50} 625 nM), was used at a concentration of 1 μM for 24 hours, and caused severe disruption to the organ of Corti (Figure 3.2 C, D), many hair bundles in the apical coil were lost, and where hair bundles remained, stereocilia had collapsed haphazardly (Figure 3.2 C). In the basal coil, mainly OHC hair bundles were lost, but where hair bundles remained, both IHC and OHC bundles were intact (Figure 3.2 D).

The Rho family of proteins consists of small GTPases, which, once activated, bind to a range of effectors to stimulate signalling downstream (Buchsbaum, 2007). Rho is involved in a wide variety of cellular processes including membrane trafficking, microtubule stability and actin polymerisation (Schwartz, 2004). Cochlear cultures were incubated with 2 mg/ml of C3 Transferase, a Rho A, B and C inhibitor, for 16 hours. C3 Transferase showed an indirect effect on hair bundles, localised expansion of the luminal surface of the organ of Corti pushed hair bundles out of their normally rigid arrangement (Figure 3.2 E, F, arrowheads). Additionally, C3 Transferase also caused expansion of the apical surfaces of individual hair cells (Figure 3.2 E, F, arrows). Gross hair bundle morphology was, however, unaffected.

Staurosporine, a broad-spectrum protein kinase inhibitor, has been used in many studies as either an inhibitor of protein kinase C or as an inducer of apoptosis (Sakamoto et al, 1998: Mookherjee et al, 2007: Pérez et al, 2006). At a concentration of 5 nM for 24 hours, staurosporine caused a consistent “rounding up” of all apical coil OHC hair bundles and the frequent elongation of IHC stereocilia with associated collapse (Figure 3.2 G). In the basal coil, the morphological effect of staurosporine on IHC stereocilia was less evident, but OHC stereocilial collapse was uniform (Figure 3.2 H).

Controls from apical and basal coils that had been incubated for 24 hours in medium containing 0.1% DMSO (Figure 3.3 A, B) or 0.1% water (Figure 3.3 C, D) showed normal hair bundle morphology.

3.1.2 Staurosporine causes hair bundle collapse, but specific inhibitors of potential staurosporine targets do not have a similar effect.

To assess which protein kinases staurosporine were targeting to cause the effects seen in Figure 3.2 G & H, individual inhibitors against known staurosporine targets (CaM kinase II, myosin light chain kinase, PKA, PKC, PKG) were used to treat cochlear cultures: inhibitors of Cam kinase II (5 μM of KN 93, K_i 370 nM), myosin light chain kinase (10 μM of ML 7, K_i 300 nM), $PKC_{\alpha/\beta I/\delta/\varepsilon}$ (1 μM of BIM I: PKC_α IC_{50} 0.008 μM, $PKC_{\beta I}$ IC_{50} 0.018 μM, PKC_δ IC_{50} 0.21 μM, PKC_ε IC_{50} 0.132 μM, PKC_ξ IC_{50} 5.8 μM), and PKG (10 μM of KT5823, K_i 234 nM) had no effect on hair bundle morphology when applied for a 24-hour period (Figure 3.4 A to H). Inhibition of PKA (10 μM of H89, K_i 48 nM) led to disruption of hair bundles in the apical coil, possibly due to the enlargement of the apical surfaces of both the inner and outer hair cells (Figure 3.5 A). Basal coils were unaffected by H89 treatment (Figure 3.5 B). A cocktail of these individual inhibitors (CaM kinase II, myosin light chain kinase, PKA, PKC, PKG) was also used to treat cochlear cultures, but staurosporine-like effects on hair bundles were not observed (results not shown).

Other PKC isoforms were inhibited using the PKC_θ inhibitor Myr-HQRRGAIKQ AKVHHVKC-NH_2 and Rottlerin, an inhibitor of $PKC_{\delta\,\&\,\theta}$ isoforms (IC_{50} 3-6 μM). At a concentration of 40 μM, Myr-HQRRGAIKQ AKVHHVKC-NH_2 caused the loss of some hair bundles of the inner and outer hair cells in apical coils after 24 hours, although bundles that remained were of normal appearance (Figure 3.5 C).

In the basal coils, the loss of hair bundles was more severe and few OHC hair bundles remained (Figure 3.5 D). After 24 hours, 5 μM Rottlerin caused loss of OHC hair bundles in apical coils, as well as loss of IHC and OHC hair bundles in basal coils (Figure 3.5 F). Where the OHCs of the apical and basal coils survived, the remaining hair bundles appeared to be shorter than the equivalent hair bundles in the 0.1% DMSO controls (Figure 3.5 I, J).

Hence the specific inhibitors of potential staurosporine targets either caused no damage to hair cells and hair bundles, or the damage caused did not resemble the type or pattern of damage caused by staurosporine, as was the case with PKA, Myr-HQRRGAIKQ AKVHHVKC-NH_2 and Rottlerin.

3.2 Staurosporine and JNK inhibitor I

Of the protein kinase inhibitors tested in the initial screen, staurosporine was chosen for further study as it had a uniform detrimental effect on hair bundles in both apical and basal coils without apparently causing hair cell death. In dose response experiments, a concentration of staurosporine as low as 2 nM was sufficient to cause hair bundle collapse after 24 hours (Figure 3.6 E, F), however, this was not always repeatable, hence staurosporine concentrations of either 5 or 10 nM were used in this set of experiments. JNK inhibitor I was also of particular interest due to studies showing the oto-protective potential of c-Jun N-terminal kinase inhibition in preventing auditory hair cell apoptosis after drug or noise induced trauma (Wang et al, 2003: Coleman et al, 2007). Therefore in order to gain further insight into the possible mechanism of hair bundle damage caused by staurosporine and JNK inhibitor I, cochlear cultures treated with these inhibitors were further examined by confocal, transmission and scanning electron microscopy.

3.2.1 Effects of staurosporine can be first seen by 5 hours

Hair bundles were unaffected by 2.5 hours of 5 nM staurosporine treatment, but by 5 hours, basal coil hair bundle collapse was seen using confocal microscopy (Figure 3.7 D). In order to examine the effects of staurosporine on hair-cell surface morphology in more detail, SEM analysis was used. Figure 3.8 shows cochlear cultures treated with 10 nM staurosporine for 14 hours, apical coil OHC hair bundles have collapsed inwards (Figure 3.8 A, C), while the hair bundles of basal coil OHCs have collapsed outwards (Figure 3.8 B, D), with the apical surfaces of the hair cells apparently reabsorbing hair bundles (Figure 3.8 D, arrows). There is also a marked decrease in the amount of supporting cell microvilli in the basal coil (Figure 3.8 B, arrows) in comparison to controls (Figure 3.8 F).

Using transmission electron microscopy, clusters of vesicles were visible that had accumulated at the base of the hair bundles after 5 hours of 5 nM staurosporine treatment (Figure 3.9 A, B, arrows). Similar clusters were not observed in the controls (Figure 3.9 E, F). At 10 hours, apical coil IHC hair bundles remained unaffected by staurosporine treatment; however, there is a separation of the cuticular plate from the overlying plasma membrane (Figure 3.9 C, double arrows). Basal coil IHC hair bundles showed collapse by 10 hours, some possibly having decoupled from their rootlets (Figure 3.9 D, arrow), whilst other stereocilia retained largely intact rootlets (Figure 3.9 D, arrowhead). The separation of the cuticular plate from the overlying plasma membrane seen in IHCs at 10 hours were already present by 5 hours in apical coil OHCs (Figure 3.10 A, double-headed arrows), as were accumulations of vesicles (Figure 3.10 A, single arrows). In basal coil OHCs at 5 hours, the plasma membranes were bulging and contained a large number of vesicles (Figure 3.10 B), with possible separation of stereocilia from their rootlets (Figure 3.10 B, arrow). By 10 hours, the area

that separated the cuticular plate and the plasma membrane had increased in size, and caused the elevation of hair bundles away from the cuticular plate (Figure 3.10 C, double arrow). In the basal coils, OHC hair bundles had collapsed completely by 10 hours (Figure 3.10 D, arrowheads), leaving rootlets in the cuticular plate (Figure 3.10 D, single arrows). Material accumulated between the cuticular plate and the plasma membrane is indicated by the double-headed arrow (Figure 3.10 D).

3.2.2 JNK inhibitor I shows a marked effect on hair bundles.

Scanning electron microscopy showed that at 14 hours, many hair bundles of the apical coil OHCs were intact and normal (Figure 3.11 A, arrowheads). In among these apparently undamaged hair bundles though, many OHC hair bundles had collapsed and individual stereocilia showed elongation (Figure 3.11 A, C, arrows). Some basal coil OHC stereocilia also showed elongation (Figure 3.11 D, arrowhead), but in contrast to the apical coil, OHC hair bundles in the basal coil had uniformly collapsed (Figure 3.11 B, D, arrows).

JNK inhibitor I caused collapse of apical and basal coil IHC stereocilia by as early as 5 hours (Figure 3.12 A, B), and by 10 hours collapsed stereocilia were in the process of being reabsorbed back into the hair cell (Figure 3.12 C, D, arrows). Basal coil OHC hair bundles had also been damaged by 5 hours (Figure 3.13 B), and by 10 hours, hair cells had died (Figure 3.13 D). In contrast, apical coil OHC hair bundles had not collapsed at 5 hours (Figure 3.13 A) and this remained the case at 10 hours, although there was some disruption of the cell membrane at the base of hair bundles (Figure 3.13 C, arrow). In both apical and basal coils, treatment with JNK inhibitor I resulted in much membrane debris seen above the hair bundles (Figure 3.12 A to C and 3.13 A to C).

3.2.3 At 8 hours, externalisation of phosphatidylserine was detected in JNK inhibitor I, but not staurosporine, treated cultures.

The translocation of phosphatidylserine from the inner leaflet to the outer leaflet of the plasma membrane can be one of the first signs of apoptosis. To ascertain whether JNK inhibitor I and staurosporine cause apoptosis in hair cells, cochlear cultures were treated with either 5 μM JNK inhibitor I or 10 nM staurosporine for 8 hours before labelling with Alexa Fluor 488 annexin V.

Annexin V labelling was observed in both apical (Figure 3.14 C) and basal (Figure 3.14 D) coils that had been treated with JNK inhibitor I, but not for either the apical (Figure 3.14 G) or basal (Figure 3.14 H) coils of staurosporine treated cultures. Over a longer period of 48 hours, toluidine blue staining of resin embedded cultures showed that 5 μM JNK inhibitor I treated apical coils retained both inner and outer hair cells (Figure 3.15 A). In the basal coils, IHCs were present, but all three rows of OHCs were missing (Figure 3.15 B). At a concentration of 10 nM, staurosporine had no adverse effects on the survival of either inner or outer hair cells in the apical and basal coils at 48 hours (Figure 3.15 E, F).

3.2.4 JNK inhibitor I–induced phosphatidylserine externalisation is rapid and dose dependent.

To establish the concentration and length of JNK inhibitor I treatment needed to cause translocation of phosphatidylserine, dose response experiments were carried out using 1, 2 and 5 μM JNK inhibitor I for 5 minutes. A JNK inhibitor I concentration of 5 μM caused some phosphatidylserine externalisation in apical coils (Figure 3.16 C), with increased phosphatidylserine detection in the basal coils (Figure 3.16 D). A concentration of 2 μM JNK inhibitor I was also sufficient to cause occasional

phosphatidylserine externalisation in apical coils (Figure 3.16 G), with a greater amount detected in the basal coils (Figure 3.16 H). No labelling of phosphatidylserine occurred at 1 μM JNK inhibitor I for either apical (Figure 3.16 K) or basal (Figure 3.16 L) coils.

3.2.5 Staurosporine treatment does not block neomycin–induced phosphatidylserine externalisation.

The aminoglycoside antibiotic neomycin is known to induce phosphatidylserine externalisation in hair cells, and is thought to enter hair cells via their mechanotransducer channels (Gale et al, 2001: Marcotti et al, 2005: Goodyear et al, 2008). In order to assess how staurosporine-induced stereocilia collapse affects neomycin-induced phosphatidylserine externalisation, cochlear cultures were treated with neomycin in the presence of annexin V after 8 hours of treatment with 10 nM staurosporine. Despite the staurosporine-induced hair bundle disruption observed in the apical (Figure 3.17 A) and basal (Figure 3.17 B) coils, a robust neomycin–induced phosphatidylserine externalisation response was observed in both the apical and the basal coils (Figure 3.17 G, H).

The finding that staurosporine treatment does not eliminate mechanotransducer function is supported by the results of FM1-43 loading. FM1-43 is a styryl pyridinium dye that is lipophilic, non-toxic, and fluorescent when incorporated into the cell membrane. In the inner ear, FM1-43 has been shown to selectively label hair cells (Nishikawa and Sasaki, 1996: Meyer et al, 2001), although there was uncertainty as to whether FM1-43 enters via endocytosis or through the mechanically gated transduction channel situated on the tips of the stereocilia. More recent studies indicate that longer incubation times allows cell entry via endocytosis while shorter incubation times result in entry via the mechanotransduction channels (Gale et al, 2001: Griesinger et al, 2004: Kaneko et al,

2006: Meyers et al, 2003). Cochlear cultures treated with 10 nM staurosporine for 10 hours were exposed to 3 μM FM1-43 for 10 seconds. Both apical and basal coils (Figure 3.18 C, D) showed FM1-43 loading, but this was reduced in comparison to their 0.1% DMSO controls (Figure 3.18 E, F).

3.3 Effects of staurosporine and JNK inhibitor I treatment on the distribution of ezrin-radixin-moesin (ERM) proteins.

While both staurosporine and JNK inhibitor I treatment resulted in collapsed hair bundles, staurosporine treatment also caused a reduction in the number of microvilli on the apical surfaces of supporting cells (Figure 3.8 B) as well as a separation of the hair cell cell membrane from the cuticular plate (Figure 3.9 C, Figure 3.10 A-D). The separation of the plasma membrane from the cuticular plate is a feature similar to that seen in the OHCs of radixin deficient mice at P21 (Kitajiri et al, 2004). Therefore, the presence and distribution of radixin, as well as of phosphorylated ezrin-radixin-moesin (phos-ERM) were examined in staurosporine treated cochlear cultures by Western blotting and immunofluorescence microscopy.

JNK is one of the protein kinases potentially activated downstream of the small GTPases Rho, Rac and Cdc42 (Yamauchi et al, 2001: Potin et al, 2007), which are known to be major binding partners for ERM proteins (Hirao et al, 1996: Kotani et al, 1997: Matsui et al, 1998). More recently, JNK has also been suggested to have a role in the Rho associated kinase (ROCK)-ERM activation pathway during disassembly of epithelial junctions (Naydenov et al, 2009). Therefore, to assess whether JNK inhibition affected the presence and distribution of radixin and phos-ERM, JNK inhibitor I treated cochlear cultures were also examined by Western blotting and immunofluorescence microscopy.

3.3.1 Staurosporine treatment has no effect on the presence of radixin, but reduces the presence of phos-ERM in hair bundles.

After 16 hours of incubation in 5 nM staurosporine, radixin was still present in both apical coil and basal coil inner and outer hair bundles (Figure 3.19 A, E) as well as in the microvilli of supporting cells (Figure 3.19 A, E, arrows). The presence of radixin was also examined by Western blotting of cochlear cultures incubated with 10 nM staurosporine for 1, 2.5, 5, 10 and 14 hours. A representative Western blot for cochlear cultures treated with 14 hours of staurosporine and probed for radixin showed no difference between the staurosporine treated cultures and the 0.1% DMSO controls (Figure 3.20). In contrast to radixin, 14 hours of 10 nM staurosporine treatment resulted in greatly attenuated levels of phos-ERM in hair bundles for both apical and basal coils (Figure 3.21 B, H, arrows). Additionally, the presence of phos-ERM in the microvilli of supporting cells was also greatly attenuated (Figure 3.21 B, H, arrowheads). The presence of phos-ERM was also examined by Western blotting of cochlear cultures incubated with 10 nM staurosporine for 1, 2.5, 5, 10 and 14 hours. Figure 3.22 shows a representative Western blot for cochlear cultures treated with 14 hours of staurosporine and probed for phos-ERM, and illustrates a reduction of phos-ERM in staurosporine treated cultures in comparison to 0.1% DMSO controls.

Densitometric analysis of scanned PVDF membranes showed that the radixin grey-scale values of staurosporine treated cochlear cultures differed very little from the radixin grey-scale values of 0.1% DMSO control cultures over time (Figure 3.23, orange bars). This result was supported by statistical analysis of grey-scale values at 14 hours, which showed no significant difference ($p = 0.70$) between radixin values of staurosporine and DMSO treated cochlear cultures (Figure 3.23). For phos-ERM, densitometric analysis indicated a trend of decreasing grey-scale values against 0.1% DMSO over time, and

this was confirmed by statistical analysis at 14 hours which showed a significant reduction ($p = 0.04$) of phos-ERM levels in staurosporine treated cochlear cultures against 0.1% DMSO control values (Figure 3.23).

3.3.2 Staurosporine does not affect PIP_2 distribution in the hair bundle

A previous study suggested that levels of PIP_2 could be reduced in rat basophilic leukemia cells as a result of PKC inhibition by staurosporine (Apgar, 1995). Therefore in order to assess whether the attenuation of phos-ERM levels in staurosporine treated cochlear cultures was due to an adverse effect of staurosporine on the presence of PIP_2, cochlear cultures were transfected with the PIP_2 reporter $PLC_{\delta 1}PH$ by gene gun and treated with 10 nM staurosporine for 7 hours. The presence and distribution of PIP_2 in hair cells and hair bundles were unaffected by staurosporine treatment (Figure 3.24 B, H) when compared to 0.1% DMSO controls (Figure 3.24 E, K).

3.3.3 JNK inhibitor I treatment has no effect on the presence of either phos-ERM or radixin in hair bundles.

Where hair bundles remained after treatment with 5 μM JNK inhibitor I for 14 hours, phos-ERM was present in apical coil hair bundles (Figure 3.25 B, arrows). Anti-phos-ERM labelling of supporting cell microvilli was present in both apical and basal coils (Figure 3.25 B, H, arrowheads). Figure 3.26 shows a representative Western blot for cochlear cultures treated with 14 hours of 5 μM JNK inhibitor I and probed for phos-ERM and radixin. Densitometric analysis of scanned PVDF membranes showed that there were no significant differences between either radixin ($p = 0.77$) or phos-ERM ($p = 0.77$) grey-scale values against their 0.1% water controls (Figure 3.27).

3.4 Endocytosis is not adversely affected by staurosporine treatment.

Staurosporine treatment of cochlear cultures often resulted in the bulging of the hair cell apical membrane (Figure 3.10 B, C). To examine whether this bulging was caused by the expansion of the apical surface due to a failure in endocytosis, cochlear cultures were treated with 10 nM staurosporine for 4 hours at 37 ºC, incubated with cationic ferritin for one hour on ice and incubated for a further 4 hours at 37 ºC with staurosporine. Transmission electron micrographs showed that the areas beneath the bulging membrane contain endocytic vesicles encapsulating cationic ferritin (Figure 3.28 A, B, arrows), as well as vesicles without cationic ferritin (Figure 3.28 A, B, arrowheads). Transmission electron micrographs also showed vesicles containing cationic ferritin in the cuticular plates of hair cells in both apical and basal coils of 0.1% DMSO controls (Figure 3.28 C, D, arrows).

3.5 Hair bundle recovery

As it has been shown that auditory hair cells and hair bundles can recover from damage under certain conditions (Sobkowicz et al, 1995: Tsuprun et al, 2003: Goodyear et al, 2008), immature (P1-P2) mouse hair bundles were examined by fluorescent and scanning electron microscopy at various time points after brief treatment with either staurosporine or neomycin and assessed for signs of hair bundle recovery.

3.5.1 Staurosporine causes irreversible hair-bundle collapse as well as continued hair bundle degeneration even after short treatment duration.

Cochlear cultures were treated with 5 nM staurosporine for 14 hours and returned to fresh staurosporine-free media for a further 48 hours (Figure 3.29). OHC hair-bundle collapse seen at 14 hours (Figure 3.29 A, B) remained after 48 hours (Figure 3.29 C, D),

and IHC hair bundles, which showed little damage at 14 hours (Figure 3.29 A, B), had collapsed after 48 hours (Figure 3.29 C, D), indicating no recovery of normal hair bundle morphology for the hair bundles of either inner or outer hair cells.

Even where a short duration of 10 nM staurosporine treatment caused no visible hair bundle damage at an early time point of 2.5 hours (Figure 3.30 A, B), return to fresh staurosporine-free media for 7.5 hours resulted in collapse of OHC hair bundles from both apical and basal coils (Figure 3.30 C, D). Hair bundle deterioration continued though the 24-hour recovery period (Figure 3.30 E, F) and by 48 hours, some collapsed apical and basal coil OHC hair bundles also showed elongated stereocilia (Figure 3.30 G, H, arrows).

3.5.2 Hair cells show some recovery from blebbing caused by neomycin, but hair bundles do not recover from 1, 2 or 4 hours of neomycin treatment.

Using basal coil cochlear cultures, 1 hour of treatment with 1 mM neomycin at 23 °C caused blebbing on the surface of the hair cell (Figure 3.31 A). Some blebs appeared to be associated with the hair bundles (Figure 3.31 A, arrows), while others were not (Figure 3.31 A, arrowheads). When neomycin was removed after 1 hour and the cochlear cultures placed in neomycin-free media for a further 23 hours at 37 °C, blebbing had reduced, but many mid sections of the hair bundles were missing (Figure 3.31 B, arrows) and the density of supporting cell microvilli appeared reduced (Figure 3.31 B, arrowheads).

Cochlear cultures incubated for 2 hours with 1 mM neomycin at 23 °C showed some surface blebbing (Figure 3.32 A, arrows). After 22 hours recovery time in media at 37 °C, blebs and hair bundle degeneration remained visible (Figure 3.32 B, arrows).

Some hair cells also appeared to be in the process of being extruded (Figure 3.32 B, arrowheads).

After 4 hours of 1 mM neomycin incubation at 23 °C, there were a few hair bundles that appeared to be normal (Figure 3.33 A, arrows), but many showed signs of degeneration (Figure 3.33 A, right angle arrows). Numerous small blebs resided on the surface of the cochlear culture, but very large blebs were also present (Figure 3.33 A, arrowheads), and some cells were in the process of being extruded (Figure 3.33 A, bendy arrows).

After 20 hours recovery, intact IHC hair bundles were still visible (Figure 3.33 B, arrows). However, no OHC hair bundles were observed, and there was a band of debris above the position where the OHCs would normally be situated (Figure 3.33 B, arrowheads).

3.5.3 A lower concentration of 10 μM neomycin caused no hair bundle loss after 3 days, but hair bundles were eventually lost even after cessation of neomycin treatment.

In studies where neomycin has been used to cause damage or degeneration to mammalian auditory or vestibular hair cells, the typical concentration of neomycin used was 1 mM (Zine and de Ribaupierre, 1998: Quint et al, 1998: Gale et al, 2001). To assess the effect of a lower concentration of neomycin over a number of days, cochlear cultures were incubated with 10 μM neomycin for 72 hours at 37 °C.

When cochlear cultures were fixed and examined after 72 hours in neomycin, neither apical or basal coil hair bundles showed any sign of morphological damage (Figure 3.34 A, B). However, when neomycin was removed and the cochlear cultures were incubated in fresh neomycin-free media for a further 72 hours, both inner and outer hair cells of the apical coil showed disrupted hair bundles (Figure 3.34 C). In the basal coil, IHC hair

bundles were still intact, but no OHC hair bundles remained (Figure 3.34 D). As hair bundles were undamaged after 72 hours of incubation with neomycin, but were lost after a further 72 hours in neomycin-free medium, hair cell viability was assessed after 24 and 72 hours in 10 μM neomycin by dipping in propidium iodide. Propidium iodide (PI) is a nucleic acid stain that is impermeant and normally excluded from viable cells. After 24 hours neomycin treatment, hair cells remained impermeable to PI (Figure 3.35 C), but after 72 hours, there was clear PI uptake by the OHCs (Figure 3.35 D).

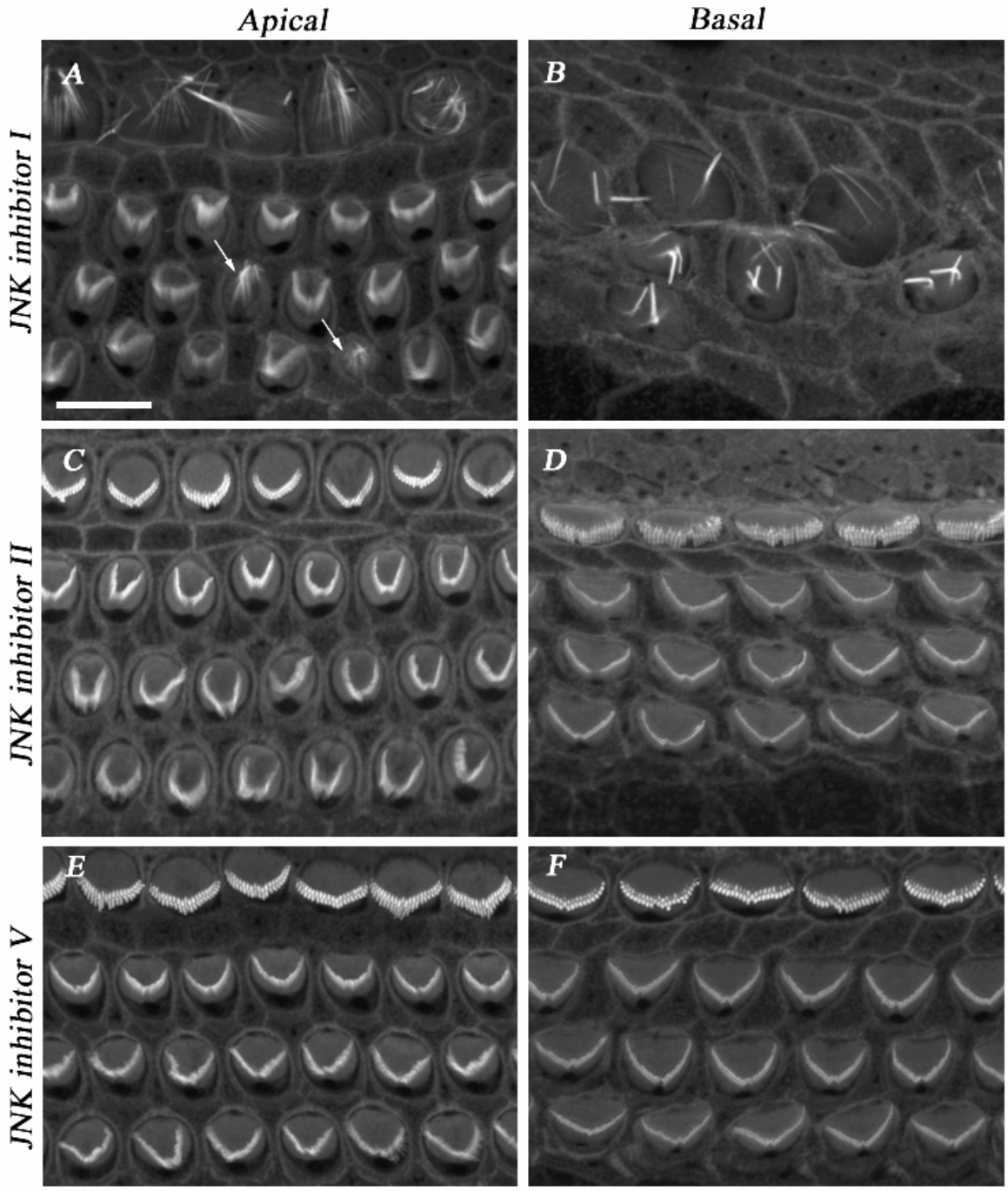

Figure 3.1 Confocal images of phalloidin stained cochlear cultures treated with JNK inhibitor I, JNK inhibitor II and JNK inhibitor V for 24 hours. Apical (A, C, E) and basal (B, D, F) coil cochlear cultures incubated with 5 μM JNK inhibitor I (A, B), 50 μM JNK inhibitor II (C, E), 2 μM JNK inhibitor V (E, F). Arrows indicate disruption to apical OHC hair bundles. Scale bar = 10 μm.

Figure 3.2 Confocal images of phalloidin stained cochlear cultures treated with protein kinase inhibitors. Apical (A, C, E, G) and basal (B, D, F, H) coil cochlear cultures incubated with 100 nM GSK 3 for 24 hours (A, B), 1μM Akt IV for 24 hours (C, D), 2 mg/ml C3 transferase for 16 hours (E, F) and 10 nM staurosporine for 24 hours (G, H). Arrows and arrowheads (E, F) indicate expanded apical surfaces of hair cells (arrows) and supporting cells (arrowheads). Scale bar = 10 μm.

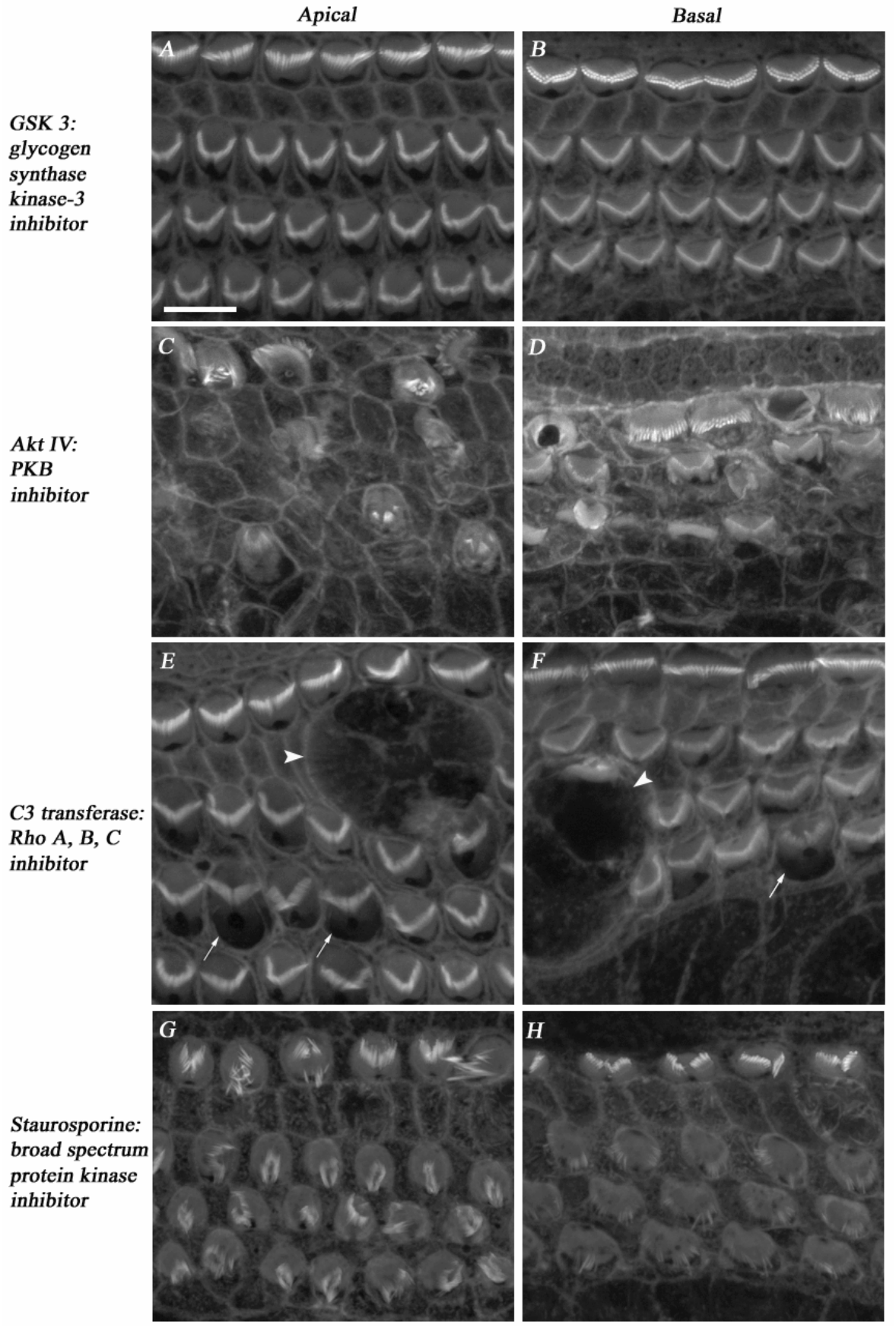
Apical
Basal
A
B
GSK 3:
glycogen
synthase
kinase-3
inhibitor
C
D
Akt IV:
PKB
inhibitor
E
F
C3 transferase:
Rho A, B, C
inhibitor
G
H
Staurosporine:
broad spectrum
protein kinase
inhibitor

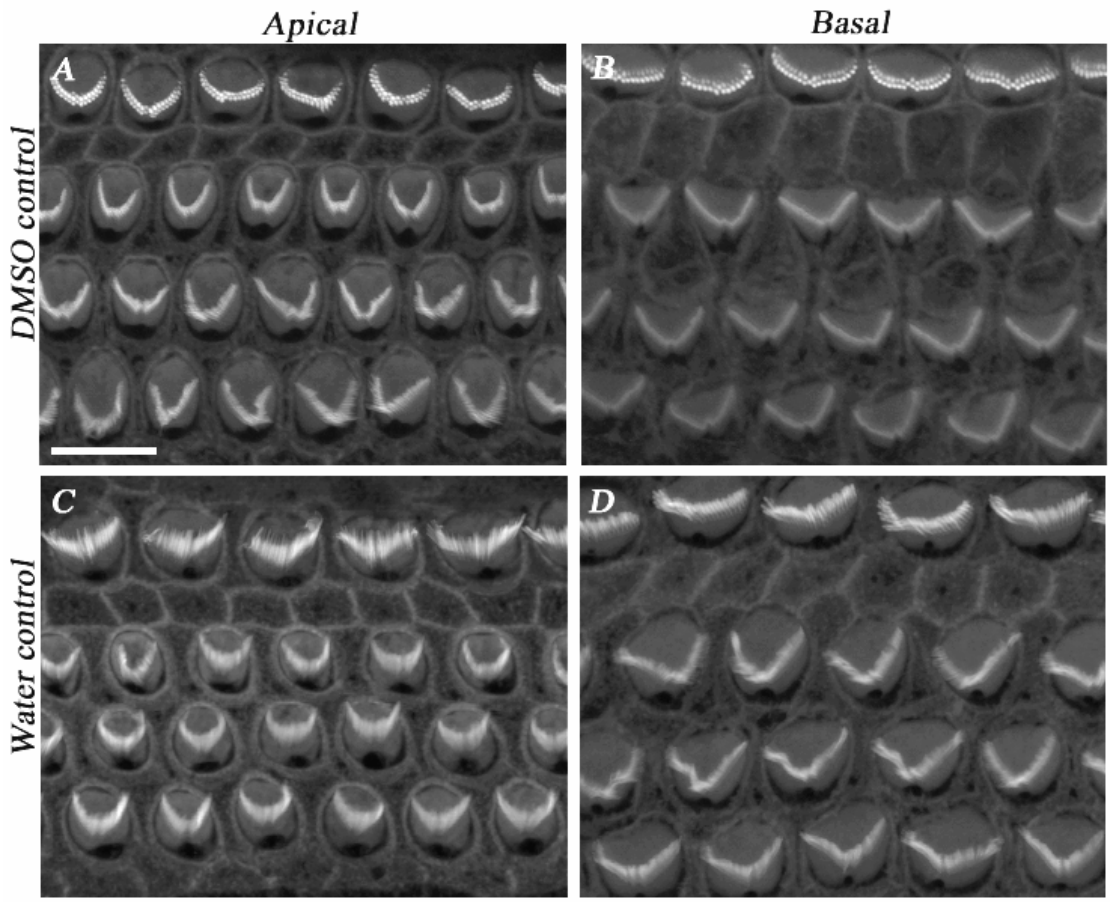

Figure 3.3 Confocal images of control phalloidin-stained cochlear cultures. Apical (A, C) and basal (B, D) region cochlear cultures incubated with medium containing 0.1% DMSO (A, B) or 0.1% water (C, D) for 24 hours. Scale bar = 10 μm.

Figure 3.4 Confocal images of phalloidin-stained cochlear cultures treated with specific inhibitors of potential staurosporine targets for 24 hours. Apical (A, C, E, G) and basal (B, D, F, H) coil cochlear cultures treated with 5 μM KN93 (A, B), 10 μM ML7 (C, D), 1 μM BIM I (E, F) and 10 μM KT5823 (G, H). Apical (I) and basal (J) coil cochlear cultures incubated with medium containing 0.1% DMSO as controls. Scale bar = 10 μm.

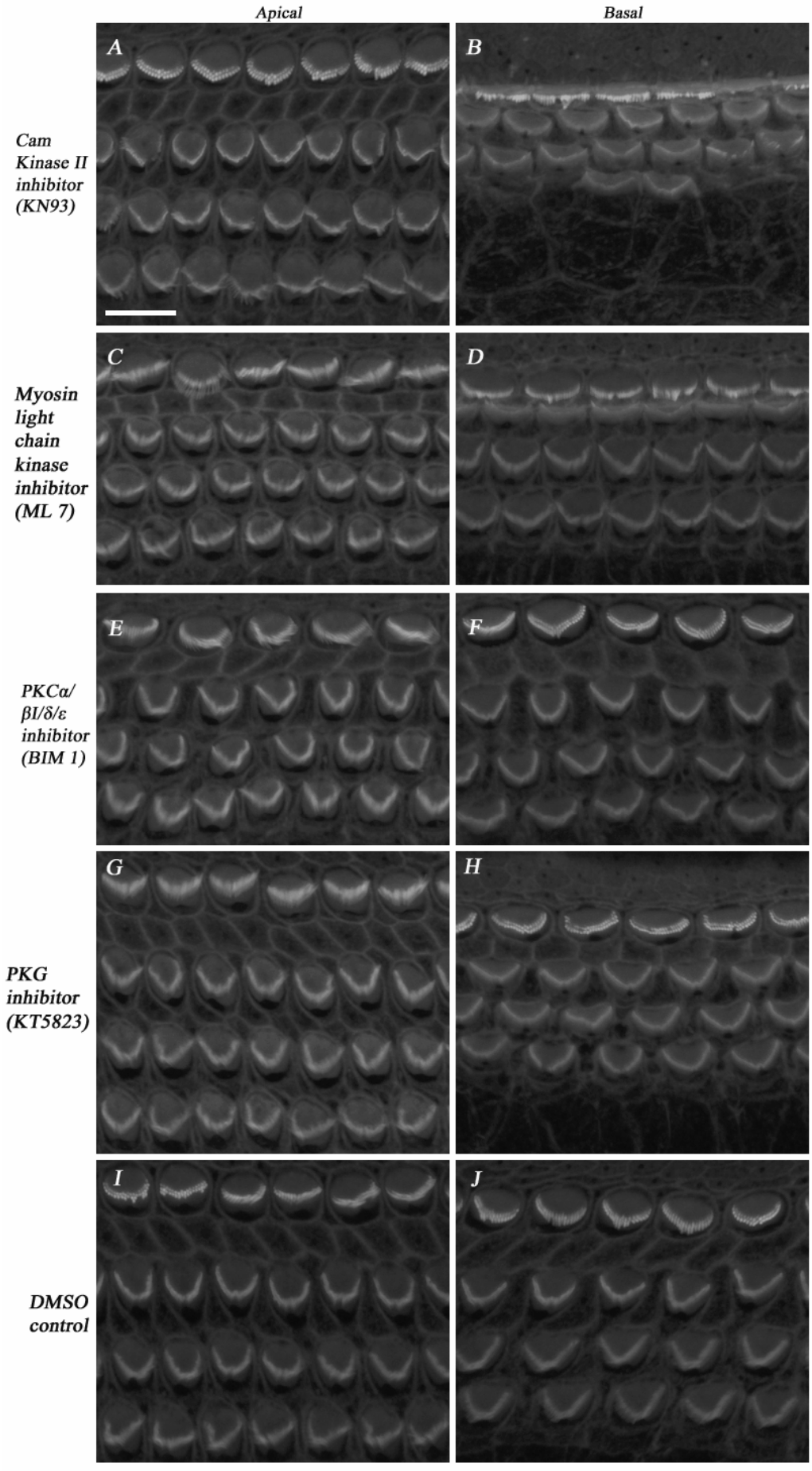
Apical
Basal
A
B
Cam Kinase II inhibitor (KN93)
C
D
Myosin light chain kinase inhibitor (ML 7)
E
F
PKCα/ βI/δ/ε inhibitor (BIM 1)
G
H
PKG inhibitor (KT5823)
I
J
DMSO control

Figure 3.5 Confocal images of phalloidin-stained cochlear cultures treated with potential PKC staurosporine targets for 24 hours. Apical (A, C, E) and basal (B, D, F) coil cochlear cultures incubated with 10 μM H89 (A, B), 40 μM PKC_{θ} inhibitor (Myr-HQRRGAIKQ AKV HHVKC-NH2) (C, D) and 5 μM Rottlerin (E, F). Apical (G, I) and basal (H, J) coil cochlear cultures incubated with medium containing 0.1% water (G, H) and 0.1% DMSO (I, J) as controls. Scale bar = 10 μm.

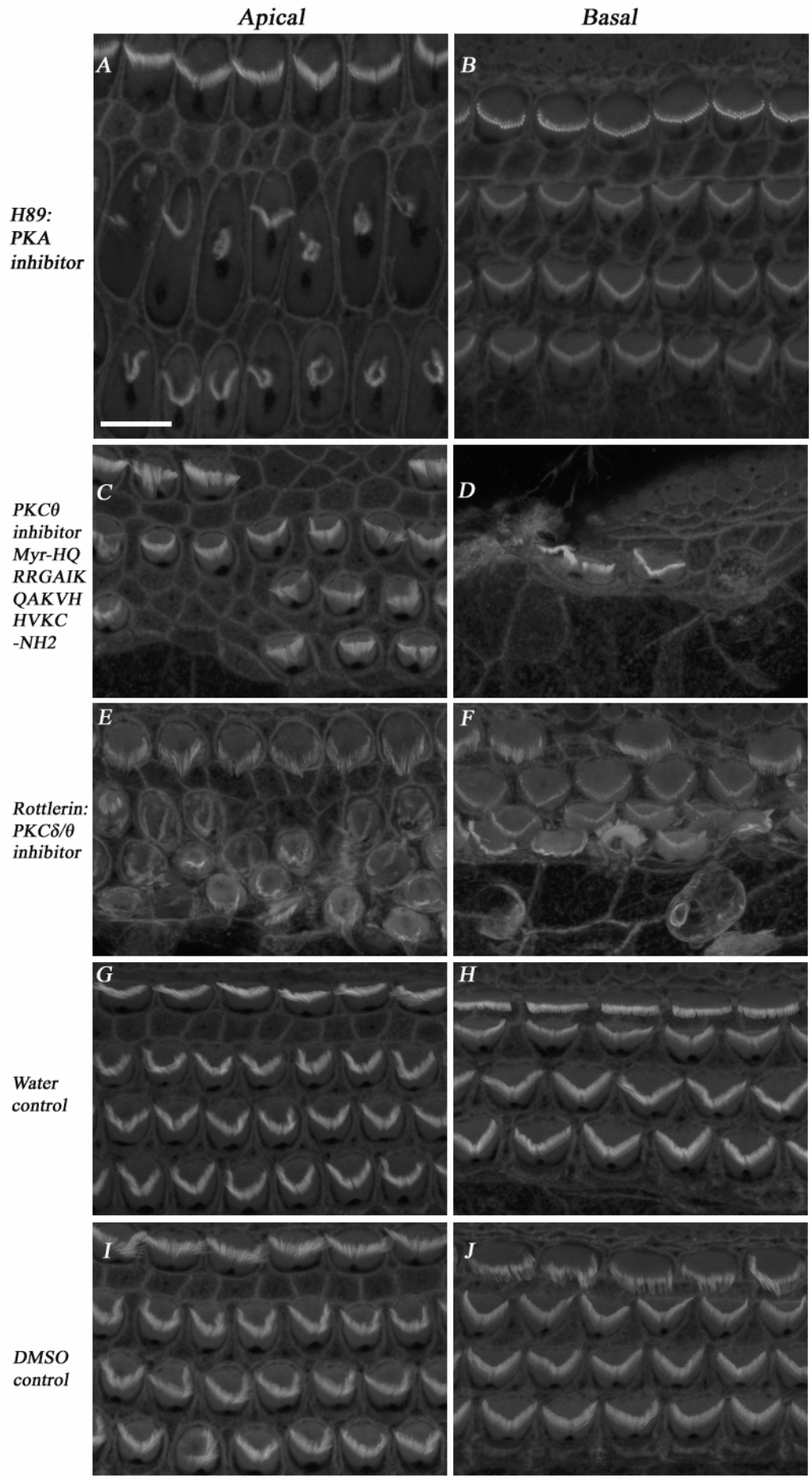
Apical
Basal
A
B
H89:
PKA
inhibitor
C
D
PKCθ
inhibitor
Myr-HQ
RRGAIK
QAKVH
HVKC
-NH2
E
F
Rottlerin:
PKCδ/θ
inhibitor
G
H
Water
control
I
J
DMSO
control

Figure 3.6 Confocal images of phalloidin-stained cochlear cultures treated with different staurosporine concentrations for 24 hours. Apical (A, C, E) and basal (B, D, F) coil cochlear cultures incubated with 10 nM staurosporine (A, B), 5 nM staurosporine (C, D), 2 nM staurosporine (E, F) for 24 hours. Apical (G) and basal (H) coil cochlear cultures incubated with medium containing 0.1% DMSO for 24 hours. Scale bar = 10 µm.

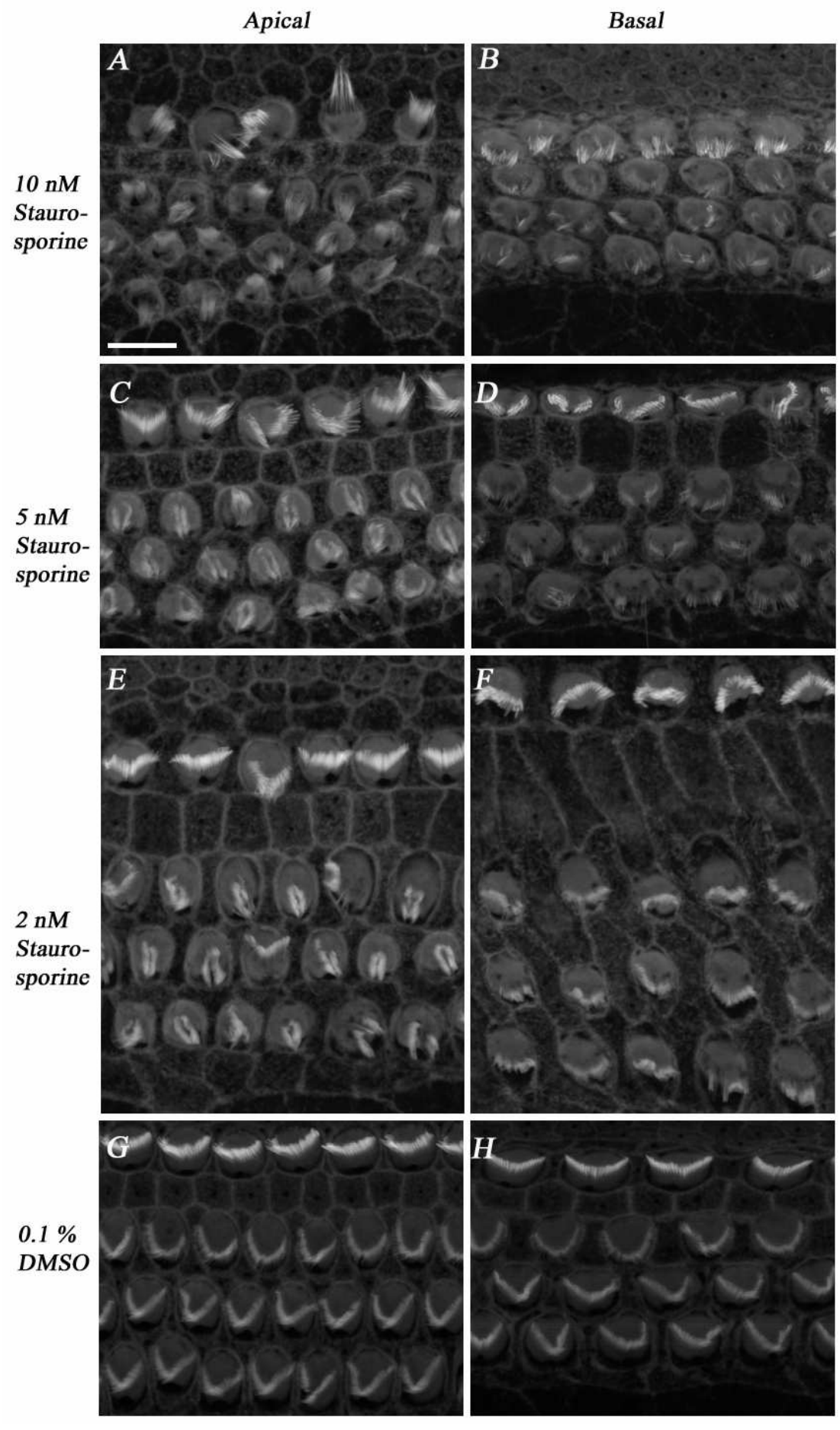
Apical
Basal
A
B
10 nM Staurosporine
C
D
5 nM Staurosporine
E
F
2 nM Staurosporine
G
H
0.1 % DMSO

Figure 3.7 Confocal images of phalloidin-stained cochlear cultures treated with 5 nM staurosporine for 2.5, 5 and 10 hours. Apical (A, C, E) and basal (B, D, F) coil cochlear cultures treated with 5 nM staurosporine for 2.5 hours (A, B), 5 hours (C, D) and 10 hours (E, F). Apical (G) and basal (H) coil cochlear cultures incubated with medium containing 0.1% DMSO for 10 hours. Scale bar = 10 µm.

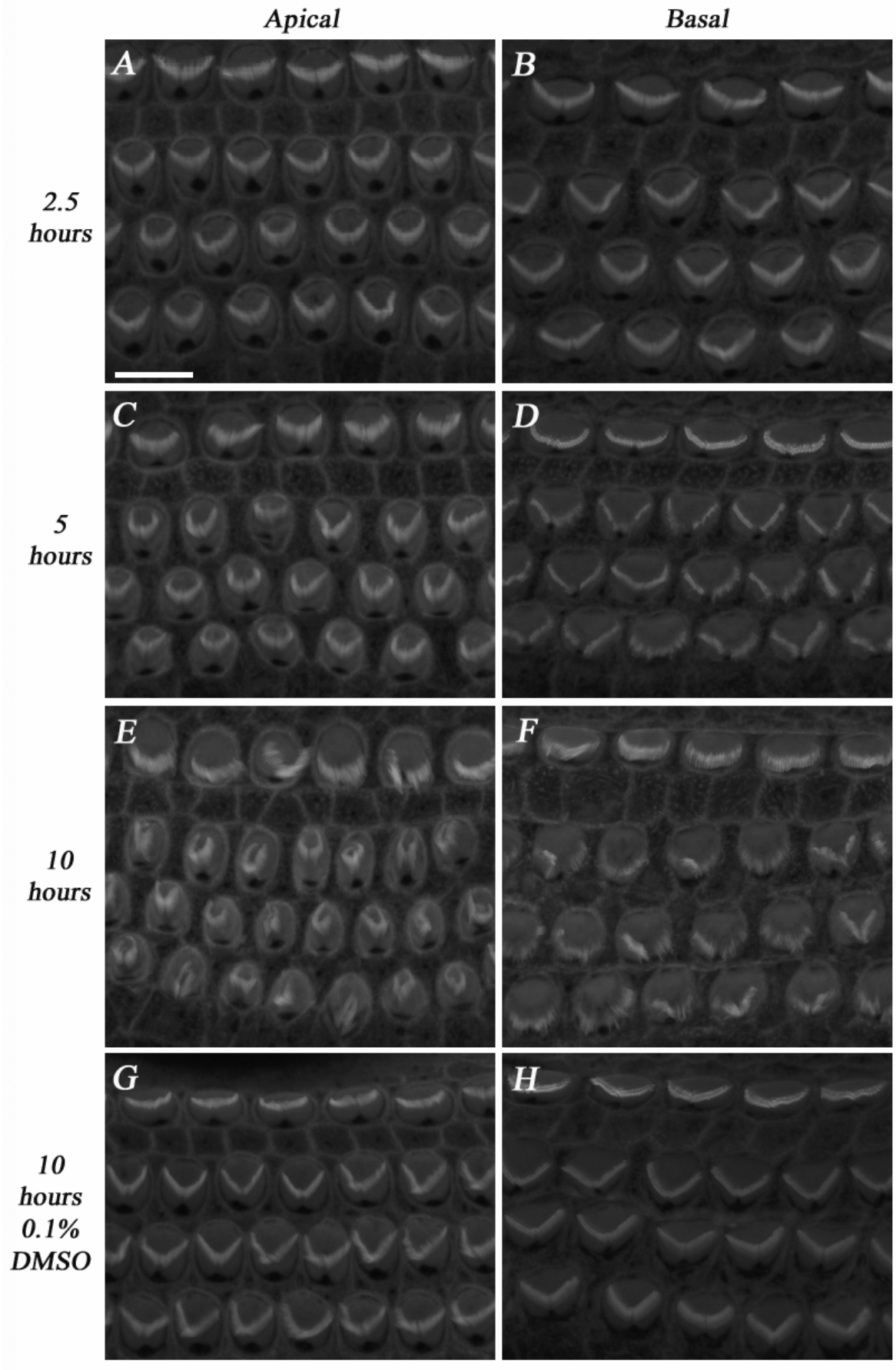
Apical
Basal
A
B
2.5 hours
C
D
5 hours
E
F
10 hours
G
H
10 hours 0.1% DMSO

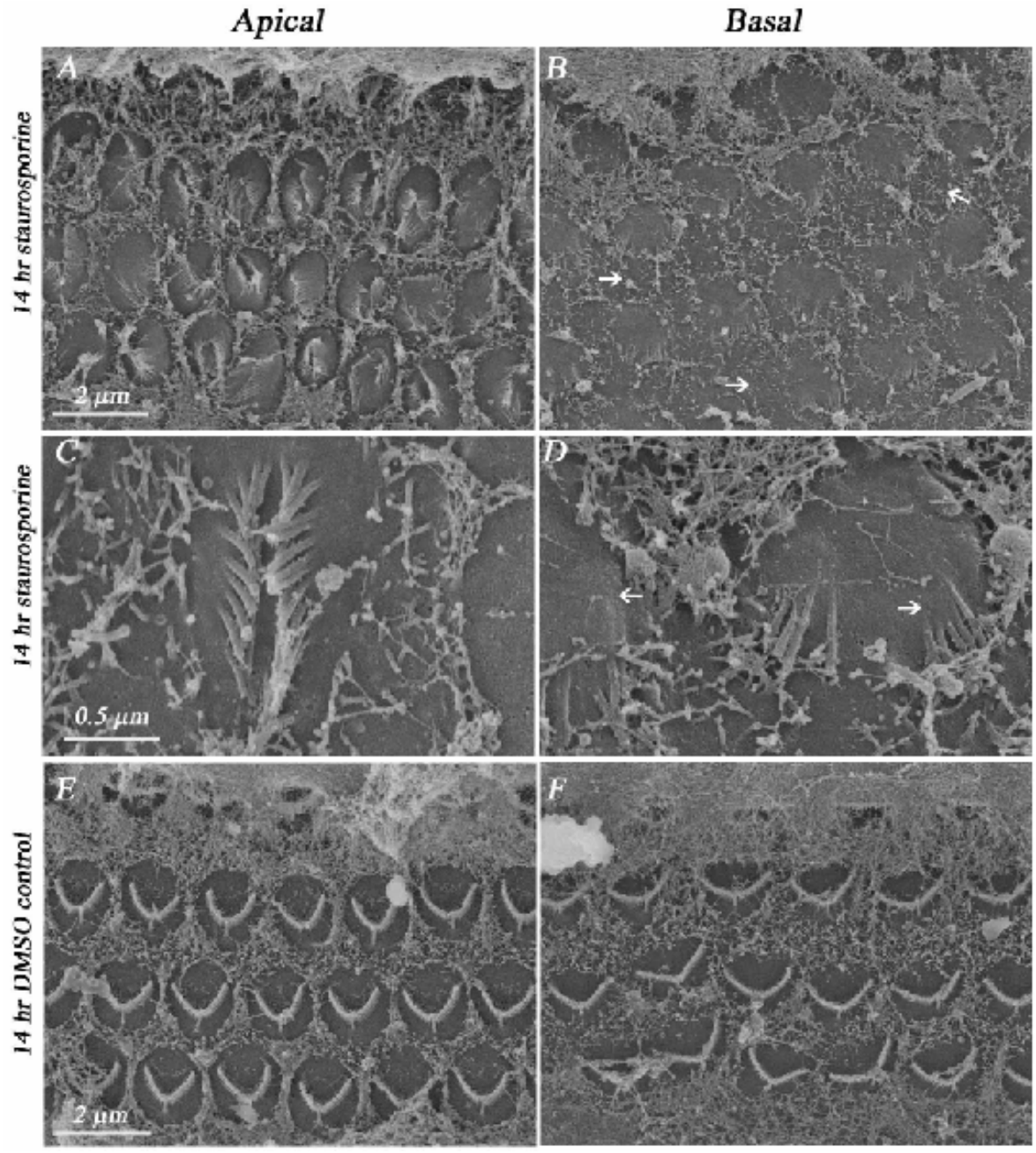

Figure 3.8 Scanning electron micrographs of P2 mouse auditory hair cells after treatment with 10 nM staurosporine for 14 hours. Apical (A, C, E) and basal coil (B, D, F) cochlear cultures treated with 10 nM staurosporine (A, B, C, D) and medium containing 0.1 % DMSO control (E, F). Staurosporine treated apical (C) and basal (D) coil outer hair cells shown at higher magnification. Panel B arrows indicates the paucity of supporting cell microvilli, and panel D arrows show hair bundle bases being reabsorbed back into hair cell apical surfaces. Scale bars = 0.5 µm, 2 µm.

Figure 3.9 Transmission electron micrographs of P2 mouse auditory inner hair cells after treatment with 5 nM staurosporine for 5 or 10 hours. Apical (A, C) coil inner hair cells treated with 5 nM staurosporine for 5 hours (A) or 10 hours (C). Basal (B, D) coil inner hair cells treated with 5 nM staurosporine for 5 hours (B) or 10 hours (D). Apical (E) and basal coil (F) inner hair cells incubated with medium containing 0.1% DMSO control for 10 hours. Panel A and B arrows indicate accumulation of vesicles. In panel C, double-headed arrows indicate a separation of the cuticular plate from the overlying plasma membrane and in panel D, the arrow shows an isolated rootlet, and the arrowhead shows an intact rootlet. Scale bar = 0.5 µm

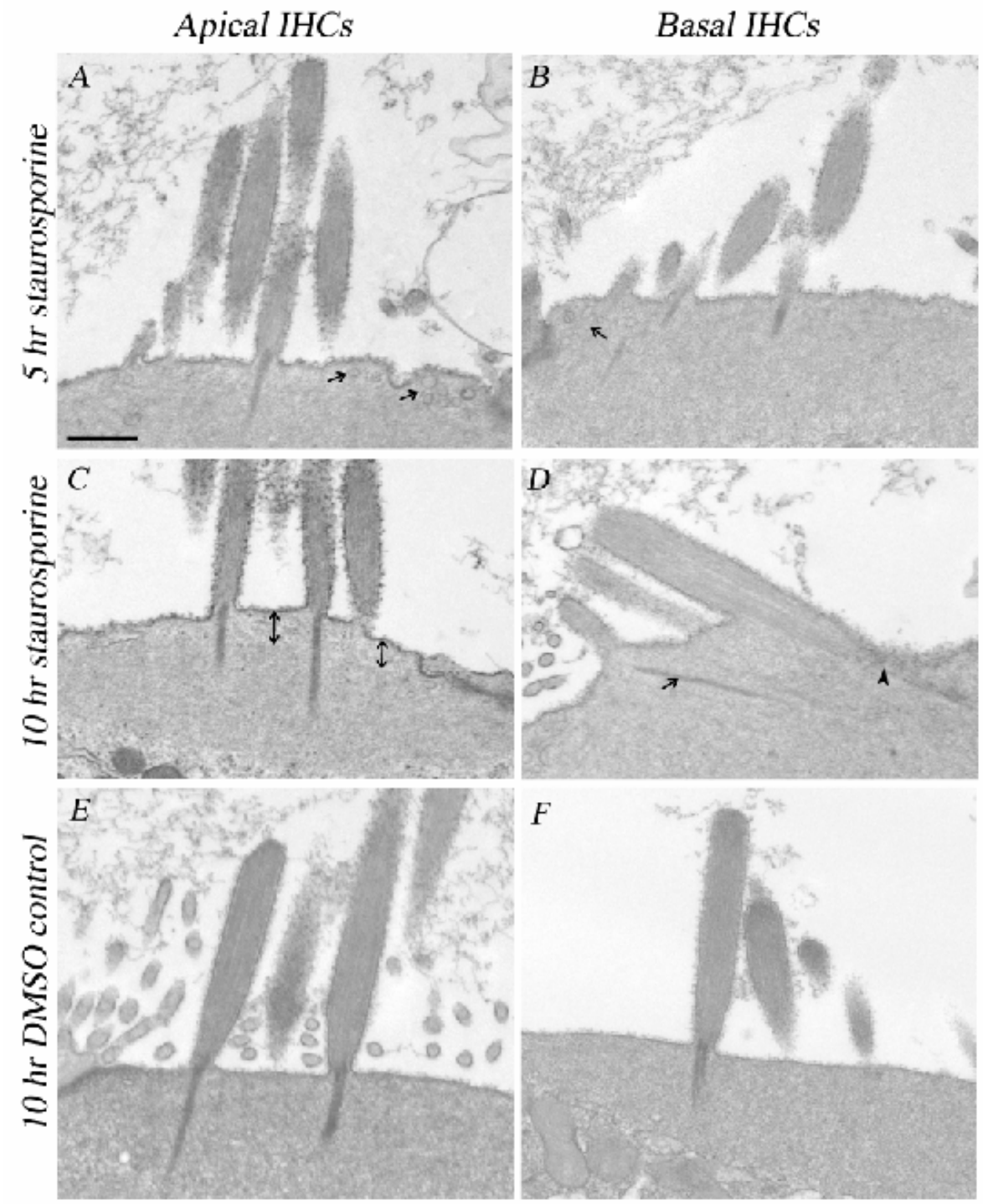
Apical IHCs
Basal IHCs
5 hr staurosporine
10 hr staurosporine
10 hr DMSO control
A
B
C
D
E
F

Figure 3.10 Transmission electron micrographs of P2 mouse auditory outer hair cells after treatment with 5 nM staurosporine for 5 or 10 hours. Apical (A, C) coil outer hair cells incubated with 5 nM staurosporine for 5 hours (A) and 10 hours (C). Basal (B, D) coil outer hair cells incubated with 5 nM staurosporine for 5 hours (B) and 10 hours (D). Apical (E) and basal coil (F) outer hair cells incubated with medium containing 0.1% DMSO control for 10 hours. Panel A, C and D double-headed arrows indicate a separation of the cuticular plate from the overlying plasma membrane, and panel A single arrows show vesicles in the cuticular plate. Panel B and D single arrows shows isolated rootlets. Panel D arrowheads indicate hair bundle collapse. Scale bar = 0.5 µm

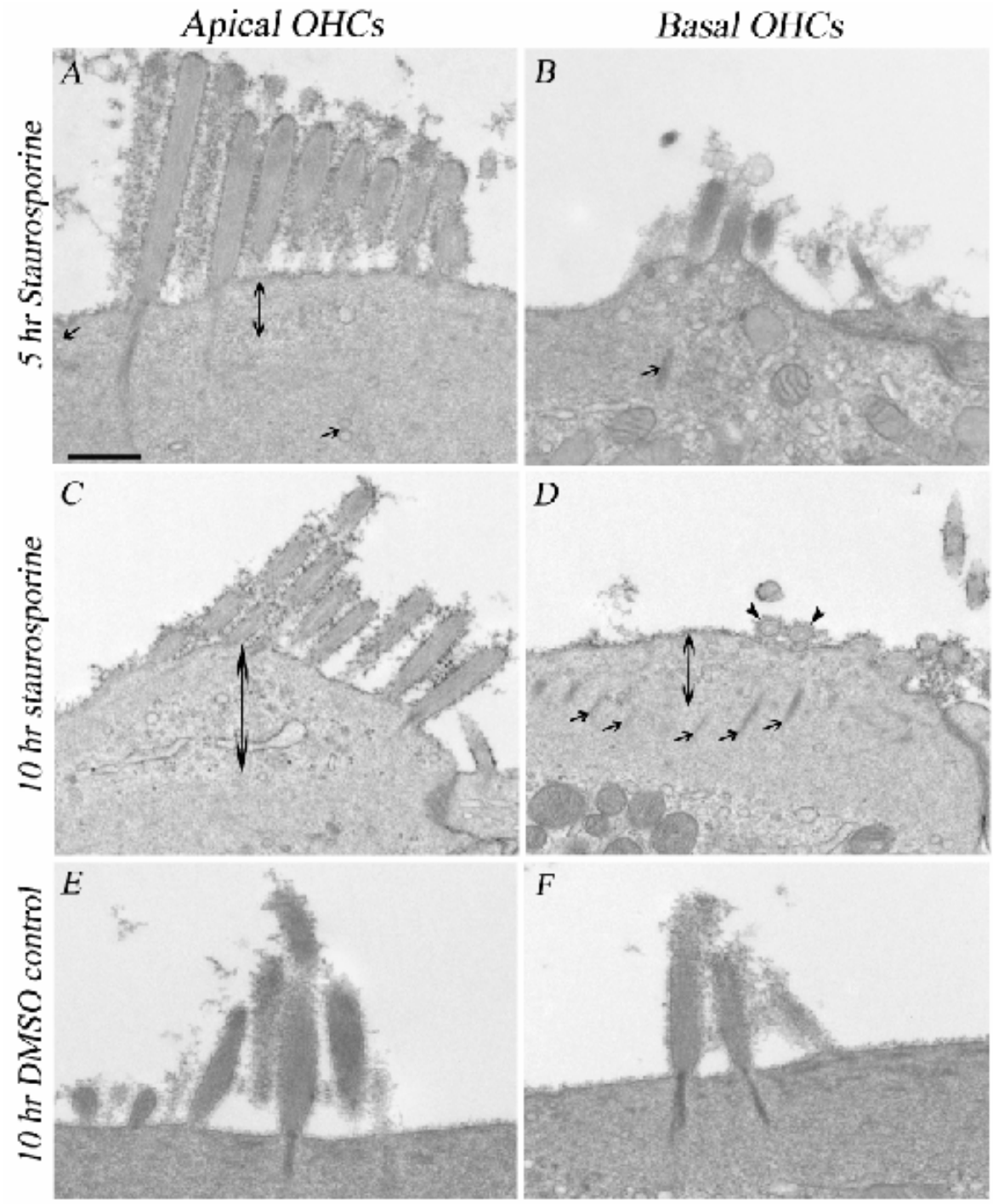
Apical OHCs
Basal OHCs
5 hr Staurosporine
10 hr staurosporine
10 hr DMSO control
A
B
C
D
E
F

Figure 3.11 Scanning electron micrographs illustrating the effect of JNK inhibitor I on mouse cochlear cultures at 14 hours. Apical (A, C, E) and basal coil (B, D, F) cochlear cultures incubated with 5 μM JNK inhibitor I (A, B, C, D) or in medium containing 0.1% JNK inhibitor I negative control (E, F). JNK inhibitor I treated apical (C) and basal (D) coil outer hair cells shown at higher magnification. Arrowheads in panel A indicate apparently normal hair bundles and arrows in panel A and C show hair bundle collapse and elongation. Arrows in panel B and D show hair-bundle collapse and arrowhead in panel D shows stereocilia elongation. Scale bars = 0.5 μm, 2 μm.

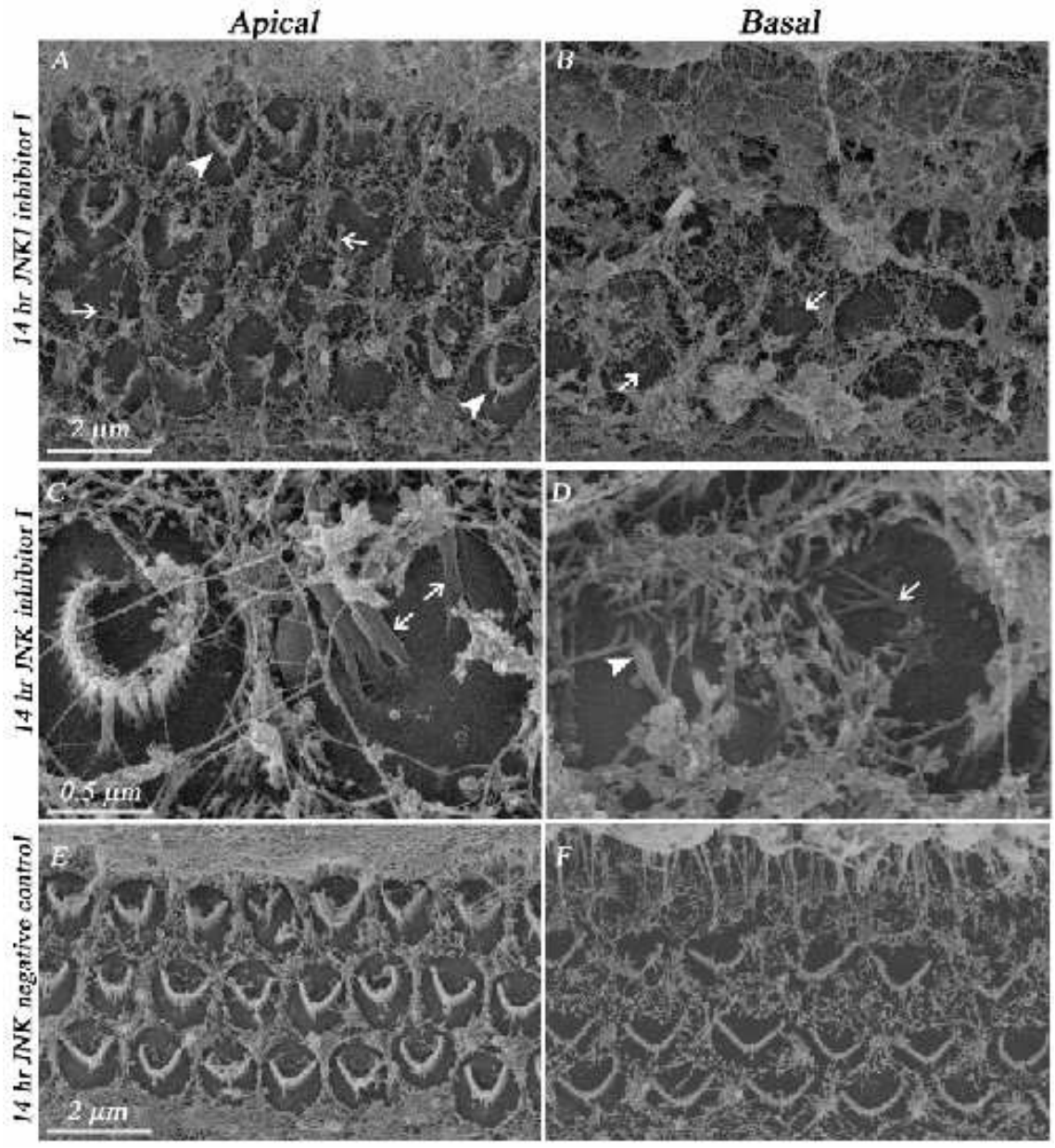
Apical
Basal
14 hr JNK1 inhibitor I
14 hr JNK inhibitor I
14 hr JNK negative control
A
B
C
D
E
F
2 μm
0.5 μm
2 μm

Figure 3.12 Transmission electron micrographs of P2 mouse auditory inner hair cells after treatment with 5 μM JNK inhibitor I for 5 and 10 hours. Apical (A, C) coil inner hair cells treated with 5 μM JNK inhibitor I for 5 hours (A) and 10 hours (C). Basal (B, D) coil inner hair cells incubated with 5 μM JNK inhibitor I for 5 hours (B) and 10 hours (D). Apical (E) and basal coil (F) inner hair cells incubated with medium containing 0.1% water control for 10 hours. Arrows in panels C and D indicates re-absorption of stereocilia back into hair cells. Scale bar = 0.5 μm

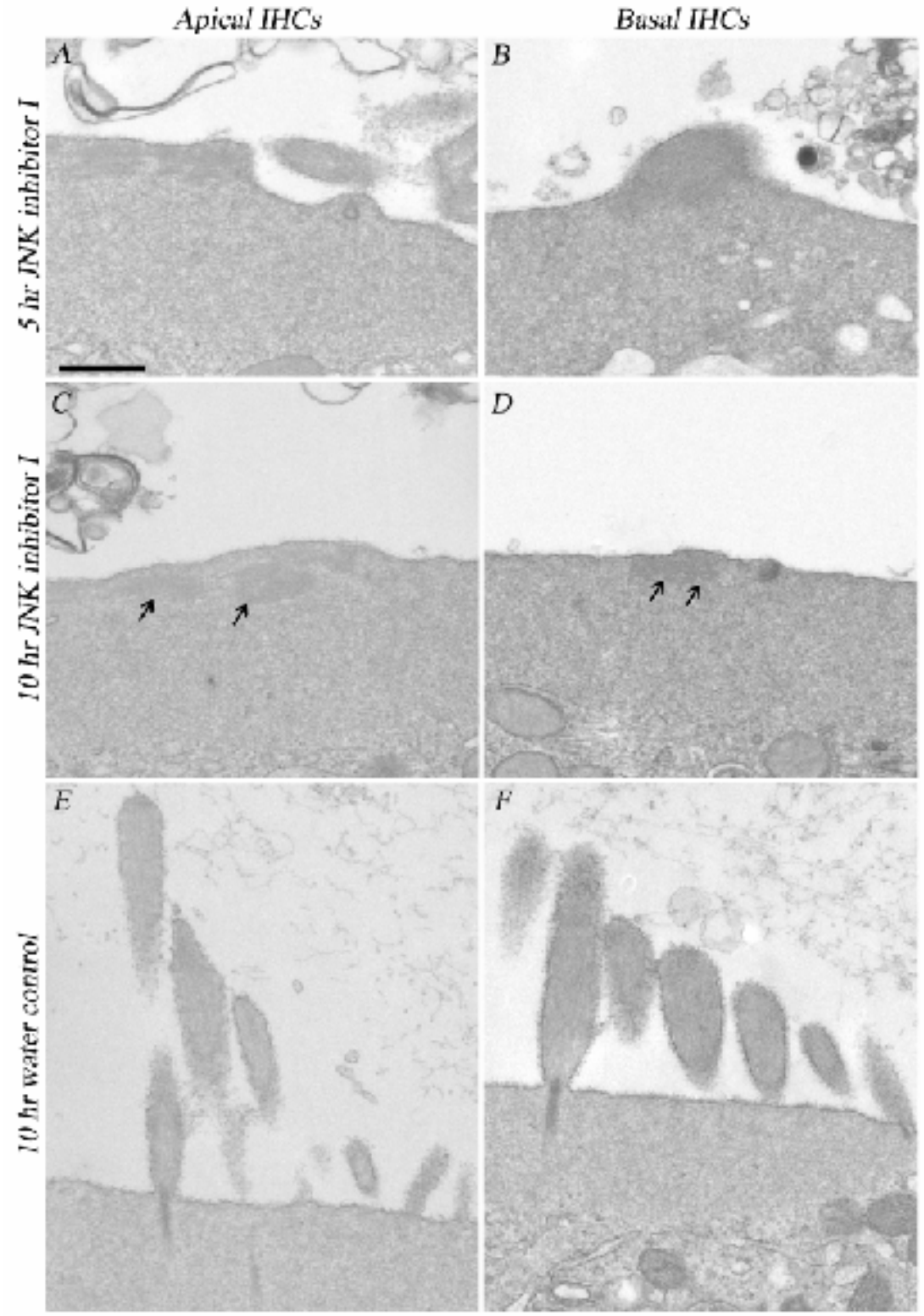
Apical IHCs
Basal IHCs
5 hr JNK inhibitor I
10 hr JNK inhibitor I
10 hr water control
A
B
C
D
E
F

Figure 3.13 Transmission electron micrographs of P2 mouse auditory outer hair cells after treatment with 5 µM JNK inhibitor I for 5 and 10 hours. Apical (A, C) coil outer hair cells treated with 5 µM JNK inhibitor I for 5 hours (A) and 10 hours (C). Basal (B, D) coil outer hair cells treated with 5 µM JNK inhibitor I for 5 hours (B) and 10 hours (D). Apical (E) and basal (F) coil outer hair cells incubated with medium containing 0.1% water control for 10 hours. Panel C arrow indicates disruption of plasma membrane at the base of the stereocilia. Scale bar = 0.5 µm

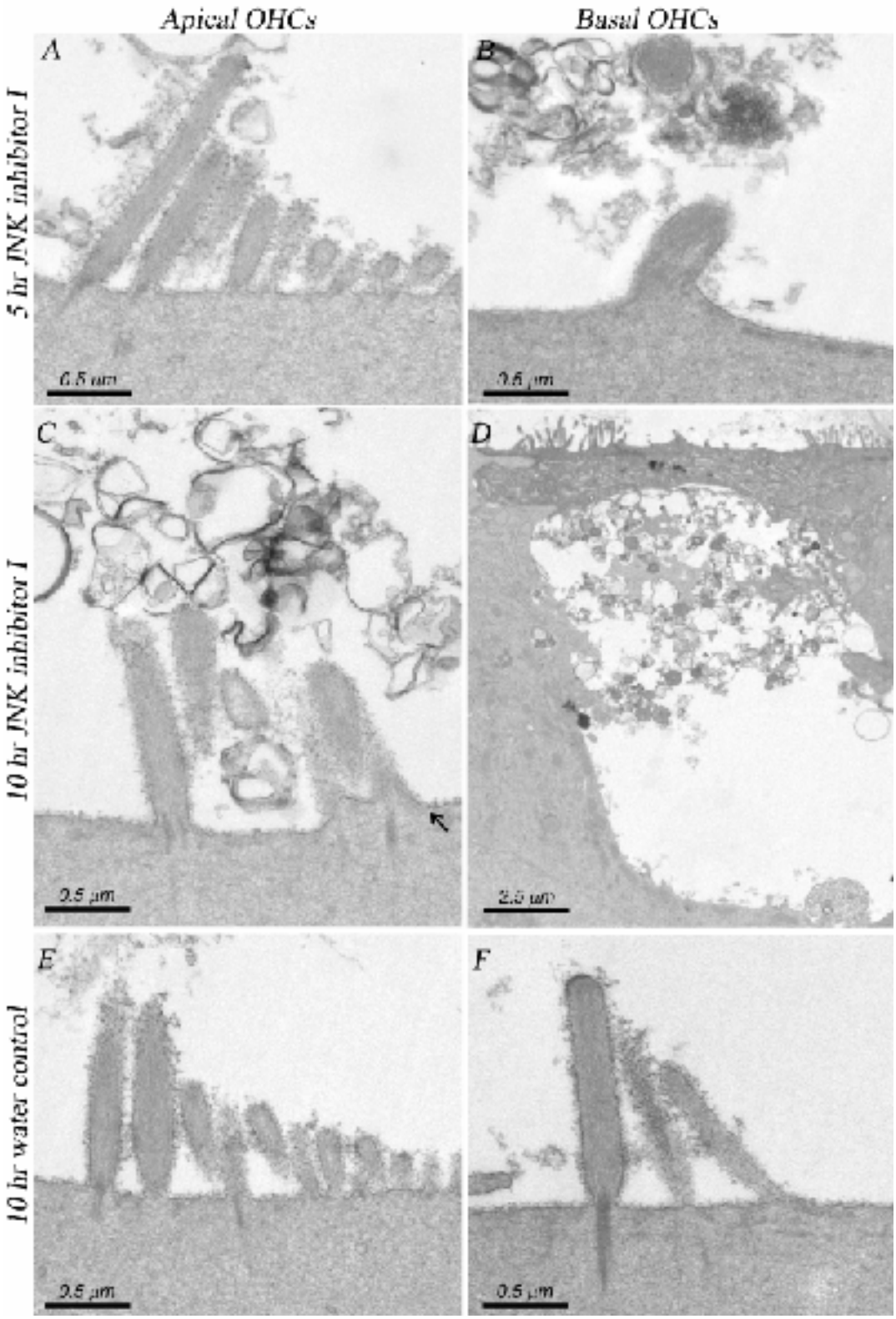
Apical OHCs
Basal OHCs
5 hr JNK inhibitor I
10 hr JNK inhibitor I
10 hr water control
A
B
C
D
E
F
0.5 μm
0.5 μm
0.5 μm
0.5 μm
0.5 μm
0.5 μm

Figure 3.14 Annexin V detection of phosphatidylserine externalization in JNK inhibitor I and staurosporine treated cochlear cultures. Normarski interference contrast (A, B, E, F, I, J) and fluorescent (C, D, G, H, K, L) images of apical (A, C, E, G, I, K) and basal (B, D, F, H, J, L) coil cultures treated for 8 hours with 5 μM JNK inhibitor I (A-D), 10 nM staurosporine (E-H) and medium containing 0.1% DMSO (I-L) as control and imaged 5 minutes after onset of annexin V labelling.
Scale bar = 50 μm.

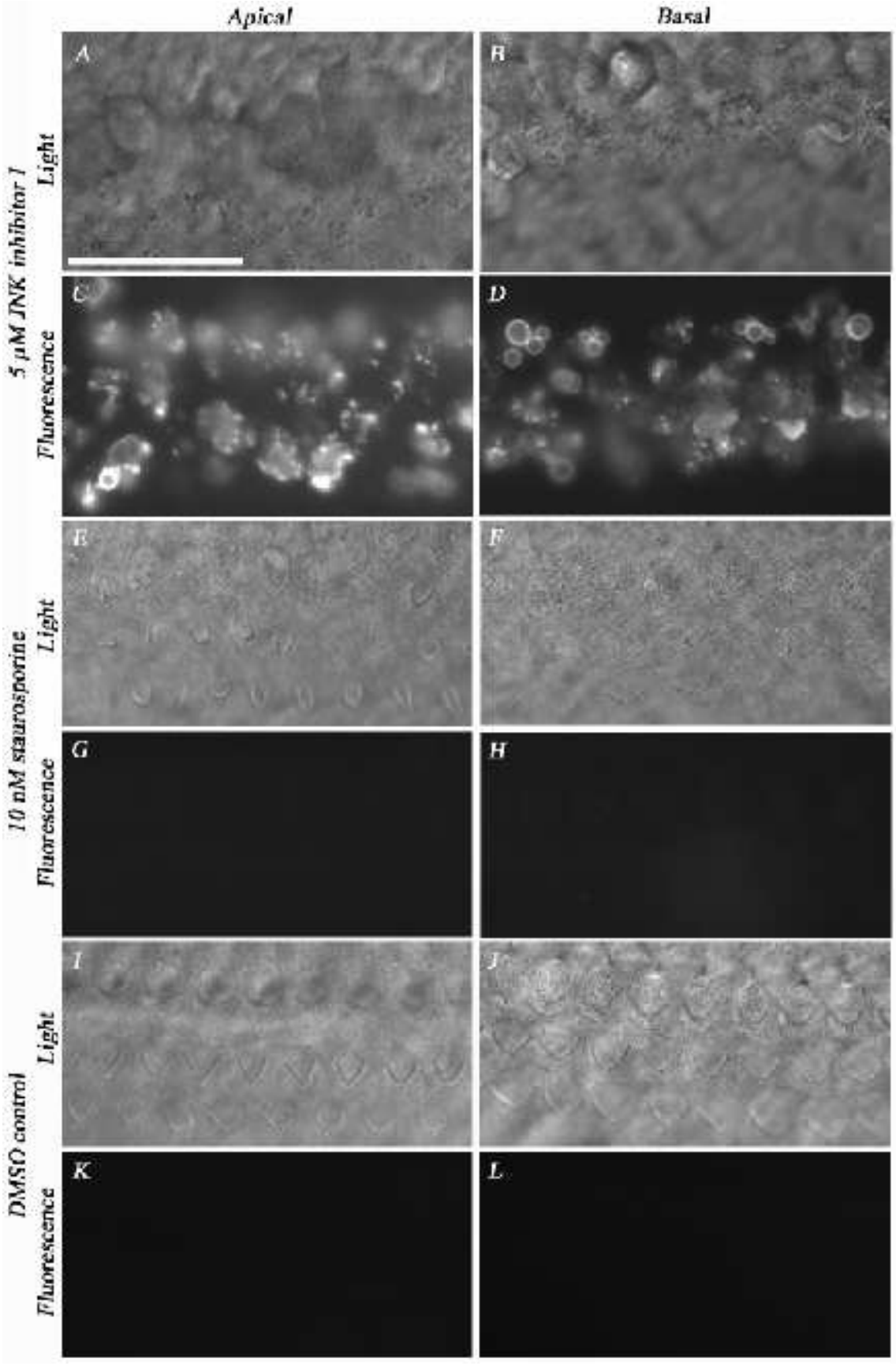
Apical
Basal
5 μM JNK inhibitor I
Light
Fluorescence
10 nM staurosporine
Light
Fluorescence
DMSO control
Light
Fluorescence
A
B
C
D
E
F
G
H
I
J
K
L

Figure 3.15 Toluidine blue staining showing the effect of JNK inhibitor I and staurosporine on mouse cochlear cultures at 48 hours. Apical (A, C, E, G) and basal coil (B, D, F, H) cochlear cultures treated with 5 μM JNK inhibitor I (A, B), 5 μM JNK inhibitor I negative control (C, D), 10 nM staurosporine (E, F) and medium containing 0.1% DMSO as a control (G, H). Scale bar = 10μm.

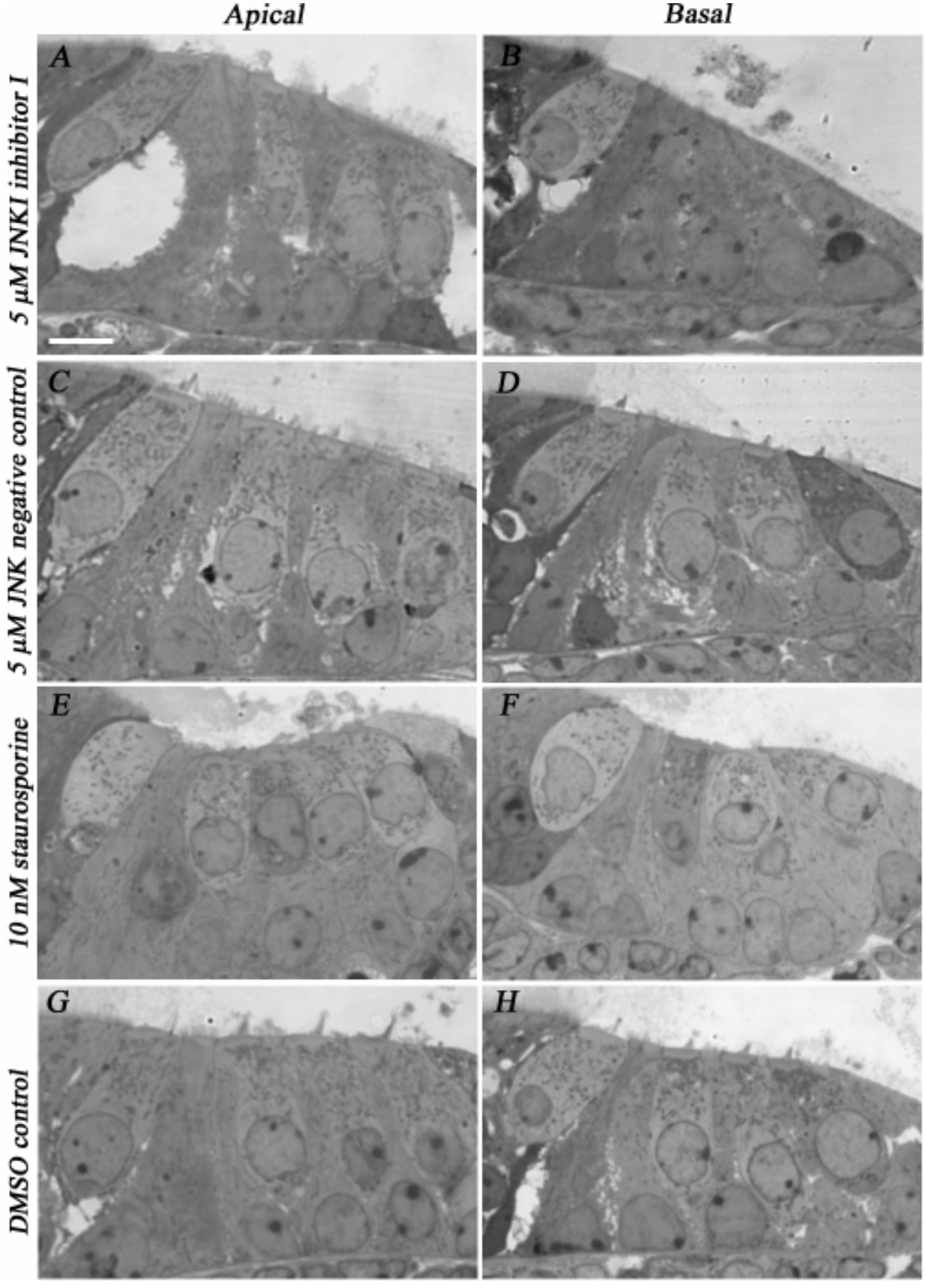
Apical
Basal
A
B
C
D
E
F
G
H
5 μM JNKI inhibitor I
5 μM JNK negative control
10 nM staurosporine
DMSO control

Figure 3.16 Annexin V detection of phosphatidylserine externalization in cochlear cultures treated with different concentrations of JNK inhibitor I for 10 minutes at room temperature. Normarski interference contrast (A, B, E, F, I, J) and fluorescent (C, D, G, H, K, L) images of apical (A, C, E, G, I, K) and basal (B, D, F, H, J, L) coil cultures treated for 8 hours with 5 μM JNK inhibitor I (A-D), 2 μM JNK inhibitor I (E-H) and 1 μM JNK inhibitor I (I-L), for 5 minutes prior to imaging. Scale bar = 50 μm.

Apical
Basal
5 μM JNK inhibitor I
Light
Fluorescence
2 μM JNK inhibitor I
Light
Fluorescence
1 μM JNK inhibitor I
Light
Fluorescence
A
B
C
D
E
F
G
H
I
J
K
L

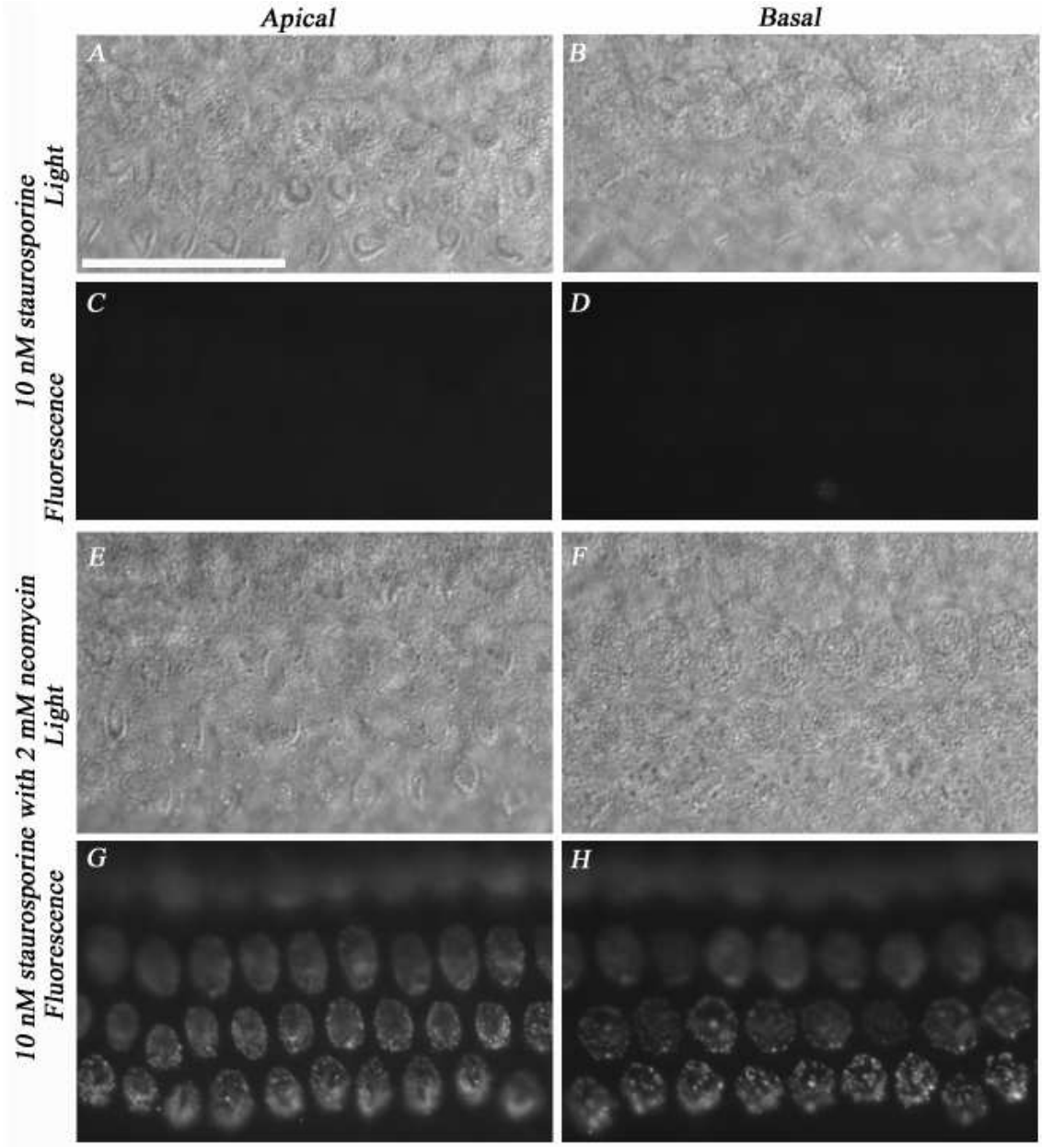

Figure 3.17 Annexin V detection of phosphatidylserine externalization in staurosporine treated cochlear cultures. Normarski interference contrast (A, B, E, F) and fluorescent (C, D, G, H) images of apical (A, C, E, G) and basal (B, D, F, H) coil cultures treated with 10 nM staurosporine for 8 hours and imaged before (A-D) and 5 minutes after (E-H) treatment with 2 mM neomycin. Scale bar = 50 µm.

Figure 3.18 FM1-43 loading in staurosporine treated cultures. Apical (A, C, E, G) and basal coil (B, D, F, H) cochlear cultures treated with 10 nM staurosporine (A, B, C, D) or medium containing 0.1% DMSO as a control (E, F, G, H) for 10 hours and dipped in 3 μM FM1-43 (C, D, E F). Confocal scale bar = 10 μm, fluorescence scale bar = 50 μm.

Apical
Basal
Staurosporine
Hair bundles
A
B
Staurosporine
Hair cell FM1-43 loading
C
D
0.1 % DMSO control
Hair cell FM1-43 loading
E
F
0.1 % DMSO control
Hair bundles
G
H

Figure 3.19 Confocal images of phalloidin stained cochlear cultures treated with 5 nM staurosporine for 16 hrs and labelled with anti-radixin antibody. Apical (A, C) and basal coil (E, G) cochlear cultures incubated with 5 nM staurosporine (A, E) and medium containing 0.1% DMSO (C, G) as a control, and labelled with anti-radixin antibody. Counterstaining with phalloidin (B, D, F, H). Arrows in panel A and E indicate radixin labelling of supporting cell microvilli. Scale bar = 5 µm.

Anti-radixin
Phalloidin
A
B
C
D
E
F
G
H
Staurosporine
DMSO control
Staurosporine
DMSO control
Apical
Apical
Basal
Basal

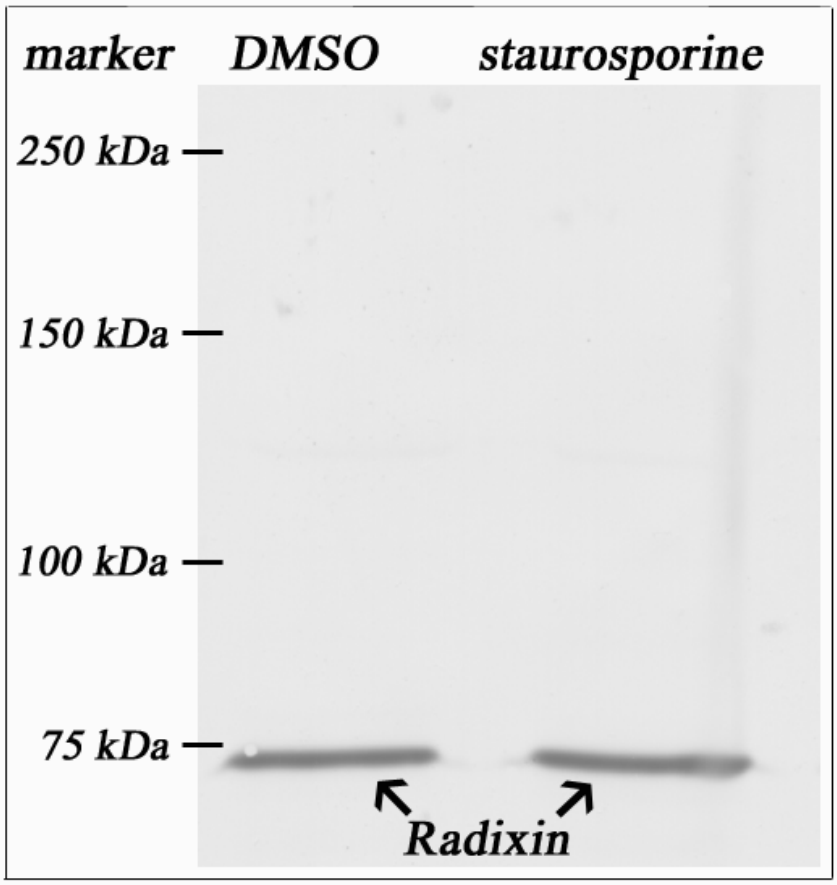

Figure 3.20 Western blotting of cochlear cultures for radixin after 14 hours of staurosporine treatment. Immuno-detection of radixin after 14 hours of 10 nM staurosporine treatment.

Figure 3.21 Confocal images of phalloidin stained cochlear cultures treated with 10 nM staurosporine for 14 hrs and labelled with anti-phospho-ERM monoclonal antibody. Apical (B, E) and basal (H, K) coil cochlear cultures treated with 10 nM staurosporine (B, H) or medium containing 0.1% DMSO as a control (E, K), and labelled with anti-phospho-ERM monoclonal antibody. Counterstaining with phalloidin (A, D, G, J). Arrows in panels B and H indicate attenuated phos-ERM levels in hair bundles, and arrowheads show attenuated phos-ERM levels in the microvilli of supporting cells. Scale bar = 10 µm.

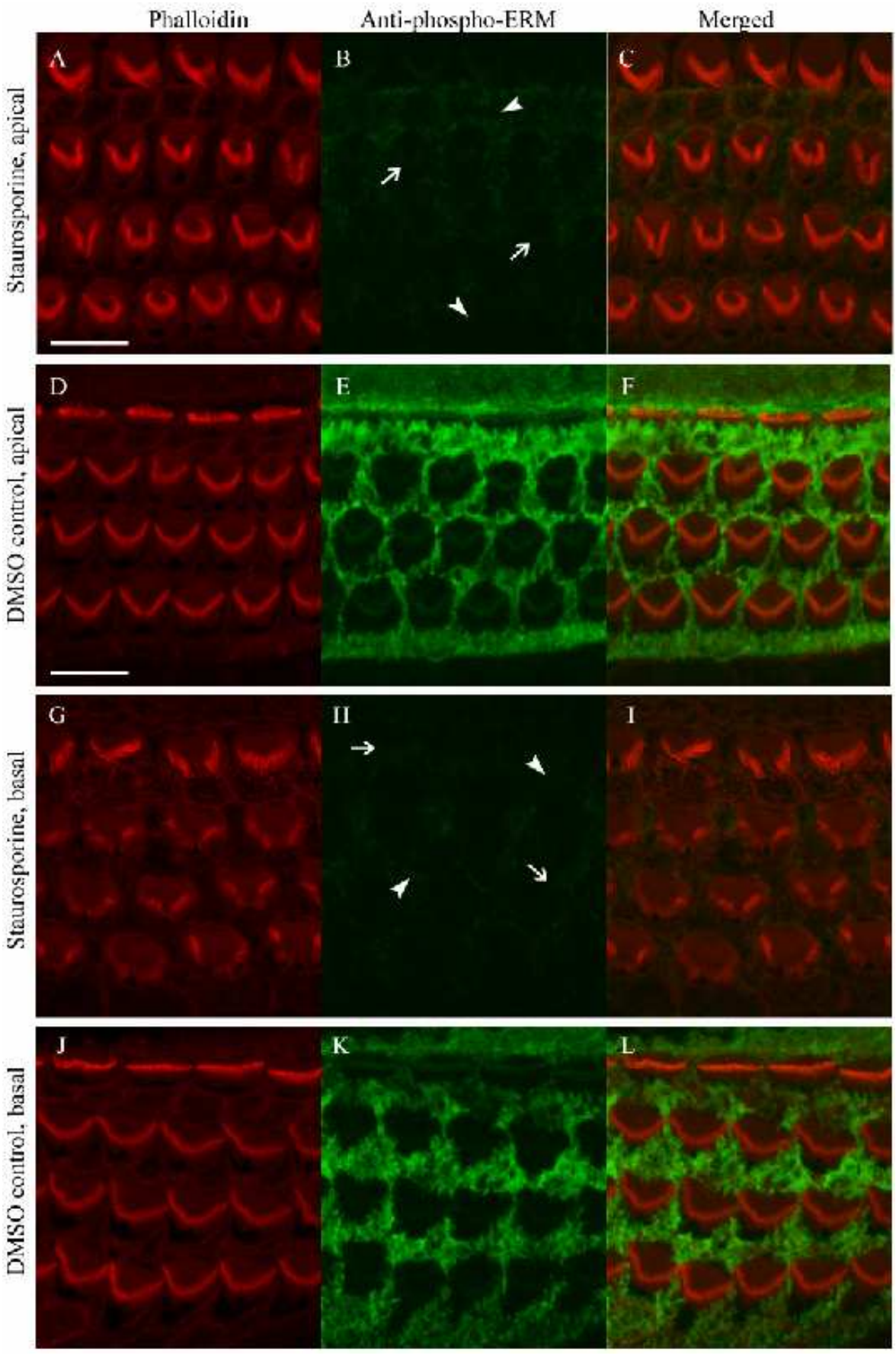
Phalloidin
Anti-phospho-ERM
Merged
Staurosporine, apical
DMSO control, apical
Staurosporine, basal
DMSO control, basal
A
B
C
D
E
F
G
H
I
J
K
L

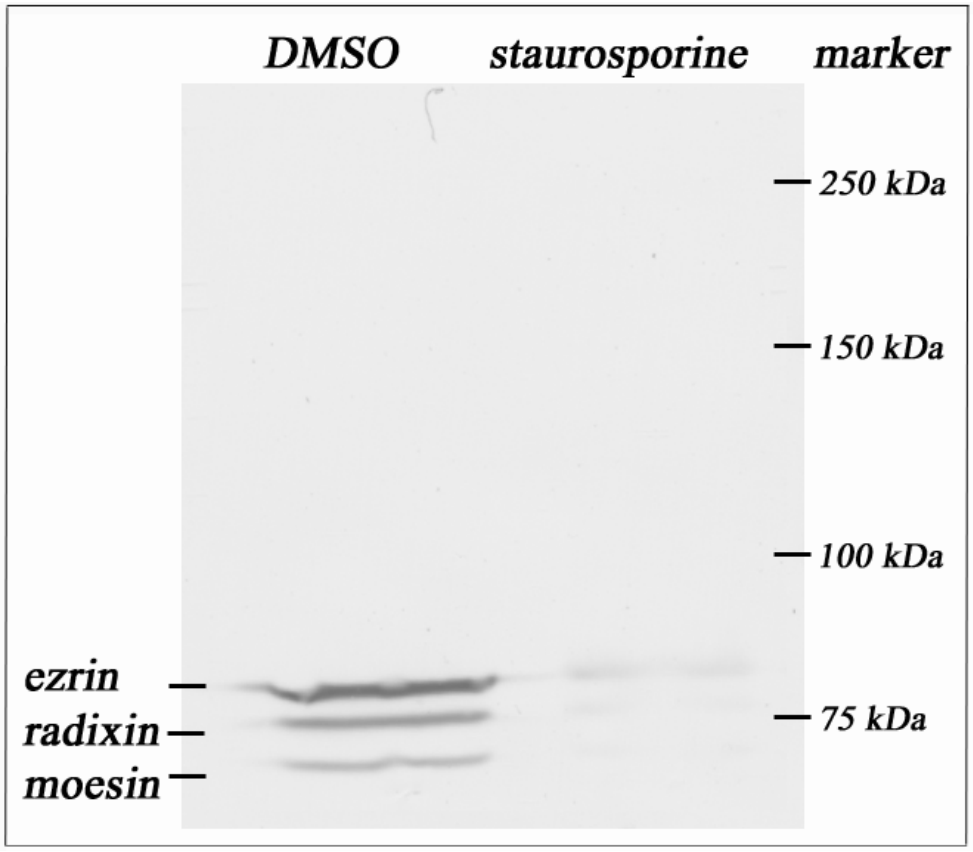

Figure 3.22 Western blotting of cochlear cultures for phos-ERM after 14 hours of staurosporine treatment. Immuno-detection of phos-ERM after 14 hours of 10 nM staurosporine treatment.

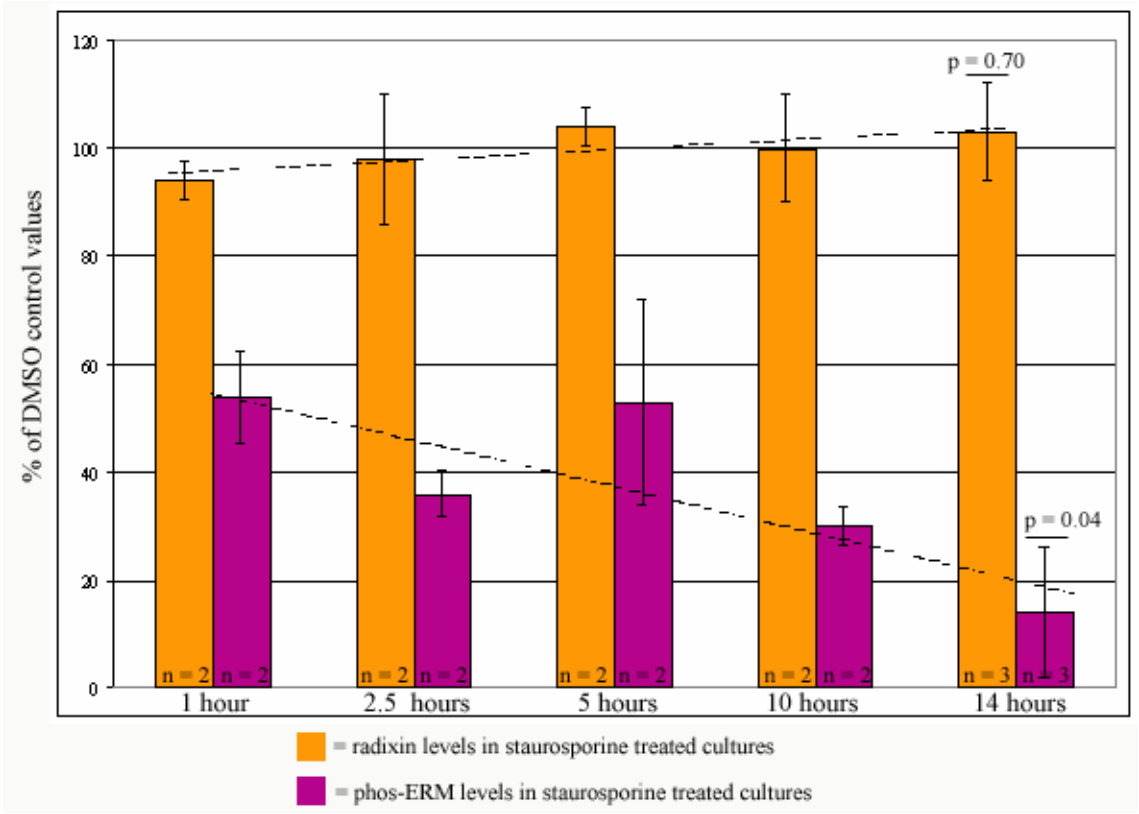

Figure 3.23 Histograms showing levels of radixin and phos-ERM in immunoblots of staurosporine treated cochlear cultures as a percentage of the DMSO control at different time points. Densitometry analysis of radixin (orange bars) and phos-ERM (purple bars) grey-scale values after 1 hour, 2.5 hours, 5 hours, 10 hours and 14 hours treatment with 10 nM staurosporine vs. medium containing 0.1% DMSO as a control. At 14 hours, radixin values show no significant difference between staurosporine and 0.1 % DMSO treated cochlear cultures ($p = 0.70$), while phos-ERM values do show a significant difference between staurosporine and medium containing 0.1% DMSO treated cochlear cultures ($p = 0.04$).

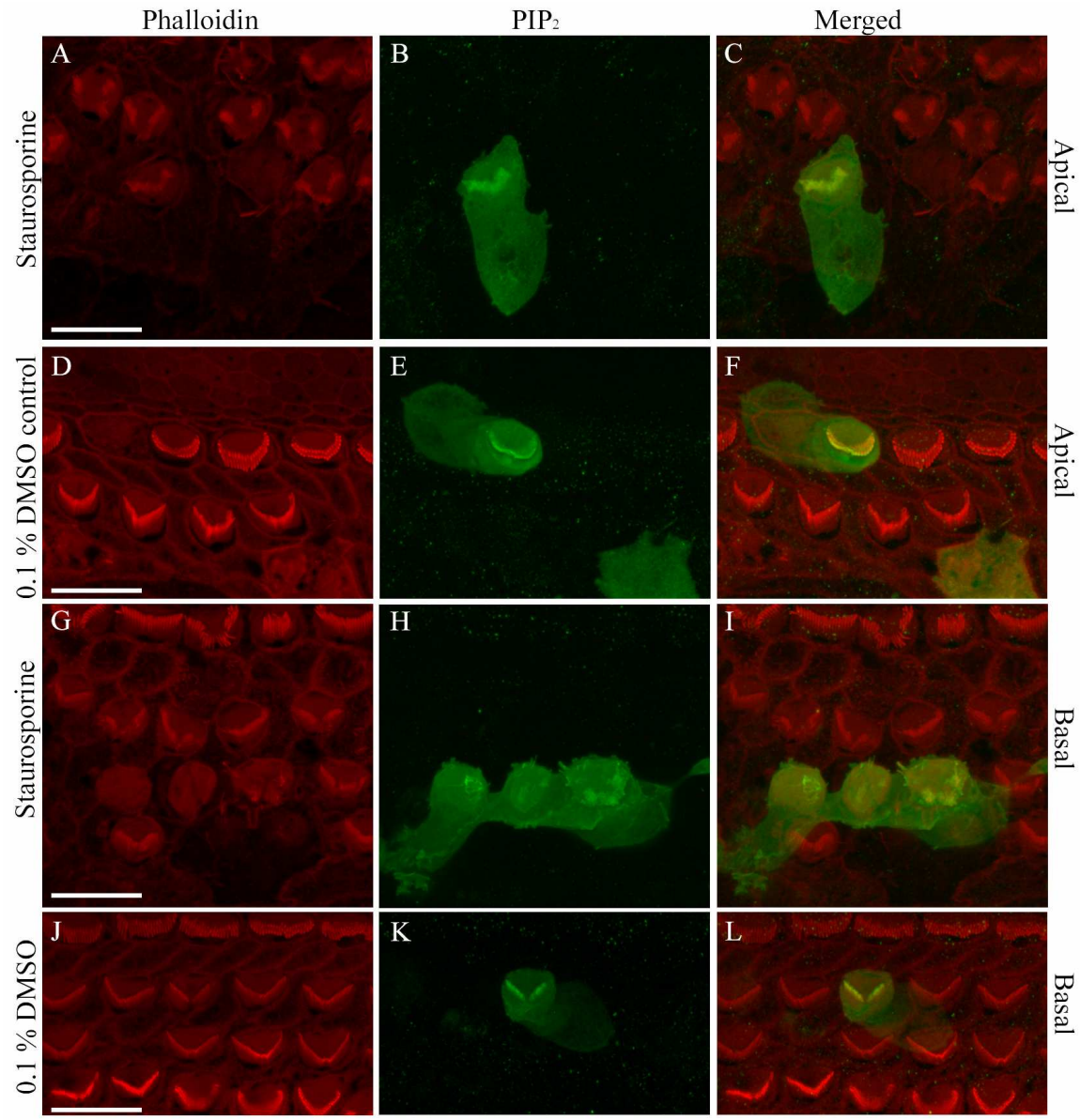

Figure 3.24 Confocal images of phalloidin stained cochlear cultures transfected with the PIP_2 reporter $PLC_{\delta 1}PH$ and treated with 10 nM staurosporine for 7 hours. Apical (B, E) and basal region (H, K) cochlear hair cells transfected with the PIP_2 reporter $PLC_{\delta 1}PH$ by gene gun and treated with 10 nM staurosporine (B, H) or medium containing 0.1% DMSO as a control (E, K) for 7 hours. Counterstaining with phalloidin (A, D, G, J). Scale bar = 10 μm.

Figure 3.25 Confocal images of phalloidin stained cochlear cultures treated with 5 µM JNK inhibitor I for 14 hrs and labelled with anti-phospho-ERM monoclonal antibody. Apical (B, E) and basal (H, K) coil cochlear cultures treated with 5 µM JNK inhibitor I (B, H) or medium containing 0.1% water as a control (E, K), and labelled with anti-phospho-ERM monoclonal antibody. Counterstaining with phalloidin (A, D, G, J). Arrows in panel B indicates phos-ERM labelling of hair bundles. Panel B and H arrowheads indicates phos-ERM labelling of supporting cell microvilli. Scale bar = 10 µm.

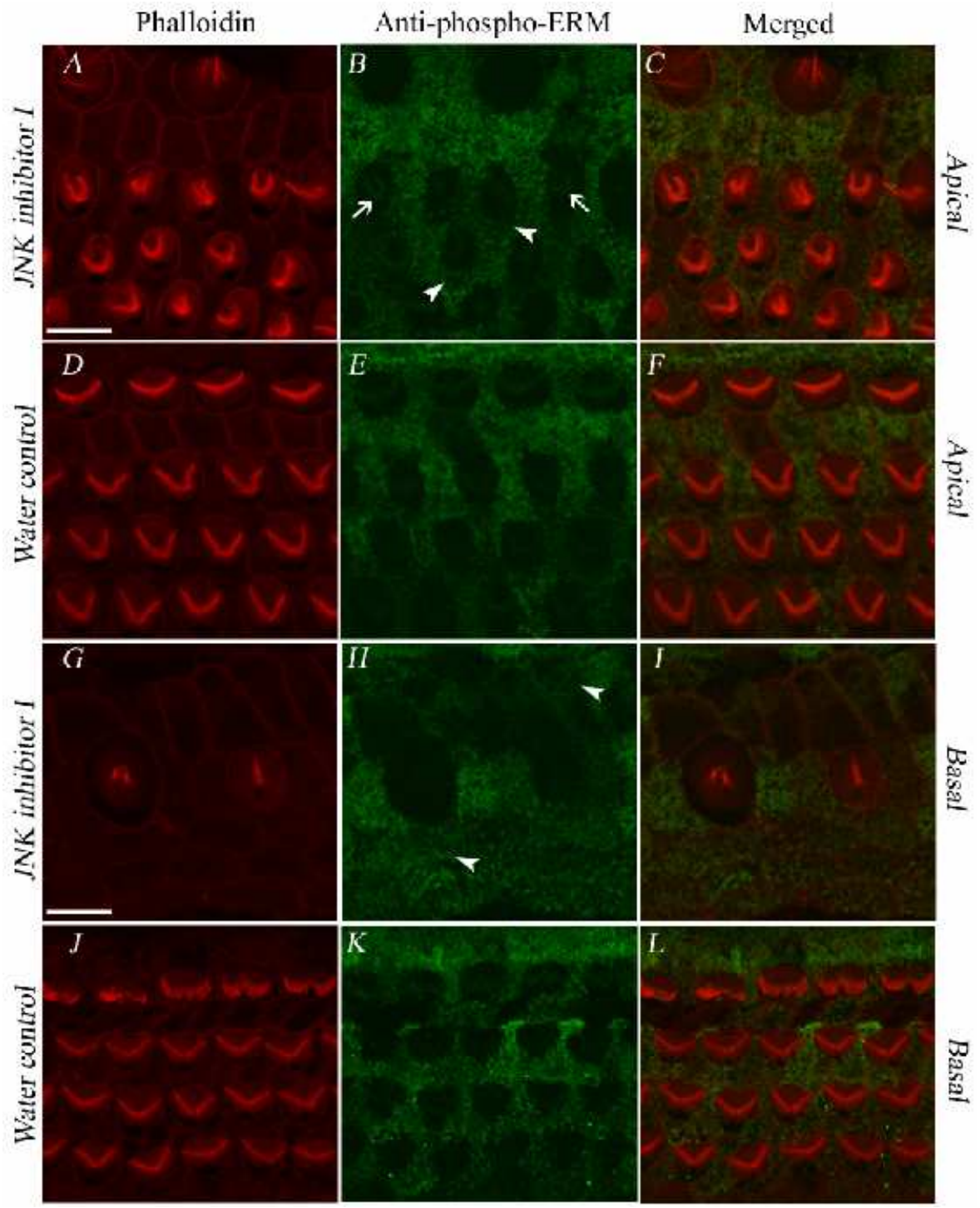
Phalloidin
Anti-phospho-ERM
Merged
A
B
C
D
E
F
G
H
I
J
K
L
JNK inhibitor I
Water control
JNK inhibitor I
Water control
Apical
Apical
Basal
Basal

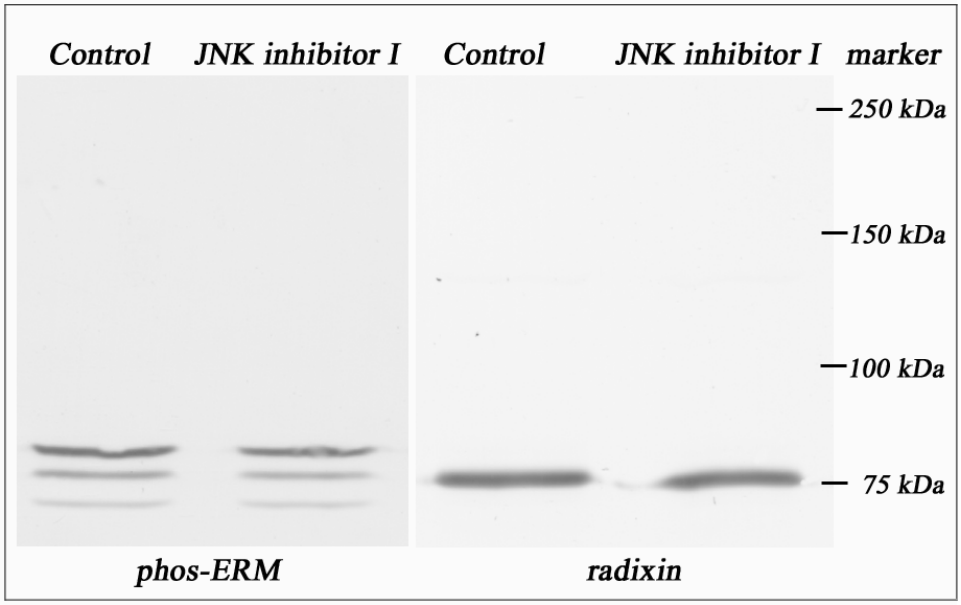

Figure 3.26 Western blotting of cochlear cultures for phos-ERM and radixin after 14 hours of JNK inhibitor I treatment.

Immuno-detection of phos-ERM and radixin after 14 hours of 5 μM JNK inhibitor I treatment.

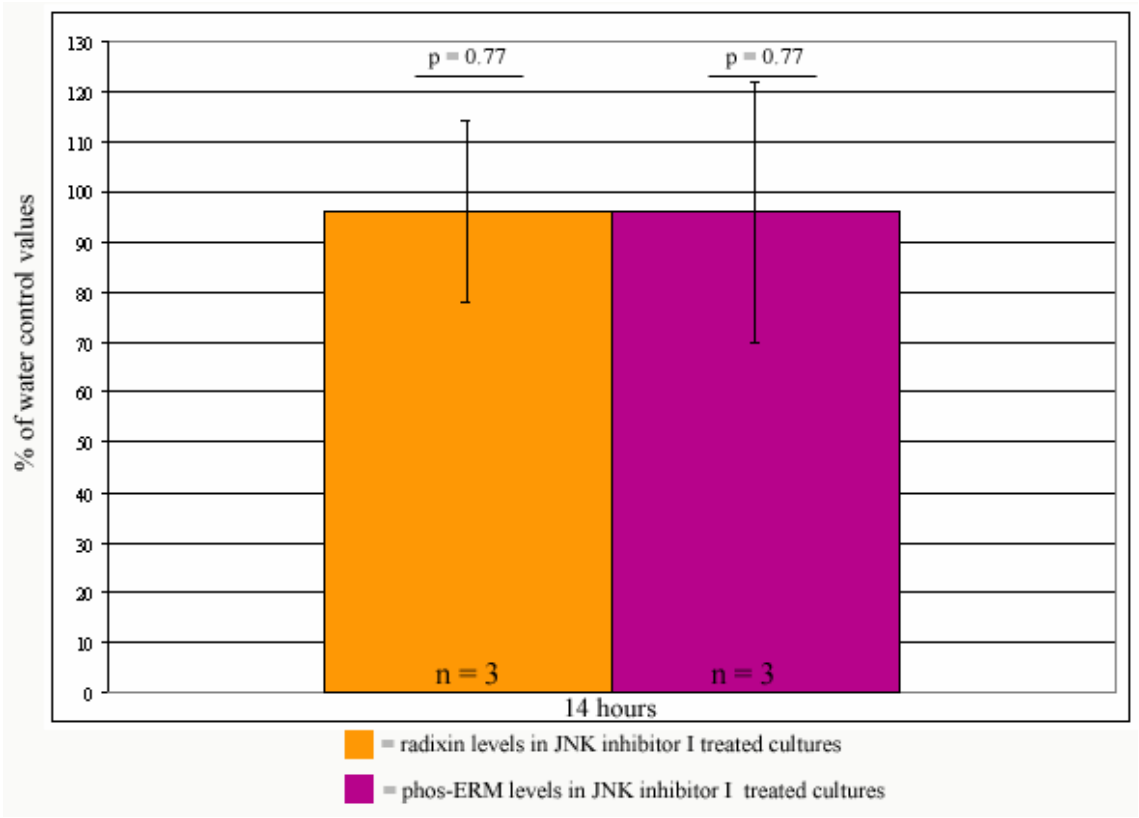

Figure 3.27 Histograms showing levels of radixin and phos-ERM in immunoblots of JNK inhibitor I treated cochlear cultures as a percentage of the control at 14 hours. Densitometry analysis of radixin (orange bar) and phos-ERM (purple bar) grey-scale values after 14 hours treatment with 5 μM JNK inhibitor I and medium containing 0.1% water as a control. At 14 hours, neither radixin nor phos-ERM values shows any significant differences between JNK inhibitor I and medium containing 0.1% water control treated cochlear cultures ($p = 0.77$).

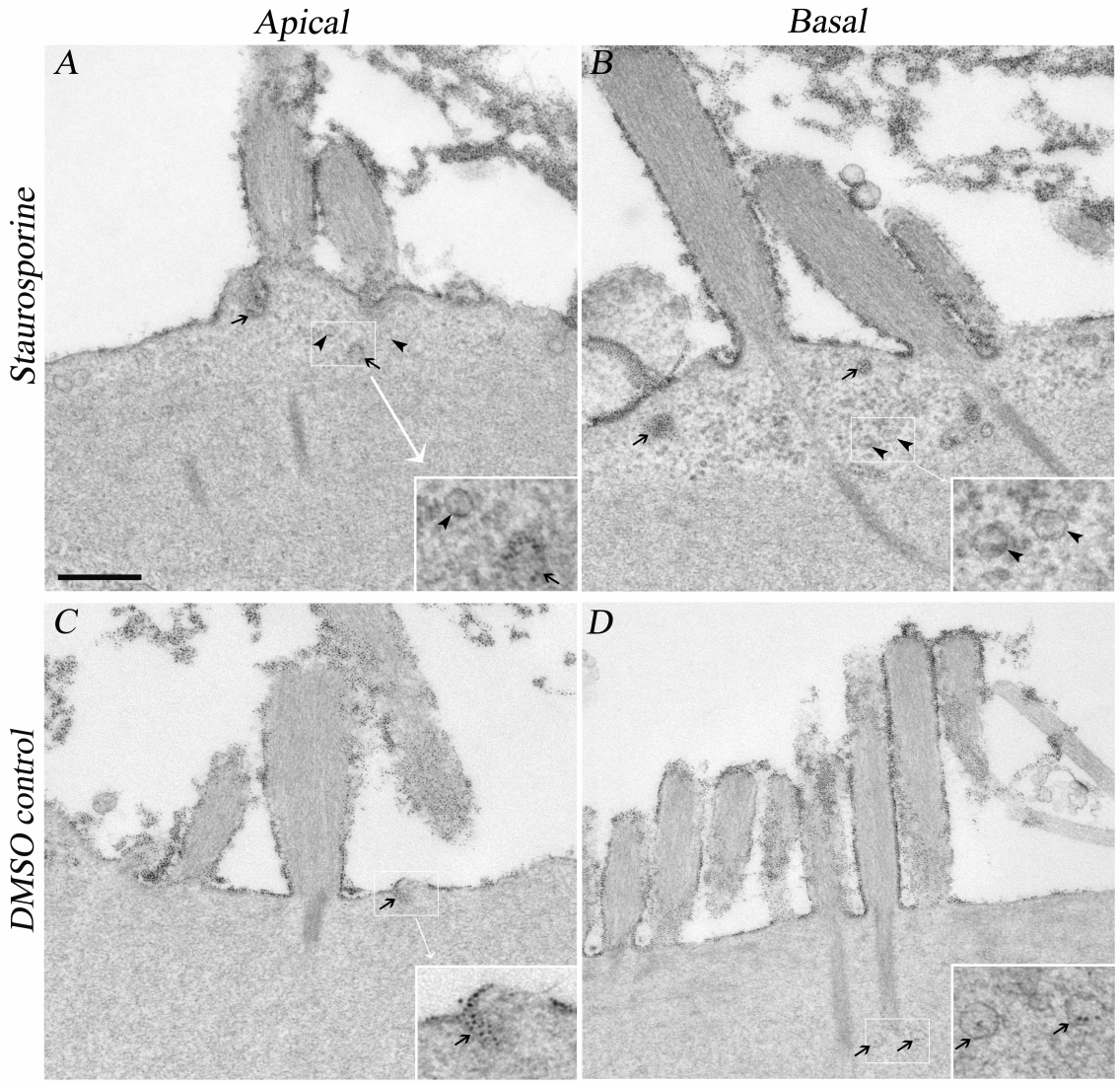

Figure 3.28 Cationic ferritin labelling of staurosporine treated cultures. Apical (A, C) and basal region (B, D) cochlear cultures treated with 10 nM staurosporine (A, B) or medium containing 0.1% DMSO (C, D) for 4 hours, then with ferritin for 1 hour, followed by a further 4 hours with 10 nM staurosporine (A, B) or medium containing 0.1% DMSO (C, D). Arrows in panels A, B, C and D shows vesicles containing cationic ferritin and arrowheads in panels A and B indicate empty vesicles. Insets for all panels magnified at x2.5. Scale bar = 0.2 μm.

Figure 3.29 Confocal images of phalloidin stained cochlear cultures treated with staurosporine for 14 hours and allowed to recover for 48 hours. Apical (A, C) and basal coil (B, D) cochlear cultures that were treated with 5 nM staurosporine for 14 hours and either fixed immediately (A, B) or allowed to recover for 48 hours and then fixed (C, D). Apical (E) and basal coil (F) cochlear cultures treated with medium containing 0.1% DMSO control for 14 hours and allowed to recover for 48 hours. Scale bar = 10 µm

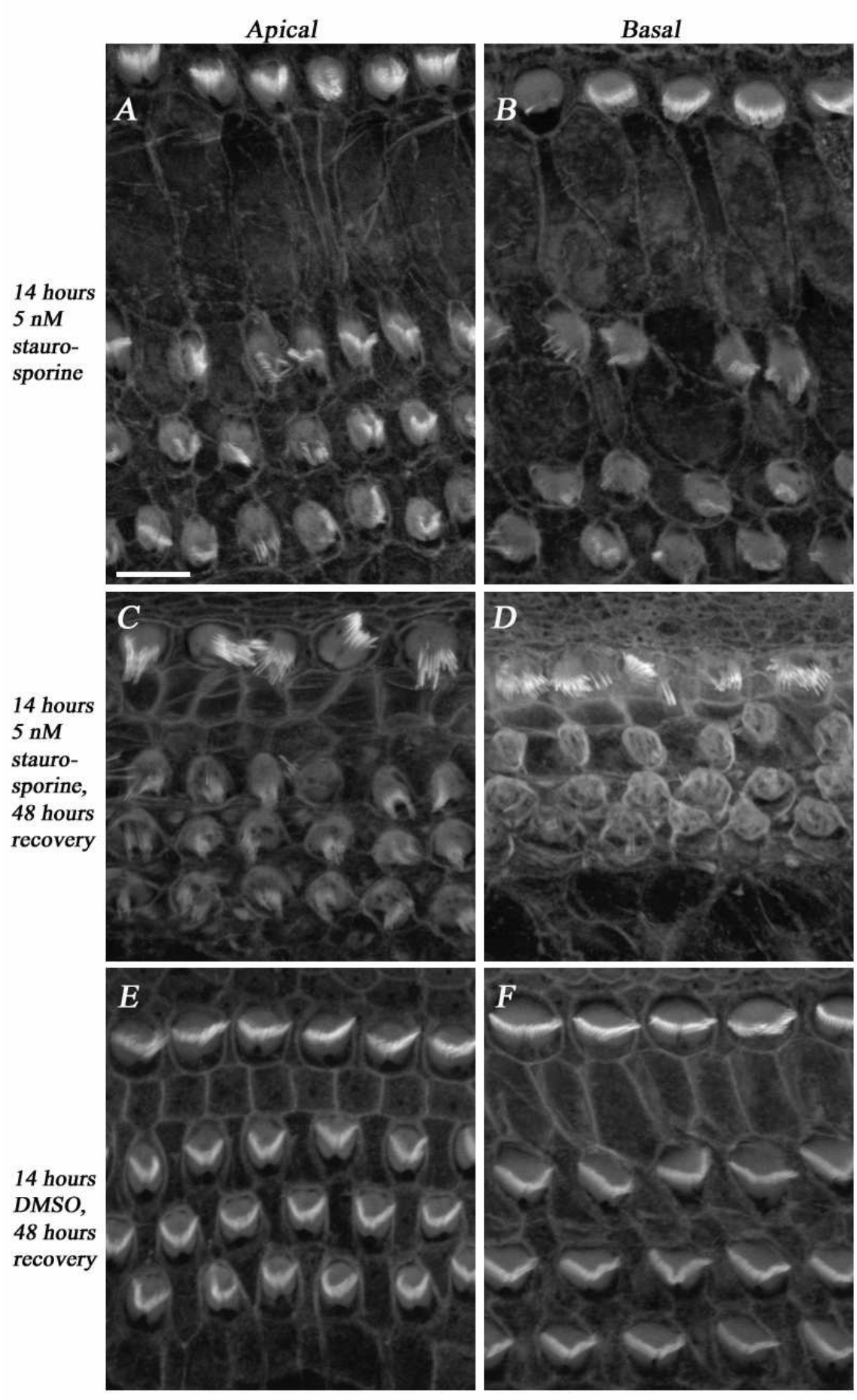
Apical
Basal
A
B
14 hours 5 nM staurosporine
C
D
14 hours 5 nM staurosporine, 48 hours recovery
E
F
14 hours DMSO, 48 hours recovery

Figure 3.30 Confocal images of phalloidin stained cochlear cultures treated with staurosporine for 2.5 hours and allowed to recover for 7.5, 24 or 48 hours.

Apical (A, C, E, G) and basal coil (B, D, F, H) cochlear cultures that were treated with 10 nM staurosporine for 2.5 hours (A, B) and then allowed to recover for 7.5 hours (C, D), 24 hours (E, F) and 48 hours (G, H). Apical (I) and basal coil (J) cochlear cultures treated with medium containing 0.1% DMSO as controls for 2.5 hours and allowed to recover for 48 hours. Arrows in panels G and H indicate elongated stereocilia. Scale bar = 10 µm

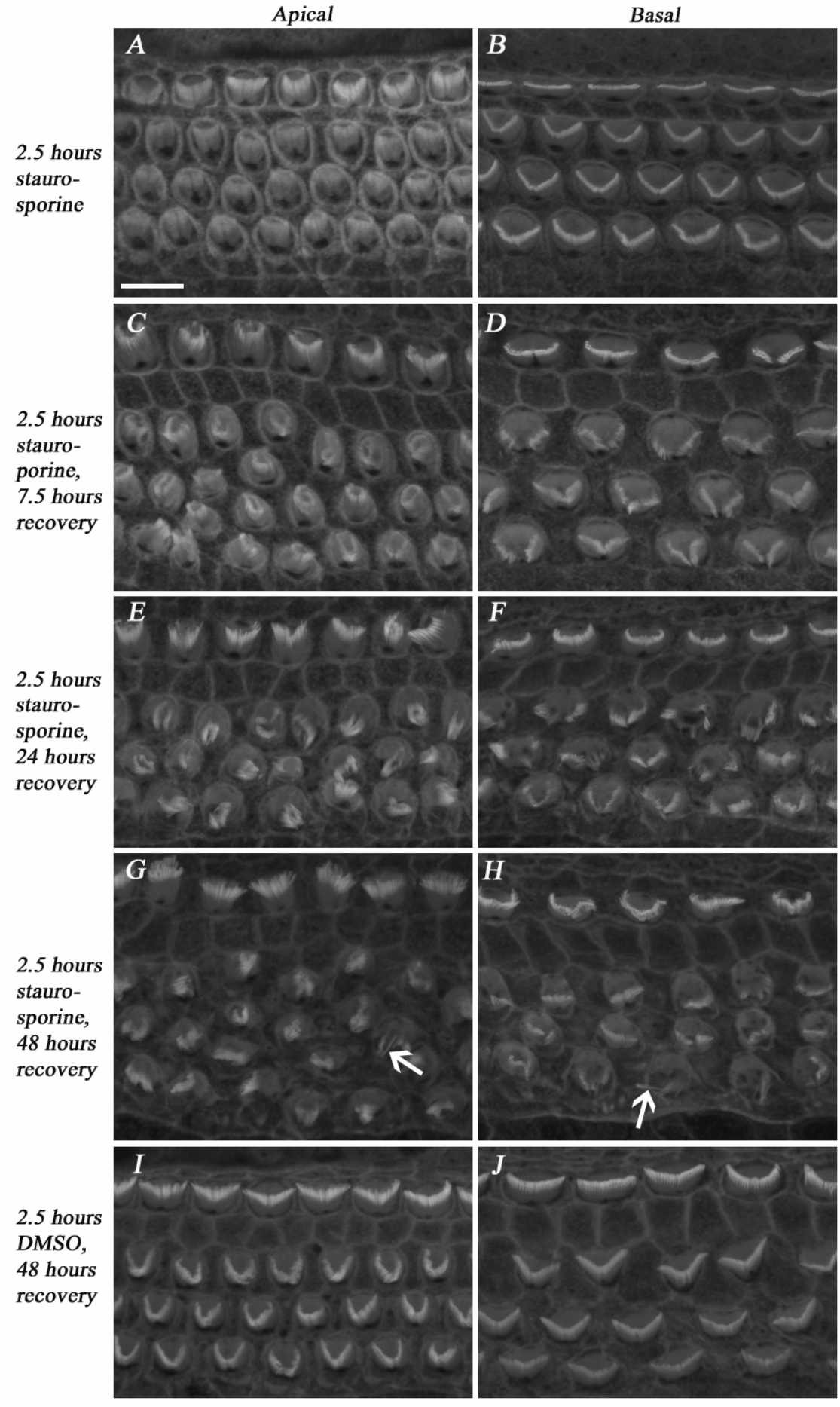
Apical
Basal
A
B
2.5 hours staurosporine
C
D
2.5 hours staurosporine, 7.5 hours recovery
E
F
2.5 hours staurosporine, 24 hours recovery
G
H
2.5 hours staurosporine, 48 hours recovery
I
J
2.5 hours DMSO, 48 hours recovery

Figure 3.31 Scanning electron micrographs showing basal cochlear cultures treated with 1 mM neomycin for 1 hour and allowed to recover for 23 hours. Basal coil cochlear cultures treated with 1 mM neomycin in media at 23 ˚C for 1 hour (A, B), and allowed to recover for 23 hours at 37 ˚C (B). Basal coil cochlear cultures treated with medium supplemented with 0.1% HBHBSS as a control at 23 ˚C for 1 hour and allowed to recover for 23 hours at 37 ˚C (C). Arrows in panel A shows hair bundle associated blebs, and arrowheads shows blebs not associated with hair bundles. Arrows in panel B shows disrupted hair bundles, while arrowheads show a reduction in the density of supporting cell microvilli. Scale bar = 2 µm.

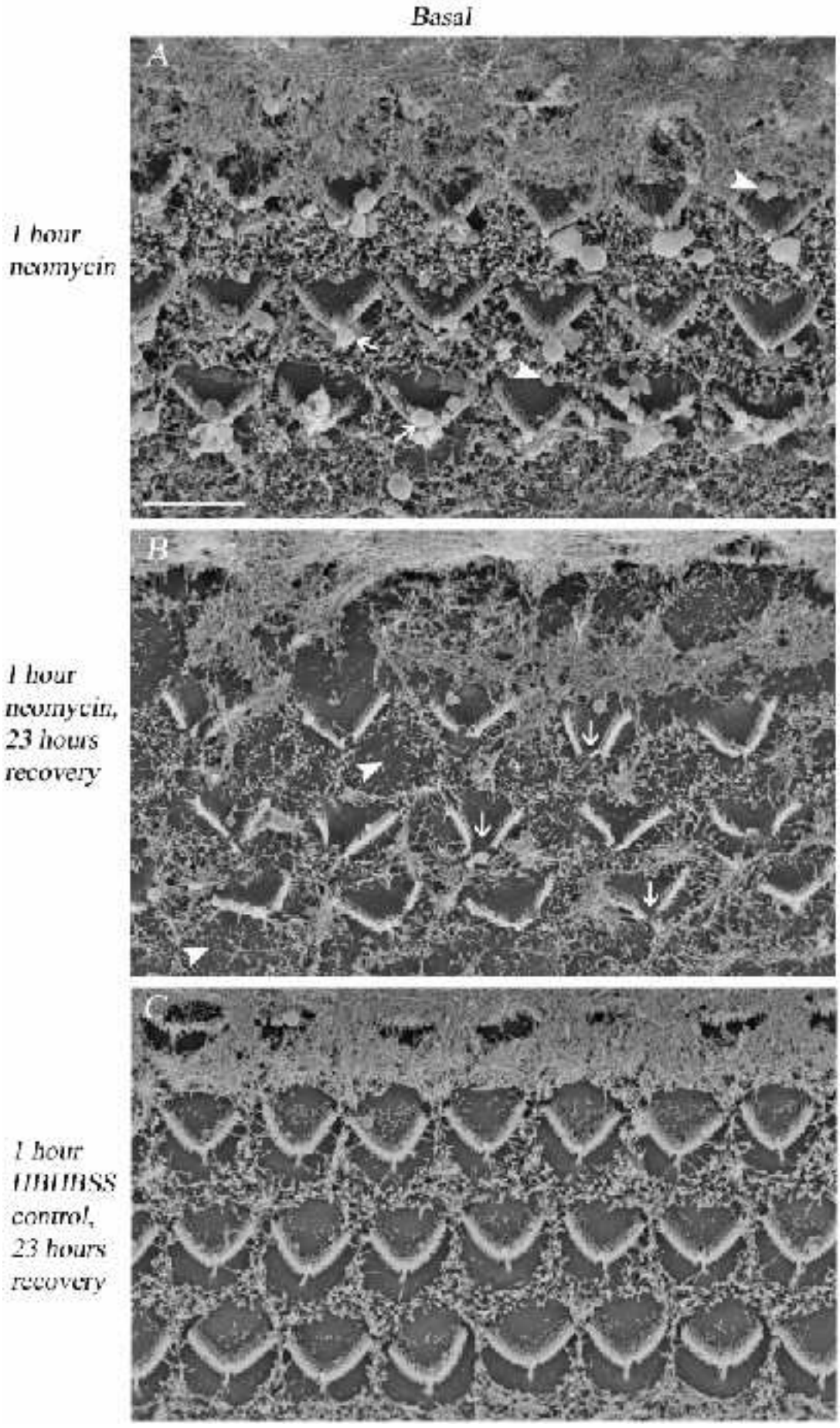
Basal
A
1 hour neomycin
B
1 hour neomycin, 23 hours recovery
C
1 hour HBHBSS control, 23 hours recovery

Figure 3.32 Scanning electron micrographs showing basal cochlear cultures treated with 1 mM neomycin for 2 hours and allowed to recover for 22 hours. Basal coil cochlear cultures treated with 1 mM neomycin in media at 23 ˚C for 2 hours (A, B), and allowed to recover for 22 hours at 37 ˚C (B). Basal coil cochlear cultures treated with medium supplemented with 0.1% HBHBSS as a control at 23 ˚C for 2 hours and allowed to recover for 22 hours at 37 ˚C (C). Arrows in panel A shows the presence of blebs. Arrows in panel B shows hair bundle disruption, while arrowheads shows possible hair cell extrusions. Scale bar = 2 µm.

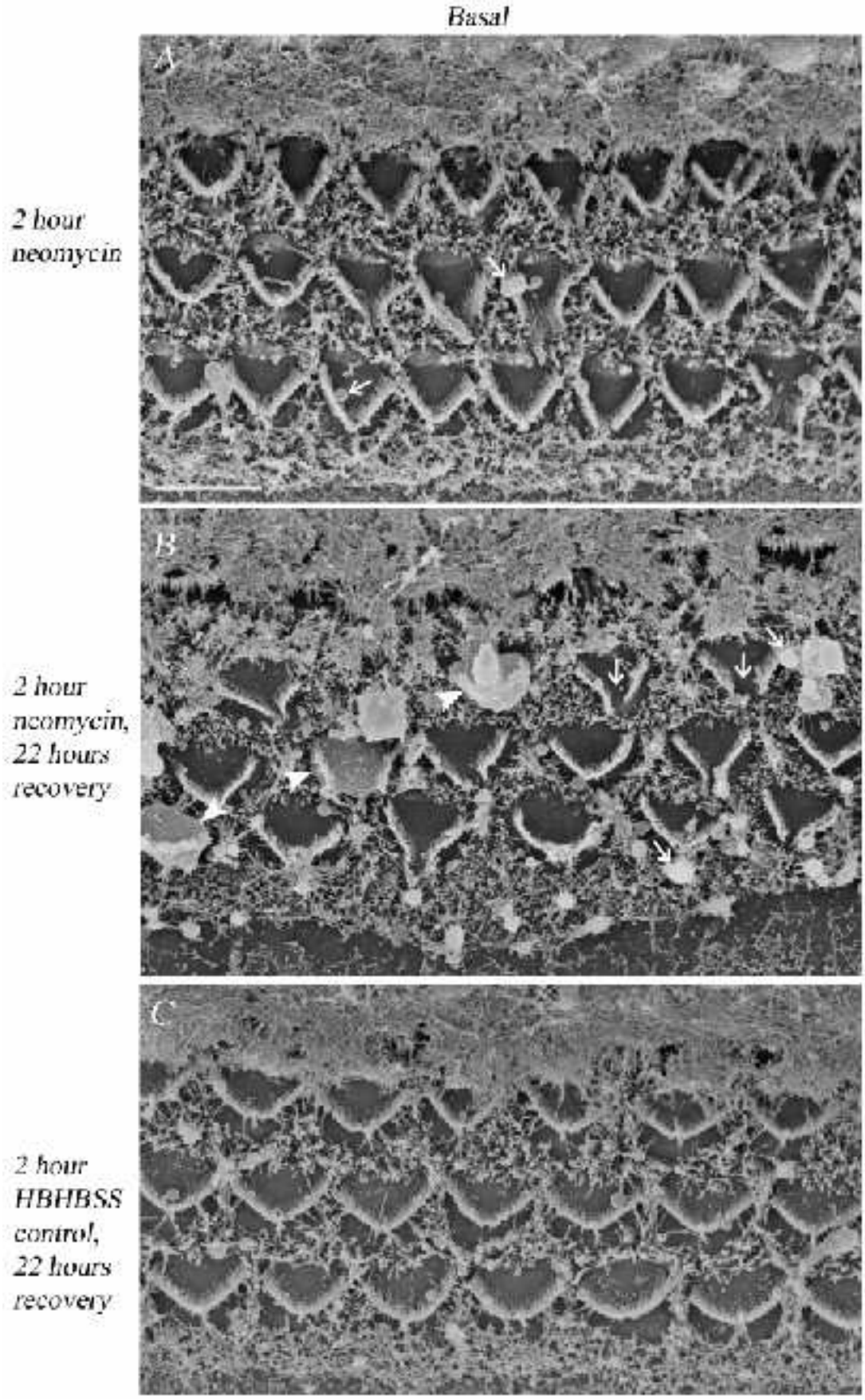
Basal
A
2 hour neomycin
B
2 hour neomycin, 22 hours recovery
C
2 hour HBHBSS control, 22 hours recovery

Figure 3.33 Scanning electron micrographs showing basal cochlear cultures treated with 1 mM neomycin for 4 hours and allowed to recover for 20 hours. Basal coil cochlear cultures treated with 1 mM neomycin in media at 23 ˚C for 4 hours (A, B), and allowed to recover for 20 hours at 37 ˚C (B). Basal coil cochlear cultures treated with medium supplemented with 0.1% HBHBSS control at 23 ˚C for 4 hours and allowed to recover for 20 hours at 37 ˚C (C). Panel A arrows: straight arrows indicates normal hair bundles, right-angle arrows indicates degenerating hair bundles, arrowheads shows the presence of large blebs and bendy arrows shows hair cells possibly being extruded. Arrows in panel B shows the presence of IHC hair bundles and the arrowheads show debris on the organ of Corti surface. Scale bar = 2 µm.

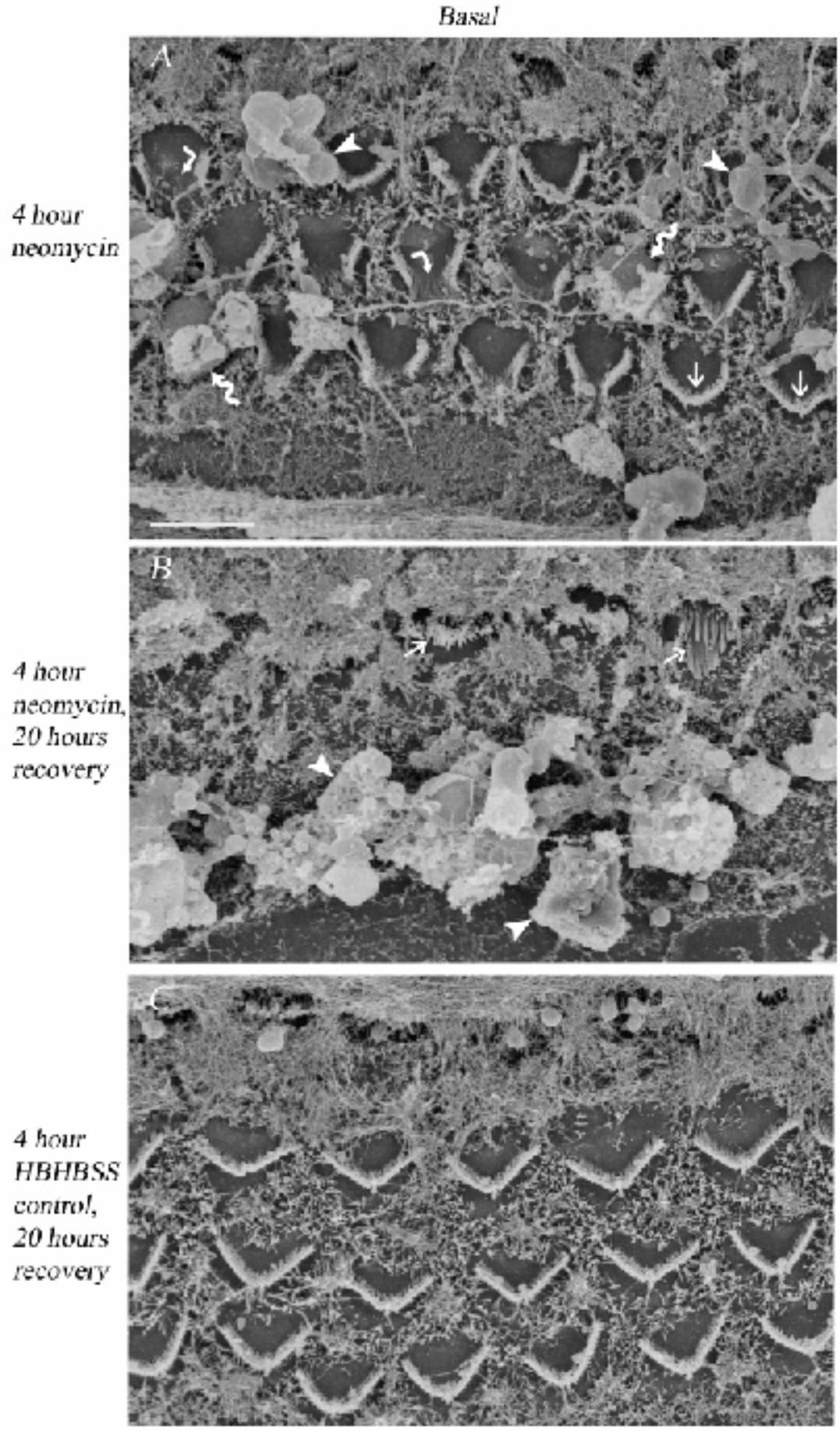
Basal
A
4 hour neomycin
B
4 hour neomycin, 20 hours recovery
C
4 hour HBHBSS control, 20 hours recovery

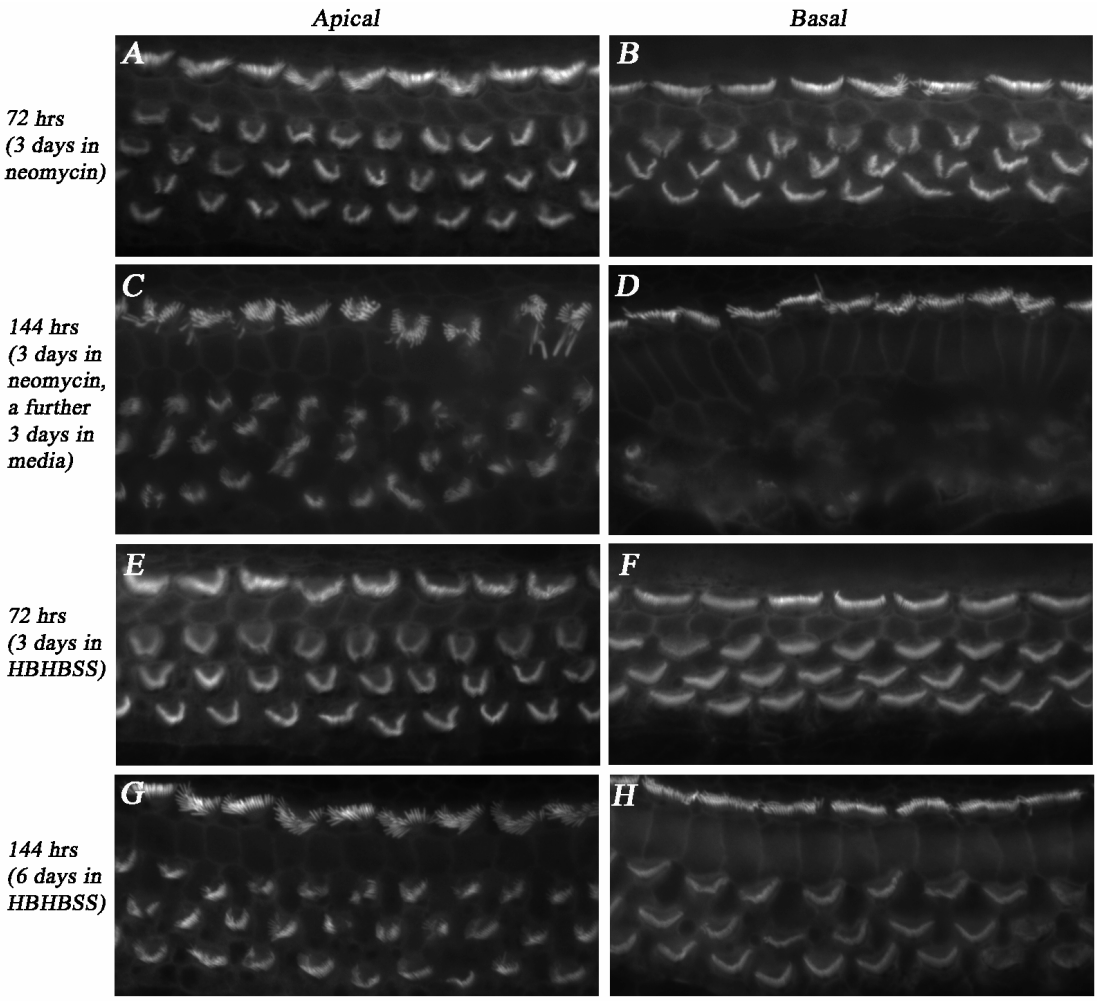

Figure 3.34 Fluorescent images of phalloidin stained cochlear cultures treated with 10 μM neomycin for 3 days and allowed to recover for a further 3 days. Apical (A, C) and basal region (B, D) cochlear cultures treated with 10 μM neomycin for 3 days (A, B) and allowed to recover for a further 3 days in neomycin-free media (C, D). Apical (E, G) and basal coil (F, H) cochlear cultures incubated with medium supplemented with 0.1 % HBHBSS control for 3 days (E, F) or for 6 days (G, H). Scale bar = 10 μm.

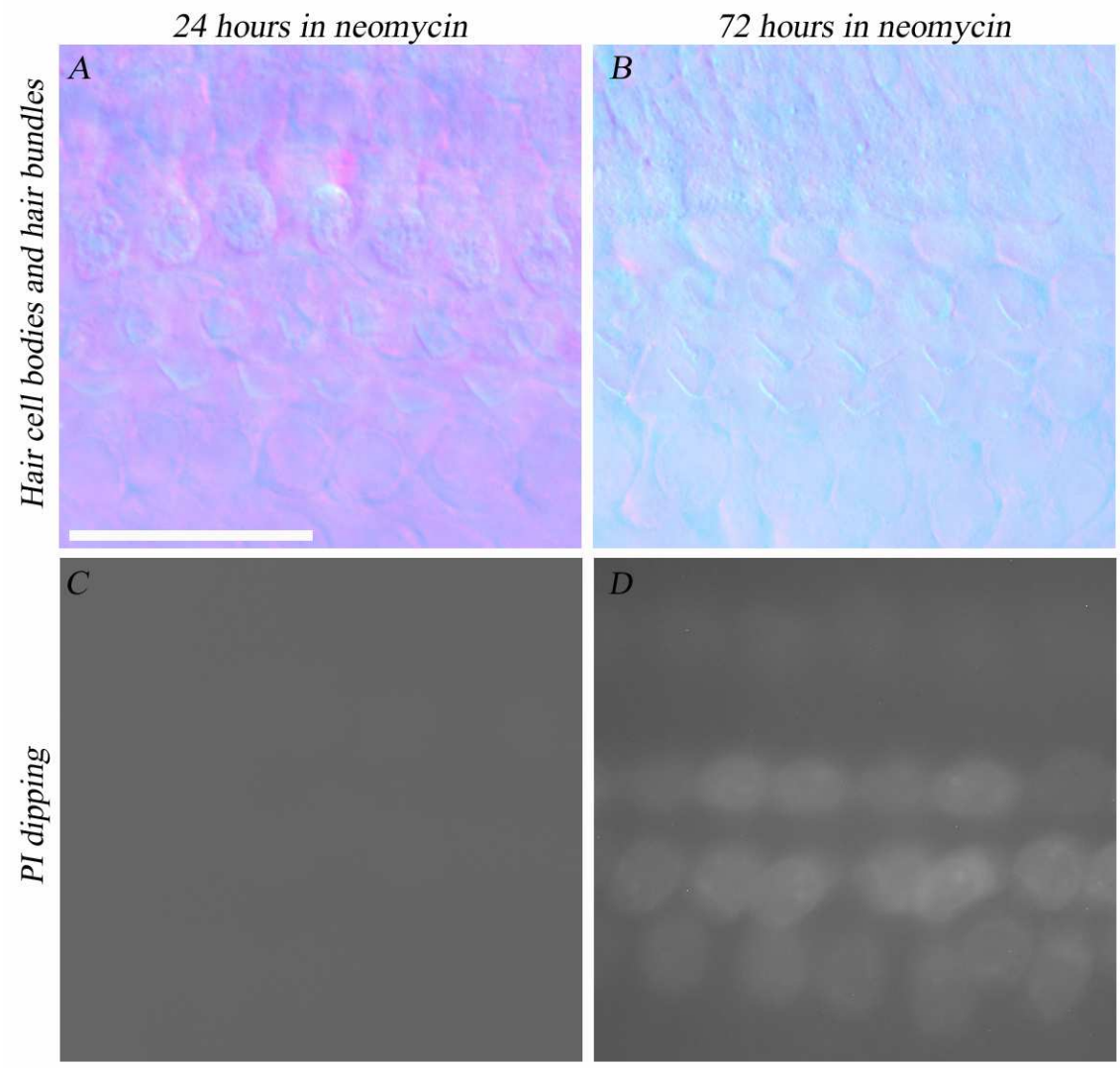

Figure 3.35 Light and fluorescent images of cochlear cultures incubated with 10 µM neomycin for 1 and 3 days prior to exposure to propidium iodide, n = 1. Basal cochlear cultures treated with 10 µM neomycin for 1 (A) and 3 (B) days, then dipped in propidium iodide (C, D). Scale bar = 50 µm.

Chapter 4

Discussion and conclusions

The key findings of this study are:

1) At low concentrations, staurosporine causes irreparable damage to auditory hair bundles but is not lethal to hair cells.

2) Staurosporine may cause hair bundle damage by affecting the functions of the phos-ERM proteins.

3) JNK inhibitor I (L-JNKI-I) is toxic to auditory hair cells.

4) Hair cells can recover from blebbing caused by neomycin treatment, but hair bundles show no recovery.

4.1 Staurosporine

Staurosporine is a microbial alkaloid first isolated in 1977 (Ōmura et al, 1977), and although initially described as a highly potent protein kinase C (PKC) inhibitor with IC_{50} values in the low nanomolar range (Tamaoki et al, 1986), it has since been shown to be a broad spectrum, ATP-competitive inhibitor of protein kinases with IC_{50} values varying from nanomolar to micro-molar concentrations depending on the protein kinase inhibited (Meggio et al, 1995). The broad spectrum of staurosporine activity may be due to its ability to cause induced-fit structural changes to protein kinase ATP-binding sites; furthermore, this induced-fit results in tight binding due to multiple non-covalent bonds, possibly explaining the low IC_{50} values that staurosporine can achieve with some protein kinases (Prade et al, 1997: Kinoshita et al, 2006: Nakano and Ōmura, 2009).

A widespread interest in staurosporine stems from its ability to induce most mammalian cell types to go into apoptosis (Stepczynska et al, 2001), leading to possible new anti-cancer treatments (Sánchez et al, 2006: Janosik et al, 2008: Olano et al, 2009).

However, the mechanism of staurosporine-induced apoptosis has yet to be fully elucidated, though it appears that staurosporine utilises both the mitochondrial

cytochrome c release pathway, and also directly activates Caspases 3 and 6 (Zhang et al, 1998: Chae et al, 2000: Belmokhtar et al, 2001: Gil et al, 2003). In addition to its common use in experiments to induce apoptosis, the low IC_{50} value of staurosporine against PKC means that staurosporine has a potential range of effects on the actin cytoskeleton through PKC inhibition (Pérez et al, 2006: Hoben and Athanasiou, 2008). In this set of experiments, staurosporine was used for the assessment of protein kinase inhibition in auditory hair cells and not for the induction of apoptosis. Hence in order to identify the most appropriate staurosporine concentration to be used, we examined previous studies that investigated staurosporine effects on auditory hair cells. Of the few studies that have used staurosporine for inhibiting protein kinases in OHCs, the range of concentrations used varied from 10 nM to 1 μM (Puschner and Schacht, 1997: Kakehata et al, 1995). Puschner and Schacht (1997) used 10 nM for 30 minutes to assess the effect of protein kinase inhibition on calmodulin-dependent protein kinase mediation of calcium-induced OHC motility, while Kakehata et al (1995) used 1 μM for 4-8 minutes to assess the effect of staurosporine on the neuropeptide substance P, which suppresses non-selective cation conductance in the OHC lateral walls. In this current study, a series of 24-hour dose response experiments showed that 5 -10 nM staurosporine treatment resulted in consistent inner and outer hair cell hair bundle damage with no concomitant hair cell loss.

4.1.1 Identifying the staurosporine target needed for maintenance of hair bundle structure.

To begin elucidating the mechanisms underlying staurosporine-induced damage of hair bundles, cochlear cultures were incubated with specific inhibitors of known staurosporine targets (CaM kinase II, myosin light chain kinase, PKA, PKC, PKG)

alone, or together as a protein kinase inhibitor cocktail. Cam kinase II, a ~ 540 kDa protein, is made up of multiple subunits (Yamauchi, 2005), and has been shown to bind and stabilise F-actin in neurons (Okamoto et al, 2007: Lin and Redmond, 2008). Cam kinase II is also thought to have a role in increasing OHC motility in response to elevated intracellular calcium (Sziklai et al, 2001). Myosin light chain kinases are calmodulin-dependent protein kinases, which phosphorylate the myosin regulatory light chain of the myosin II molecule, thus initiating interaction with actin and subsequent muscle contraction (Takashima, 2009). Although myosin light chain kinase has been localised to the cuticular plate of the OHCs (Jamesdaniel et al, 2009), its precise role has yet to be elucidated. Within the OHC, PKG has been implicated in a nitric oxide negative feedback loop that regulates ATP-induced intracellular calcium levels (Shen et al, 2005).

Despite these associations with auditory hair cells, our findings showed that inhibition of CaM kinase II, myosin light chain kinase and PKG had no effect on hair bundle morphology. PKA inhibition did not affect the cochlear basal region at all while causing the apical surfaces of both the inner and outer hair cells in the apical region of the cochlea to expand, presumably leading to hair bundle damage as a secondary effect. This apical region-only effect of PKA inhibition is unusual, as many studies of ototoxicity show a base-to-apical gradient where damage and hearing loss occurs first, and sometimes only, in the high-frequency basal region of the cochlea (Crofton et al, 1994: Löwenheim et al, 1999b: Plontke et al, 2007). Perhaps damage to the apical, but not the basal, cochlear regions indicate that the action of PKA is dependent on hair-bundle maturity, with the earlier maturing basal region hair bundles being unaffected by PKA inhibition.

4.1.2 Staurosporine is unlikely to act through inhibition of PKC.

There are currently 10 known isoforms of PKC (Roffey et al, 2009), and as the IC_{50} value of staurosporine for PKC is low at 0.7 nM, the PKC inhibitor BIM1 was anticipated to cause some hair-bundle damage akin to that seen for staurosporine. At 1 μM, BIM 1 inhibits 4 PKC isoforms (PKC_{α}, $PKC_{\beta I}$, PKC_{δ} and PKC_{ε}), but in our current set of experiments, no hair-bundle damage was seen. Rottlerin, reportedly a PKC_{δ} and PKC_{θ} specific inhibitor, caused some hair-cell loss as well as possible shortening of the surviving hair bundles.The PKC_{θ} specific inhibitor, the myristoylated PKC_{θ} pseudosubstrate sequence peptide Myr-LHQRRGAIKQAKVHHV KC-NH_2, primarily caused hair-cell loss although normal hair bundles were seen on the remaining hair cells.

There is an inconsistency in these results though, as BIM1 inhibits PKC_{δ} but caused no hair-bundle damage, the detrimental effects on hair bundles caused by Rottlerin may not be through PKC_{δ} inhibition, but via PKC_{θ} inhibition. However, the damage caused by Myr-LHQRRGAIKQAKVHHVKC-NH_2 and Rottlerin are very different.

This discrepancy we observed between Rottlerin and the other PKC inhibitors tested may perhaps be due a lack of PKC_{δ} specificity for Rottlerin despite it being widely used as a PKC_{δ} inhibitor. Davies et al (2000) tested the inhibitory actions of Rottlerin against a range of protein kinases and found that it did not inhibit PKC_{δ}, although it did inhibit many other protein kinases. The suggestion that Rottlerin could act through PKC_{δ} independent pathways or has multiple targets were supported by other studies that showed Rottlerin exerted inhibitory effects even where PKC_{δ} expression had been suppressed, or in cells from PKC_{δ} null mice (Leitges et al, 2001: Kayali et al, 2002: Zhao et al, 2002). Other studies have suggested that Rottlerin could mimic the effects of PKC_{δ} inhibition by direct action on mitochondria (Soltoff, 2001: Kurosu et al, 2007).

Hence none of the three PKC inhibitors used in our set of experiments reproduced the morphological effect of staurosporine on hair bundles.

Attempting to identify which potential staurosporine protein kinase target causes the hair-bundle damage seen in hair cells may be a lengthy process. When the inhibitory effect of staurosporine was tested against 235 protein kinases, it showed IC_{50} values for over 50 protein kinases in the nanomolar range (Nakano and Ōmura, 2009). Hence even with the efforts made here to narrow down the range of protein kinases responsible for hair-bundle damage, given the broad-spectrum nature of staurosporine activity, there are many more protein kinases, and combinations thereof, that remain to be investigated.

4.1.3 Intracellular features of staurosporine treatment.

4.1.3.1 Bulging of the apical plasma membrane may have caused hair bundle collapse.

Our TEM examination showed staurosporine treated hair cells had a bulging apical plasma membrane separated from the cuticular plate by the presence of vesicles and cytoplasmic materials. Under normal circumstances, the attachment of the apical membrane to both the stereocilia and the cuticular plate contributes to the mechanical properties of the hair bundle (Hirokawa and Tilney, 1982), hence it is possible that the bulging we observed caused hair bundle collapse in staurosporine treated hair cells. This phenomenon of the bulging apical plasma membrane resulting from staurosporine treatment differs from the hair bundle damage caused by noise seen in other studies. When rabbit and cat auditory hair bundles were subjected to noise exposure, both showed hair bundle collapse and formation of giant stereocilia. However, there was no separation of the plasma membrane from the cuticular plate, and the most common

stereocilia pathology was breaking of the stereocilia at the ankle where the rootlet enters the cuticular plate (Engström et al, 1983: Liberman, 1987).

4.1.3.2 Staurosporine does not affect endocytosis at the hair cell apical surface.

As staurosporine caused the plasma membrane to bulge, we proposed a hypothesis that this bulging might have been caused by a reduction in the rate of endocytosis compared to the rate of exocytosis. However, application of cationic ferritin showed that endocytic vesicles were present beneath the rucked plasma membrane suggesting that endocytosis has not been inhibited, although a reduction in the rate of endocytosis is still possible. An interesting feature of this result is the demonstration of endocytosis within the area of the base of the hair bundle. In other studies of endocytosis in the auditory hair cells of adult guinea pigs, it has been shown that for IHCs, endocytosis occurs primarily in the pericuticular zone with endocytic vesicles being transported by an infracuticular system (Griesinger et al, 2004). In OHCs, the site of endocytosis is reported to be very specifically in the area corresponding to the basal body of the kinocilium (Griesinger et al, 2004), with vesicles subsequently collecting beneath the cuticular plate (Meyer et al, 2001). In our experiments, given that in staurosporine treated cells there is a separation of plasma membrane from the cuticular plate, it is plausible that on separation, the plasma membrane is “released” and able to perform endocytosis. However, it should be noted that vesicles containing ferritin were also occasionally seen in control cultures. It is possible that the age of the cultures used could affect the location of the apical endocytic vesicles in control cultures. This is illustrated by the observation of a large numbers of vesicles beneath the apical surfaces of early post-natal mice (P1-P2) basal region hair cells by Forge and Richardson (1993), although in both this study and the

current set of experiments, the potential for vesicles resulting from cultural artefacts cannot be excluded.

4.1.4 Staurosporine and the ERM proteins.

The distinctive separation of the plasma membrane with the presence of vesicles under the hair bundle and rootlet disruption seen in our results was extremely similar to that seen in the OHCs of radixin deficient mice at P21 (Kitajiri et al, 2004) (Figure 4.1), suggesting that staurosporine action might involve ERM proteins.

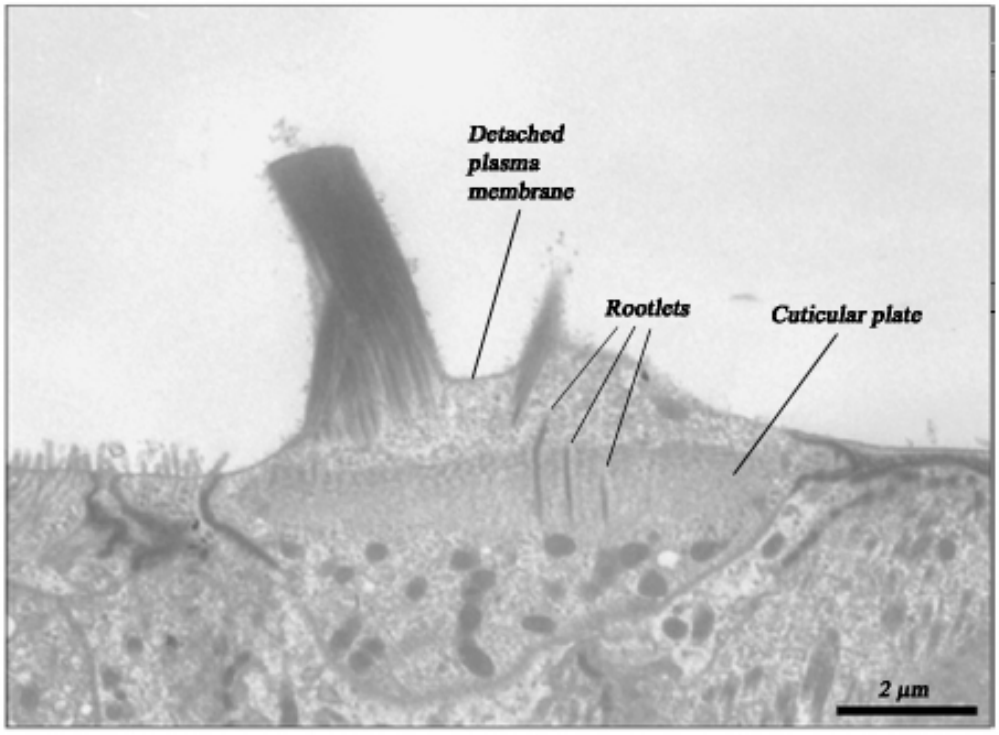

Figure 4.1 Hair cell stereocilia from P21 radixin null mice, adapted from Kitajiri et al (2004).

The ERM proteins are a highly conserved group of plasma membrane-to-cytoskeleton cross-linking proteins belonging to the band 4.1 superfamily, which share a ~ 300 amino acid common region called a FERM (**F**our point one **E**zrin, **R**adixin, **M**oesin) domain (Louvet-Vallée, 2000). The FERM domain is situated at the membrane binding

N-terminus, and is connected to the F-actin binding C-terminus by a sequence of ~ 200 amino acids named the α domain (Fiévet et al, 2007).

The activity of the ERM proteins is dependent on conformational changes, when inactive in the cytoplasm, the N-termini and C-termini show a very strong interaction via their N- and C-ERMAD (ERM association domains), effectively masking their own F-actin binding site (Gary and Bretscher, 1995). Activation of the ERM proteins is thought to be a two-stage process, where binding of the FERM domain with PIP_2 exposes a threonine residue, which is then phosphorylated, leading to ERM activation (Fiévet et al, 2004: Hao et al, 2009).

4.1.4.1 A potential model for staurosporine action in cochlear hair cells.

The antibody we used to detect radixin does not distinguish between the phosphorylated and non-phosphorylated forms; therefore an antibody to detect for the presence of phos-ERM was also used. Cochlear cultures incubated with staurosporine showed a noticeable reduction in phos-ERM levels by as early as 1 hour. At 14 hours, there was a significant decrease in the amount of phos-ERM but not of radixin in staurosporine treated cultures compared to their DMSO controls. Thus it is possible that in hair cells, staurosporine prevents activation (phosphorylation) of ERM proteins, resulting in a decrease in phosphorylated-ERM proteins, thus leading to the detachment of the apical plasma membrane from the cuticular plate (Figure 4.2).

Our hypothesis that staurosporine affects the function of the ERM proteins as plasma membrane-to-cytoskeleton cross-linkers is supported by Yonemura et al (2002), who showed that in a range of kidney-derived cell lines, 10 nM staurosporine caused inactivation of ERM proteins, redistributing them from the plasma membrane back into the cytoplasm.

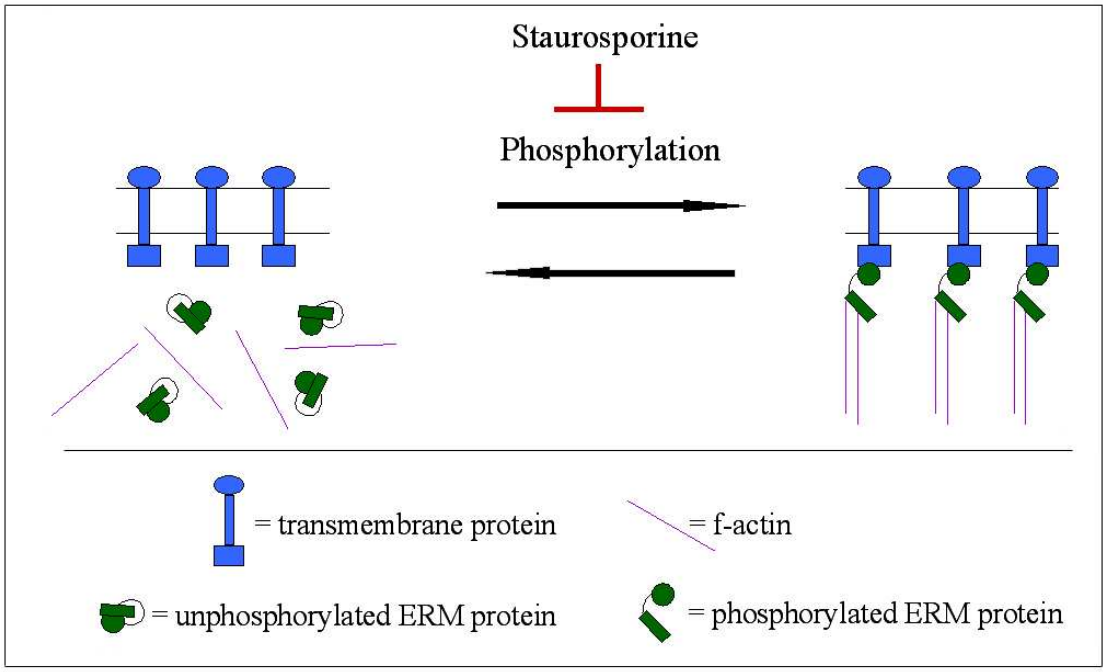

Figure 4.2 A possible mechanism for staurosporine action in hair cells: prevention of ERM protein activation could result in detachment of the plasma membrane from the cuticular plate region.

In cochlear hair cells, radixin has been localised to the hair bundle (Pataky et al, 2004: Khan et al, 2007), while ezrin was only detected faintly in hair and supporting cells and moesin was not detectable in hair cells at P20 (Kitajiri et al, 2004). However, as the Western blots carried out for this set of experiments used the entire organ of Corti, both phosphorylated ezrin and phosphorylated moesin were present, presumably from all the other cell types present in the organ of Corti. Nonetheless, the age of mice used here may also have contributed to the phosphorylated ezrin present in the Western blots, as Kitajiri et al (2004) showed that ezrin was clearly present in P1 radixin+/+ mice, although ezrin staining disappeared by P40.

4.1.4.2 Staurosporine inhibition of hair cell ERM proteins is unlikely to involve Rho A, B and C.

Several studies have shown that ERM proteins are activated by a Rho dependent pathway in a variety of cell types (Matsui et al, 1999: Haas et al, 2007). If this also applied to hair cells, then it would be reasonable to hypothesize that Rho inhibition would produce similar hair bundle damage to that seen with staurosporine. In the current set of experiments, inhibition of cochlear cultures with the Rho A, B, and C inhibitor *Clostridium botulinum* exoenzyme C3 transferase did not cause direct hair bundle damage, but rather an apparent expansion of the luminal surfaces of both hair and supporting cells.

Whether ERM protein activation relies on Rho or not appears to be highly dependent on cell type. In the same study in which the effect of staurosporine on ERM protein activation was assessed, Yonemura et al (2002) showed a number of cell lines that employ a Rho independent pathway for ERM activation. Interestingly, all of these cells lines were derived from the kidney. A close association between pathologies of the ear and in the kidney has long been noted (Taylor, 1965: Crawfurd and Toghill, 1968), and although this was attributed to parallel development times in gestation, is it now known that the inner ear and the kidney share many genes that are responsible for essential ion channel and transportation proteins (Izzedine et al, 2004: Lang et al, 2007).

Our experiments showed that staurosporine action on hair-cell ERM proteins may not involve Rho A, B and C. Other members of the Rho GTPase family however, namely Rac and Cdc42, have close associations with ERM activation in other cell types (Nakamura et al, 2000: Auvinen et al, 2007) and may well play a part in hair-cell ERM protein activation.

4.1.4.3 Staurosporine does not affect the distribution of PIP_2 in hair bundles.

Regardless of Rho pathway dependency, an important ERM activation pathway is the binding of the FERM domain to PIP_2 (Yonemura et al, 2002: Janke et al, 2008). Staurosporine could thus inhibit ERM activity by reducing the levels of available PIP_2. A study using rat basophilic leukaemia cells found that PIP_2 production increased with PKC activation, but this increase was suppressed by staurosporine-induced PKC inhibition, leading to the suggestion that PKC may somehow affect the activity of the phospholipid kinases upstream of PIP_2 (Apgar, 1995). If staurosporine does decrease PIP_2 levels in hair cells via PKC inhibition, then it is likely to be acting though PKC isoforms other than those inhibited by Myr-LHQRRGAIKQAKVHHVKC-NH_2 or BIM1 (though the 1 μM BIM1 used in the series of experiments presented here may not have inhibited PKC_ζ, which has an IC_{50} of 5.8 μM).

The broad-spectrum nature of staurosporine activity means that it may reduce PIP_2 levels in hair cells by inhibiting phosphoinositide 4-kinase (PI4K) and/or phosphoinositide 5-kinase (PI5K), the kinases involved in the PIP_2 synthesis, although currently there is no published literature to support this. There is a study using fibroblasts, however, which suggests staurosporine does not inhibit the phosphoinositide kinases, and therefore does not alter the levels of PIP_2 (Smith and Mooberry, 1992). In the current set of experiments, the PIP_2 reporter $PLC_{\delta1}PH$ showed PIP_2 distribution throughout the hair cell as well as the hair bundle in both control and staurosporine treated cochlear cultures, indicating that staurosporine probably does not affect PIP_2 distribution or levels in hair cells and hair bundles.

While there is agreement in the literature that activation of ERM requires binding to PIP_2 (Louvet-Vallée, 2000: Fiévet et al, 2007), there is less agreement on whether subsequent phosphorylation of ERM proteins is needed to either complete the activation

process, or to simply maintain the ERM proteins in an activated form (Yonemura et al, 2002). In both cases, phosphorylation remains essential to the proper function of ERM proteins, and staurosporine has been shown to inhibit two known ERM kinases, myotonic dystrophy kinase-related Cdc42-binding kinase (MRCK) and lymphocyte-oriented kinase (LOK), at nanomolar concentrations (Nakamura et al, 2000: Belkina et al, 2009: Nakano and Ōmura, 2009).

4.1.4.4 Staurosporine also causes loss of microvilli in supporting cells.

Early studies isolated ERM proteins from the brush border of chicken intestinal epithelial cells as well as microvilli of human carcinoma cells (Bretscher, 1983: Pakkanen et al, 1987). Since then, much work has been done on the essential role of ERM proteins in microvilli formation in a wide variety of cell types (Saotome et al, 2004: Bonilha et al, 2006: Lan et al, 2006). In our SEM images of basal region cochlear supporting cells, there is a distinct paucity of microvilli on their apical surfaces compared to controls after 14 hours of staurosporine treatment. This loss of microvilli may be due to the staurosporine-induced loss of ERM function in supporting cells, as antibody staining showed a clear decrease in levels of phos-ERM in microvilli of staurosporine treated supporting cells compared to controls.

4.2 Hair bundle recovery from staurosporine or neomycin treatment.

4.2.1 Hair bundles do not recover from staurosporine or neomycin treatment.

Previous studies have shown that hair cell loss is followed by hair cell regeneration in many species including fishes (Hernández et al, 2007), amphibians (Jones and Corwin, 1996) and birds (Corwin and Cotanche, 1988). Nevertheless, the fate of damaged hair bundles on hair cells that survive trauma is less clear, where tip links of P1 chick hair

bundles were lost due to noise exposure, they recovered to control numbers in approximately 3 days (Husbands et al, 1999: Kurian et al, 2003) while horizontal top connectors of chinchilla hair bundles have been shown to recover from noise trauma in 14-28 days (Tsuprun et al, 2003). However, the recoveries of tip links and horizontal top connectors shown by the studies referred to above appear to take place in hair bundles that retained good cohesion. Where the hair bundles of P10 chicks had degenerated into separate upright clumps due to noise damage, no hair bundle repair was observed after the 10-day recovery period (Cotanche, 1987b). If hair bundle recovery were dependent on the severity of disruption, then the complete hair bundle collapse caused by staurosporine would be unlikely to result in recovery.

While hair bundle collapse characterises the external morphological effect of staurosporine on cochlear hair cells in our experiments, the initial external morphological effect of neomycin manifests as blebbing on the hair cell apical surface. Neomycin is a member of the class of aminoglycoside antibiotics, which are known to cause apoptosis by either generation of reactive oxygen species (Clerici et al, 1996: Lopez-Gonzalez et al, 1999) or by caspase activation (Cunningham et al, 2002: Taylor et al, 2008). Goodyear et al (2008) showed that hair cells could recover from blebbing caused by 5 or 30 minutes of neomycin treatment at 20 °C following a 2-hour recovery period. Furthermore, Goodyear et al (2008) showed that hair cells treated with neomycin for 30 minutes could survive for at least a further 24 hours with no additional detrimental effects on the hair bundles (Goodyear et al, 2008. Supplemental material: Figure 3, available at www.jneurosci.org). Yet the time window in which hair cells can recover from neomycin treatment appears to be narrow, the current set of experiments showed that after 60 minutes of neomycin treatment at 20 °C with 23 hours of recovery

time at 37 °C, blebbing was much reduced, but the hair bundles were showing signs of disruption. Longer neomycin treatment of 2 and 4 hours resulted in severe OHC hair bundle damage and OHCs being extruded.

4.2.2 Staurosporine and neomycin causes hair bundle degeneration after cessation of treatment.

The series of experiments presented here showed that hair bundle damage and collapse caused by either staurosporine or neomycin was not reparable. We also showed that even after cessation of treatment, staurosporine and neomycin caused hair bundle degeneration, even where there was no hair bundle damage when treatment ended. This phenomenon is in line with a previous study that showed undamaged chick hair cells at the cessation of noise trauma going on to develop damaged stereocilia within 24 hours (Cotanche, 1987b).

In the brief 2.5-hour treatment period used in this study, staurosporine must be adversely affecting one or more essential processes in hair bundle maintenance. Since these processes do not recover from this short treatment time, it may be possible that staurosporine is affecting longer-term gene expression, which under normal circumstances would contribute to maintaining the hair bundle. Staurosporine has been shown to affect gene expression in other cell types from expression of the neuropeptides neurotensin and neuromedin in pheochromocytoma cells (Tischler et al, 1991), and transcription of an insulin gene promoter in pancreatic cells (Shinozuka et al, 2003) to gene expression for important matrix proteins in fibrochondrocytes (Hoben and Athanasiou, 2008). Performing a microarray analysis of hair cells treated with staurosporine or DMSO as a control will help to clarify this issue.

In the case of neomycin, our results showed that 10 μM neomycin over 3 days does not produce visible hair bundle damage, however, a further 3 days in neomycin-free media resulted in loss of all OHC hair bundles. This loss of OHC hair bundles may result from the loss of the OHCs themselves, and this is supported by the loading of propidium iodide by OHCs seen after 3 days of neomycin incubation indicating that the OHCs were already fatally compromised. This experiment will need to be repeated to confirm these findings, but it will be exciting to further explore the mechanism of neomycin action in auditory hair cells.

4.3 JNK inhibitor I

4.3.1 Different JNK inhibitors have been used in different hair cell studies.

The JNK inhibitor I used in this series of experiments was the L-stereoisomer of the small peptide inhibitor engineered by Bonny et al (2001): L-JNKI-I. This inhibitor was created from islet-brain proteins (also known as JNK-interacting proteins [JIPs]), which are scaffold proteins that are mainly expressed in the pancreatic islets and in the brain. L-JNKI-I was created by linking a minimal 20–amino acid sequence of the islet-brain JNK binding domain (the minimal sequence needed to block c-Jun activation) to the 10–amino acid HIV-TAT sequence that allows rapid cell permeability. The authors also created a D-stereoisomer (D-JNKI-I) by the retro-inverso method: biologically active peptides normally consist of only L-amino acids (Stryer, 1995), but since these are highly susceptible to proteases (Brugidou et al, 1995), a method was developed whereby L-amino acid residues are replaced by the corresponding D-amino acids and the peptide sequence is reversed, resulting in a “retro-inverso”, more stable, D-stereoisomer (Hervé et al, 1997). Both L-JNKI-I and D-JNKI-I isoforms were found to block phosphorylation (activation) of c-Jun in the murine insulinoma cell line βTC-3,

although D-JNKI-I was 15-20 fold less effective than L-JNKI-I (Bonny et al, 2001). However, D-JNKI-I showed greater intracellular stability, and was able to prevent pro-inflammatory cytokine interleukin- (IL-1β) induced apoptosis for up to two weeks after just a single application compared to two days for L-JNKI-I (Bonny et al, 2001). Another JNK inhibitor commonly used in hair cell studies is CEP 1347 (previously known as KT 7515), a semi-synthetic derivative of the indolocarbazole K-252a found in broths of *Narcodiopsis* bacterium (Maroney et al, 1998: Bogoyevitch et al, 2004). CEP 1347 inhibits the kinase activity of the mixed lineage kinase (MLK) family, members of the MAPKK kinases (Figure 4.3), thus preventing JNK activation. Previous in vivo and in vitro studies have shown that inhibition of JNK by either D-JNKI-1 (Wang et al, 2003: Wang et al, 2007: Coleman et al, 2007: Eshraghi et al, 2007) or CEP 1347 (Pirvola et al, 2000) protects mammalian auditory hair cells from the effects of aminoglycoside or noise damage.

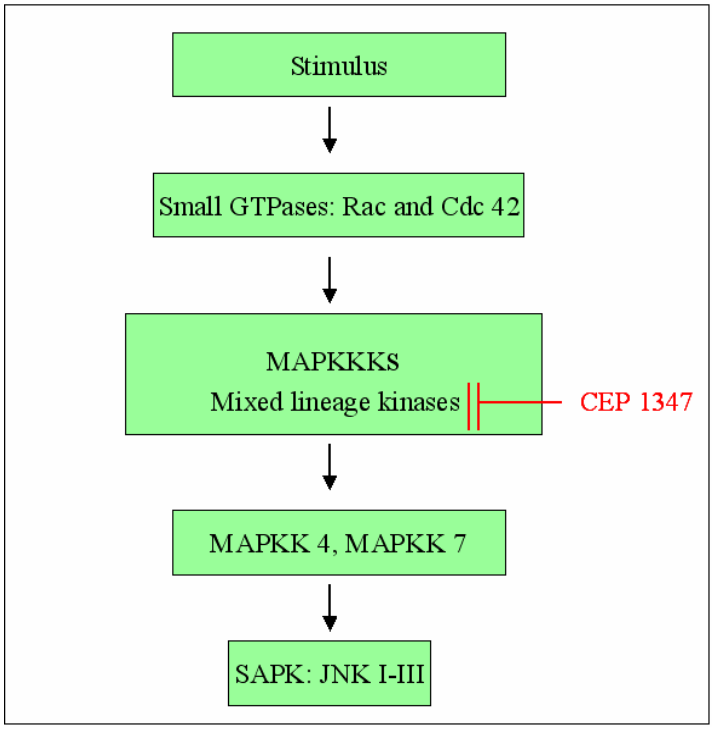

Figure 4.3 CEP 1347 prevents JNK activation by inhibition of upstream mixed lineage kinases.

4.3.2 JNK inhibitor I caused hair bundle damage and hair cell loss.

Of the JNK inhibitors used in this set of experiments, a search of the literature shows that neither JNK inhibitor V nor JNK inhibitor II (also known as SP600125) had been used previously in hair cell studies. However, in the light of studies showing JNK inhibitors conferring otoprotection, ototoxicity was not especially anticipated from the three JNK inhibitors (JNK inhibitors I, II and V) used in the current protein kinase screen. However, our experiments with L-JNKI-I unexpectedly resulted in elongation and collapse of both apical and basal region IHC stereocilia, with disrupted OHC hair bundles in the apical region, whilst OHC hair bundles were missing in the basal region, demonstrating a base to apex gradient in effect. This gradient is reflected in transmission electron micrographs as early as 5 hours after L-JNKI-I treatment, with basal region OHC hair bundles more severely disrupted than their apical region counterparts. Indeed, phosphatidylserine externalization could be detected in L-JNKI-I treated cultures as early as 5 minutes after onset the of treatment, suggesting that L-JNKI-I has a rapid effect on phospholipids, possibly as a first step in causing hair cells to undergo apoptosis. Neither JNK inhibitor II nor V had any detrimental effect when tested on cochlear cultures for 24 hours.

In other cell types, it is known that JNK inhibitor II prevents T-helper cell apoptosis as well as having anti-inflammatory actions (Bennett et al, 2001), while JNK inhibitor V protects cardiomyocytes and axons from apoptosis in response to ischaemia (Ferrandi et al, 2004: Carboni et al, 2008).

4.3.2.1 Possible methodological differences between studies.

Could differences in methodology account for the ototoxicity seen in our experiments as opposed to the otoprotection shown in other studies? In vitro experiments with either D-

JNKI-I (Wang et al, 2003) or CEP 1347 (Pirvola et al, 2000) used cultures from P3 mice or P2 rats respectively, which were similar in age to the P2 mice used in our set of experiments. The incubation times of 24-48 hours are also similar to those used in the current set of experiments, hence in terms of methodology, it is unlikely that differences in species or incubation times would have caused such a discrepancy between this study and others.

The concentration of 2 μM D-JNKI-I used by Wang et al (2003) was lower than the 5 μM L-JNKI-I used here, thus perhaps the higher concentration of JNK inhibitor used in our set of experiments may have caused hair bundle collapse and subsequent basal OHC loss. In a study of cortical neurons, Repici et al (2009) used 2 and 4 μM D-JNKI-I for in vitro experiments, but were unable to apply the higher concentration of 10 μM which they had used for their cell free conditions due to “toxic effects”, although the type and extent of the toxic effects were not stated. Bonny et al (2001) themselves used 25 μM L-JNKI-I to demonstrate suppression of c-Jun phosphorylation in the βTC-3 cell line, with no cell toxicity reported. However, the experiments presented here show that a concentration of 2 μM L-JNKI-I was sufficient to induce phosphatidylserine externalization, therefore it appears unlikely that a concentration difference between studies is the sole source of L-JNKI-I toxicity.

In terms of experimental design, previous experiments used D-JNKI-I in conjunction with other conditions such as noise (Coleman et al, 2007: Wang et al, 2007) or neomycin (Wang et al, 2003: Eshraghi et al, 2007). Although βTC-3 cells (Bonny et al, 2001) and cortical neurons (Repici et al, 2009) have been treated solely with D-JNKI-I under physiological conditions with no resultant cell death at up to a concentration of 25 μM (Bonny et al, 2001), this has yet to be carried out with D-JNKI-I in cochlear cultures.

4.3.2.2 Possible JNK inhibitor I isoform differences between studies

In both in vivo and in vitro studies of hair cells (Wang et al, 2003: Wang et al, 2004: Coleman et al, 2007: Eshraghi et al, 2007: Wang et al, 2007) as well as in a variety of other cell types (Hirt et al, 2004: Colombo et al, 2009), D-JNKI-I has been the JNK inhibitor I of choice over L-JNKI-I, in all probability for its greater intracellular stability. Stereoisomers are designated L or D according to their spatial arrangement as well as "+" or "-" according to their optical properties, and both structural and optical stereoisomers of the same compounds/drugs have been known to have different efficacy and toxic effects in a wide variety of drug groups (Stoschitzky et al, 1998: Smith, 2009). In the cochlea, this phenomenon has been documented for the loop diuretic indacrinone, where (+) indacrinone causes a dose dependent reduction in both the endocochlear potential and the compound action potential in chinchillas, while (-) indacrinone caused little or no change (Rybak et al, 1987: Rybak et al, 1991). In addition, the L-stereoisomer of the anti-cancer agent difluoromethylornithine (DFMO) has been demonstrated to significantly decrease the endocochlear potential and the compound action potential compared to D-DFMO in guinea pigs (McWilliams et al, 2000). Although Bonny et al (2001) showed that both L and D isoforms of JNKI-I inhibit phosphorylation of c-Jun in βTC-3 cells with no cell damage, another study showed that in a different murine insulinoma cell line, NIT-1, D-JNKI-I causes necrosis while L-JNKI-I prevents IL-1β-induced apoptosis by inhibition of c-Jun phosphorylation (Fornoni et al, 2007).

4.4 Summary of future directions

1) Although the fluorescence data from the current set of experiments suggest that staurosporine acts through inhibition of ERM protein phosphorylation, the

immunoblotting data that support this are derived from lysates obtained from the entire organ of Corti. In order to evaluate radixin and phos-ERM levels specifically in hair and supporting cells, separation of these cell types from the organ of Corti prior to immunoblotting would be necessary. This could be carried out by fluorescence-activated cell sorting (FACS) using antibodies against a hair cell marker such as Ptprq and $p27^{Kip1}$ for supporting cells.

2) It may be that in addition to causing hair bundle collapse, inhibition of phos-ERM function by staurosporine also prevents hair bundle recovery. It would therefore be informative to ascertain whether phos-ERM levels return to pre-treatment levels after cessation of staurosporine treatment.

3) The degeneration of hair bundles after the cessation of a brief period of staurosporine treatment suggests that staurosporine may affect gene expression that regulates hair bundle maintenance. Microarray analysis of hair cells treated with staurosporine could be carried out to investigate this possibility,

4) Early work suggested that JNK inhibitors may have a role in otoprotection against insults such as noise or aminoglycosides, but the JNK inhibitor used in the current experiments proved toxic to hair cells. Therefore, in order to clarify the potentially different effects of L-JNKI-I and D-JNKI-I on hair cells, it is important that experiments are carried out to assess cochlear cultures after treatment with these two stereoisomers at different concentrations over different times points.

4.5 Conclusions

Although staurosporine has been more conventionally used in studies to induce apoptosis, its use at low doses in our set of experiments revealed a vital role for protein phosphorylation in maintaining the integrity of the hair bundle. The attachment of the hair-cell apical membrane to the cuticular plate, as well as hair bundle morphology, are both disrupted by staurosporine treatment. The detachment of the hair-cell apical membrane may be caused by staurosporine inhibition of ERM protein phosphorylation, and further experiments are needed to confirm this.

We showed that staurosporine is not toxic to hair cells, but hair cells are unable to maintain or repair their hair bundles even after brief staurosporine treatment, indicating that staurosporine, in addition to inhibiting phos-ERM phosphorylation, may affect gene expression. All of the protein kinases that were inhibited in the initial screen are known to influence actin regulation in a variety of cell types. Despite this, inhibiting many of these protein kinases had either no effect on hair bundles or was lethal to hair cells, demonstrating that there is much yet to be learnt about the role of protein kinases in hair cell and hair-bundle maintenance. The inability of mammalian auditory hair cells to regenerate after trauma has led to the investigation of compounds that may confer otoprotection from both acoustic and pharmacological insults that would otherwise cause hair cells to undergo apoptosis. The JNK inhibitors D-JNKI-I and CEP1347 have been shown by several groups to achieve this. However, the use of L-JNKI-I in this set of experiments has shown for the first time that this compound is toxic to cochlear hair cells. Further investigation will confirm whether all JNK inhibitors exhibit otoprotective effects under the same experimental conditions, or whether otoprotection is confined to specific JNK inhibitors, a vital distinction if JNK inhibitors are to be considered for future clinical application.

References

Abelló G, Alsina B. 2007. Establishment of a proneural field in the inner ear. Int J Dev Biol 51:483-493.

Abou-Kheir W, Isaac B, Yamaguchi H, Cox D. 2008. Membrane targeting of WAVE2 is not sufficient for WAVE2-dependent actin polymerization: a role for IRSp53 in mediating the interaction between Rac and WAVE2. J Cell Sci 121:379-390.

Adato A, Lèfevre G, Delprat B, Michel V, Michalski N, Chardenoux S, Weil D, El-Amraoui A, Petit C. 2005. Usherin, the defective protein in Usher syndrome type IIA, is likely to be a component of interstereocilia ankle links in the inner ear sensory cells. Hum Mol Genet 14:3921-3932.

Adato A, Vreugde S, Joensuu T, Avidan N, Hamalainen R, Belenkiy O, Olender T, Bonne-Tamir B, Ben-Asher E, Espinos C, Millan JM, Lehesjoki AE, Flannery JG, Avraham KB, Pietrokovski S, Sankila EM, Beckmann JS, Lancet D. 2002. USH3A transcripts encode clarin-1, a four-transmembrane-domain protein with a possible role in sensory synapses. Eur J Hum Genet 10:339-350.

Ahmed ZM, Goodyear R, Riazuddin S, Lagziel A, Legan PK, Behra M, Burgess SM, Lilley KS, Wilcox ER, Griffith AJ, Frolenkov GI, Belyantseva IA, Richardson GP, Friedman TB. 2006. The tip-link antigen, a protein associated with the transduction complex of sensory hair cells, is protocadherin-15. J Neurosci 26:7022-7034.

Ahmed ZM, Riazuddin S, Aye S, Ali RA, Venselaar H, Anwar S, Belyantseva PP, Qasim M, Friedman TB. 2008. Gene structure and mutant alleles of PCDH15: nonsyndromic deafness DFNB23 and type 1 Usher syndrome. Hum Genet 124:215-223.

Ahmed ZM, Riazuddin S, Bernstein SL, Ahmed Z, Khan S, Griffith AJ, Morell RJ, Friedman TB, Wilcox ER. 2001. Mutations of the protocadherin gene PCDH15 cause Usher syndrome type 1F. Am J Hum Genet 69:25-34.

Ahmed ZM, Riazuddin S, Khan SN, Friedman PL, Friedman TB. 2009. USH1H, a novel locus for type I Usher syndrome, maps to chromosome 15q22-23. Clin Genet 75:86-91.

Alagramam KN, Yuan H, Kuehn MH, Murcia CL, Wayne S, Srisailpathy CR, Lowry RB, Knaus R, Van Laer L, Bernier FP, Schwartz S, Lee C, Morton CC, Mullins RF, Ramesh A, Van Camp G, Hageman GS, Woychik RP, Smith RJ. 2001. Mutations in the novel protocadherin PCDH15 cause Usher syndrome type 1F. Hum Mol Genet 10:1709-1718.

Altan ZM, Fenteany G. 2004. c-Jun N-terminal kinase regulates lamellipodial protrusion and cell sheet migration during epithelial wound closure by a gene expression-independent mechanism. Biochem Biophys Res Commun 322:56-67.

Anderson DW, Probst FJ, Belyantseva IA, Fridell RA, Beyer L, Martin DM, Wu D, Kachar B, Friedman TB, Raphael Y, Camper SA. 2000. The motor and tail regions of myosin XV are critical for normal structure and function of auditory and vestibular hair cells. Hum Mol Genet 9:1729-1738.

Andrianantoandro E, Pollard TD. 2006. Mechanism of actin filament turnover by severing and nucleation at different concentrations of ADF/cofilin. Mol Cell 24:13-23.

Aoki H, Kang PM, Hampe J, Yoshimura K, Noma T, Matsuzaki M, Izumo S. 2002. Direct activation of mitochondrial apoptosis machinery by c-Jun N-terminal kinase in adult cardiac myocytes. J Biol Chem 277:10244-10250.

Apgar JR. 1995. Activation of protein kinase C in rat basophilic leukemia cells stimulates increased production of phosphatidylinositol 4-phosphate and phosphatidylinositol 4,5-bisphosphate: correlation with actin polymerization. Mol Biol Cell 6:97-108.

Arima T, Uemura T, Yamamoto T. 1987. Three-dimensional visualizations of the inner ear hair cell of the guinea pig. A rapid-freeze, deep-etch study of filamentous and membranous organelles. Hear Res 25:61-68.

Arndt PG, Young SK, Lieber JG, Fessler MB, Nick JA, Worthen GS. 2005. Inhibition of c-Jun N-terminal kinase limits lipopolysaccharide-induced pulmonary neutrophil influx. Am J Respir Crit Care Med 171:978-986.

Assad JA, Shepherd GM, Corey DP. 1991. Tip-link integrity and mechanical transduction in vertebrate hair cells. Neuron 7:985-994.

Auvinen E, Kivi N, Vaheri A. 2007. Regulation of ezrin localization by Rac1 and PIPK in human epithelial cells. Exp Cell Res 313:824-833.

Avallone B, Fascio U, Balsamo G, Marmo F. 2008. Gentamicin ototoxicity in the saccule of the lizard Podarcis Sicula induces hair cell recovery and regeneration. Hear Res 235:15-22.

Baird RA, Burton MD, Lysakowski A, Fashena DS, Naeger RA. 2000. Hair cell recovery in mitotically blocked cultures of the bullfrog saccule. Proc Natl Acad Sci U S A 97:11722-11729.

Balak KJ, Corwin JT, Jones JE. 1990. Regenerated hair cells can originate from supporting cell progeny: evidence from phototoxicity and laser ablation experiments in the lateral line system. J Neurosci 10:2502-2512.

Bamburg JR. 1999. Proteins of the ADF/cofilin family: essential regulators of actin dynamics. Annu Rev Cell Dev Biol 15:185-230.

Bartles JR, Wierda A, Zheng L. 1996. Identification and characterization of espin, an actin-binding protein localized to the F-actin-rich junctional plaques of Sertoli cell ectoplasmic specializations. J Cell Sci 109 (Pt 6):1229-1239.

Barzik M, Kotova TI, Higgs HN, Hazelwood L, Hanein D, Gertler FB, Schafer DA. 2005. Ena/VASP proteins enhance actin polymerization in the presence of barbed end capping proteins. J Biol Chem 280:28653-28662.

Batts SA, Shoemaker CR, Raphael Y. 2009. Notch signaling and Hes labeling in the normal and drug-damaged organ of Corti. Hear Res 249:15-22.

Bear JE, Gertler FB. 2009. Ena/VASP: towards resolving a pointed controversy at the barbed end. J Cell Sci 122:1947-1953.

Belkina NV, Liu Y, Hao JJ, Karasuyama H, Shaw S. 2009. LOK is a major ERM kinase in resting lymphocytes and regulates cytoskeletal rearrangement through ERM phosphorylation. Proc Natl Acad Sci U S A 106:4707-4712.

Belmokhtar CA, Hillion J, Segal-Bendirdjian E. 2001. Staurosporine induces apoptosis through both caspase-dependent and caspase-independent mechanisms. Oncogene 20:3354-3362.

Belyantseva IA, Boger ET, Naz S, Frolenkov GI, Sellers JR, Ahmed ZM, Griffith AJ, Friedman TB. 2005. Myosin-XVa is required for tip localization of whirlin and differential elongation of hair-cell stereocilia. Nat Cell Biol 7:148-156.

Bennett BL, Sasaki DT, Murray BW, O'Leary EC, Sakata ST, Xu W, Leisten JC, Motiwala A, Pierce S, Satoh Y, Bhagwat SS, Manning AM, Anderson DW. 2001. SP600125, an anthrapyrazolone inhibitor of Jun N-terminal kinase. Proc Natl Acad Sci U S A 98:13681-13686.

Benz PM, Blume C, Seifert S, Wilhelm S, Waschke J, Schuh K, Gertler F, Munzel T, Renne T. 2009. Differential VASP phosphorylation controls remodeling of the actin cytoskeleton. J Cell Sci 122:3954-3965.

Beurg M, Fettiplace R, Nam JH, Ricci AJ. 2009. Localization of inner hair cell mechanotransducer channels using high-speed calcium imaging. Nat Neurosci 12:553-558.

Blundell MP, Bouma G, Metelo J, Worth A, Calle Y, Cowell LA, Westerberg LS, Moulding DA, Mirando S, Kinnon C, Cory GO, Jones GE, Snapper SB, Burns SO,

Thrasher AJ. 2009. Phosphorylation of WASp is a key regulator of activity and stability in vivo. Proc Natl Acad Sci U S A 106:15738-15743.

Bobkov AA, Muhlrad A, Pavlov DA, Kokabi K, Yilmaz A, Reisler E. 2006. Cooperative effects of cofilin (ADF) on actin structure suggest allosteric mechanism of cofilin function. J Mol Biol 356:325-334.

Boëda B, El-Amraoui A, Bahloul A, Goodyear R, Daviet L, Blanchard S, Perfettini I, Fath KR, Shorte S, Reiners J, Houdusse A, Legrain P, Wolfrum U, Richardson G, Petit C. 2002. Myosin VIIa, harmonin and cadherin 23, three Usher I gene products that cooperate to shape the sensory hair cell bundle. Embo J 21:6689-6699.

Bogoyevitch MA, Boehm I, Oakley A, Ketterman AJ, Barr RK. 2004. Targeting the JNK MAPK cascade for inhibition: basic science and therapeutic potential. Biochim Biophys Acta 1697:89-101.

Bonilha VL, Rayborn ME, Saotome I, McClatchey AI, Hollyfield JG. 2006. Microvilli defects in retinas of ezrin knockout mice. Exp Eye Res 82:720-729.

Bonny C, Oberson A, Negri S, Sauser C, Schorderet DF. 2001. Cell-permeable peptide inhibitors of JNK: novel blockers of beta-cell death. Diabetes 50:77-82.

Bork JM, Peters LM, Riazuddin S, Bernstein SL, Ahmed ZM, Ness SL, Polomeno R, Ramesh A, Schloss M, Srisailpathy CR, Wayne S, Bellman S, Desmukh D, Ahmed Z, Khan SN, Kaloustian VM, Li XC, Lalwani A, Bitner-Glindzicz M, Nance WE, Liu XZ, Wistow G, Smith RJ, Griffith AJ, Wilcox ER, Friedman TB, Morell RJ. 2001. Usher syndrome 1D and nonsyndromic autosomal recessive deafness DFNB12 are caused by allelic mutations of the novel cadherin-like gene CDH23. Am J Hum Genet 68:26-37.

Boulouiz R, Li Y, Soualhine H, Abidi O, Chafik A, Nurnberg G, Becker C, Nurnberg P, Kubisch C, Wollnik B, Barakat A. 2008. A novel mutation in the Espin gene causes autosomal recessive nonsyndromic hearing loss but no apparent vestibular dysfunction in a Moroccan family. Am J Med Genet A 146A:3086-3089.

Bretscher A. 1983. Purification of an 80,000-dalton protein that is a component of the isolated microvillus cytoskeleton, and its localization in nonmuscle cells. J Cell Biol 97:425-432.

Brugidou J, Legrand C, Mery J, Rabie A. 1995. The retro-inverso form of a homeobox-derived short peptide is rapidly internalised by cultured neurones: a new basis for an efficient intracellular delivery system. Biochem Biophys Res Commun 214:685-693.
Buchsbaum RJ. 2007. Rho activation at a glance. J Cell Sci 120:1149-1152.

Bustelo XR, Sauzeau V, Berenjeno IM. 2007. GTP-binding proteins of the Rho/Rac family: regulation, effectors and functions in vivo. Bioessays 29:356-370.

Cafaro J, Lee GS, Stone JS. 2007. Atoh1 expression defines activated progenitors and differentiating hair cells during avian hair cell regeneration. Dev Dyn 236:156-170.

Caldwell JE, Heiss SG, Mermall V, Cooper JA. 1989. Effects of CapZ, an actin capping protein of muscle, on the polymerization of actin. Biochemistry 28:8506-8514.

Carboni S, Boschert U, Gaillard P, Gotteland JP, Gillon JY, Vitte PA. 2008. AS601245, a c-Jun NH_2-terminal kinase (JNK) inhibitor, reduces axon/dendrite damage and cognitive deficits after global cerebral ischaemia in gerbils. Br J Pharmacol 153:157-163.

Casella JF, Maack DJ, Lin S. 1986. Purification and initial characterization of a protein from skeletal muscle that caps the barbed ends of actin filaments. J Biol Chem 261:10915-10921.

Chae HJ, Kang JS, Byun JO, Han KS, Kim DU, Oh SM, Kim HM, Chae SW, Kim HR. 2000. Molecular mechanism of staurosporine-induced apoptosis in osteoblasts. Pharmacol Res 42:373-381.

Chakrabarti A, Kelkar DA, Chattopadhyay A. 2006. Spectrin organization and dynamics: new insights. Biosci Rep 26:369-386.

Chaponnier C, Janmey PA, Yin HL. 1986. The actin filament-severing domain of plasma gelsolin. J Cell Biol 103:1473-1481.

Chen B, Li A, Wang D, Wang M, Zheng L, Bartles JR. 1999. Espin contains an additional actin-binding site in its N terminus and is a major actin-bundling protein of the Sertoli cell-spermatid ectoplasmic specialization junctional plaque. Mol Biol Cell 10:4327-4339.

Chen H, Bernstein BW, Bamburg JR. 2000. Regulating actin-filament dynamics in vivo. Trends Biochem Sci 25:19-23.

Chen ZY, Hasson T, Kelley PM, Schwender BJ, Schwartz MF, Ramakrishnan M, Kimberling WJ, Mooseker MS, Corey DP. 1996. Molecular cloning and domain structure of human myosin-VIIa, the gene product defective in Usher syndrome 1B. Genomics 36:440-448.

Clark JA, Pickles JO. 1996. The effects of moderate and low levels of acoustic overstimulation on stereocilia and their tip links in the guinea pig. Hear Res 99:119-128.

Clerici WJ, Hensley K, DiMartino DL, Butterfield DA. 1996. Direct detection of ototoxicant-induced reactive oxygen species generation in cochlear explants. Hear Res 98:116-124.

Cochran SL, Correia MJ. 1995. Functional support of glutamate as a vestibular hair cell transmitter in an amniote. Brain Res 670:321-325.

Coleman JK, Littlesunday C, Jackson R, Meyer T. 2007. AM-111 protects against permanent hearing loss from impulse noise trauma. Hear Res 226:70-78.

Colombo A, Bastone A, Ploia C, Sclip A, Salmona M, Forloni G, Borsello T. 2009. JNK regulates APP cleavage and degradation in a model of Alzheimer's disease. Neurobiol Dis 33:518-525.

Comis SD, Pickles JO, Osborne MP. 1985. Osmium tetroxide postfixation in relation to the crosslinkage and spatial organization of stereocilia in the guinea-pig cochlea. J Neurocytol 14:113-130.

Corwin JT. 1992. Regeneration in the auditory system. Exp Neurol 115:7-12.

Corwin JT, Cotanche DA. 1988. Regeneration of sensory hair cells after acoustic trauma. Science 240:1772-1774.

Cotanche DA. 1987a. Development of hair cell stereocilia in the avian cochlea. Hear Res 28:35-44.

Cotanche DA. 1987b. Regeneration of hair cell stereociliary bundles in the chick cochlea following severe acoustic trauma. Hear Res 30:181-195.

Crawfurd MD, Toghill PJ. 1968. Alport's syndrome of hereditary nephritis and deafness. Q J Med 37:563-576.

Crofton KM, Janssen R, Prazma J, Pulver S, Barone S, Jr. 1994. The ototoxicity of 3,3'-iminodipropionitrile: functional and morphological evidence of cochlear damage. Hear Res 80:129-140.

Cunningham LL, Cheng AG, Rubel EW. 2002. Caspase activation in hair cells of the mouse utricle exposed to neomycin. J Neurosci 22:8532-8540.

Daudet N, Lebart MC. 2002. Transient expression of the t-isoform of plastins/fimbrin in the stereocilia of developing auditory hair cells. Cell Motil Cytoskeleton 53:326-336.

Daudet N, Ripoll C, Lenoir M. 2002. Transforming growth factor-alpha-induced cellular changes in organotypic cultures of juvenile, amikacin-treated rat organ of corti. J Comp Neurol 442:6-22.

Davies SP, Reddy H, Caivano M, Cohen P. 2000. Specificity and mechanism of action of some commonly used protein kinase inhibitors. Biochem J 351:95-105.

de Arruda MV, Watson S, Lin CS, Leavitt J, Matsudaira P. 1990. Fimbrin is a homologue of the cytoplasmic phosphoprotein plastin and has domains homologous with calmodulin and actin gelation proteins. J Cell Biol 111:1069-1079.

Delanote V, Vandekerckhove J, Gettemans J. 2005. Plastins: versatile modulators of actin organization in (patho) physiological cellular processes. Acta Pharmacol Sin 26:769-779.

Delprat B, Michel V, Goodyear R, Yamasaki Y, Michalski N, El-Amraoui A, Perfettini I, Legrain P, Richardson G, Hardelin JP, Petit C. 2005. Myosin XVa and whirlin, two deafness gene products required for hair bundle growth, are located at the stereocilia tips and interact directly. Hum Mol Genet 14:401-410.

Demêmes D, Scarfone E. 1992. Fodrin immunocytochemical localization in the striated organelles of the rat vestibular hair cells. Hear Res 61:155-160.

Dérijard B, Hibi M, Wu IH, Barrett T, Su B, Deng T, Karin M, Davis RJ. 1994. JNK1: a protein kinase stimulated by UV light and Ha-Ras that binds and phosphorylates the c-Jun activation domain. Cell 76:1025-1037.

Després G, Hafidi A, Romand R. 1991. Immunohistochemical localization of nerve growth factor receptor in the cochlea and in the brainstem of the perinatal rat. Hear Res 52:157-165.

Di Palma F, Pellegrino R, Noben-Trauth K. 2001. Genomic structure, alternative splice forms and normal and mutant alleles of cadherin 23 (Cdh23). Gene 281:31-41.

Dickens M, Rogers JS, Cavanagh J, Raitano A, Xia Z, Halpern JR, Greenberg ME, Sawyers CL, Davis RJ. 1997. A cytoplasmic inhibitor of the JNK signal transduction pathway. Science 277:693-696.

DiNubile MJ, Huang S. 1997. High concentrations of phosphatidylinositol-4,5-bisphosphate may promote actin filament growth by three potential mechanisms:

inhibiting capping by neutrophil lysates, severing actin filaments and removing capping protein-beta2 from barbed ends. Biochim Biophys Acta 1358:261-278.

Doetzlhofer A, White PM, Johnson JE, Segil N, Groves AK. 2004. In vitro growth and differentiation of mammalian sensory hair cell progenitors: a requirement for EGF and periotic mesenchyme. Dev Biol 272:432-447.

Dooling RJ, Ryals BM, Manabe K. 1997. Recovery of hearing and vocal behavior after hair-cell regeneration. Proc Natl Acad Sci U S A 94:14206-14210.

Drenckhahn D, Engel K, Hofer D, Merte C, Tilney L, Tilney M. 1991. Three different actin filament assemblies occur in every hair cell: each contains a specific actin crosslinking protein. J Cell Biol 112:641-651.

Duncan LJ, Mangiardi DA, Matsui JI, Anderson JK, McLaughlin-Williamson K, Cotanche DA. 2006. Differential expression of unconventional myosins in apoptotic and regenerating chick hair cells confirms two regeneration mechanisms. J Comp Neurol 499:691-701.

Duncan RK, Saunders JC. 2000. Stereocilium injury mediates hair bundle stiffness loss and recovery following intense water-jet stimulation. J Comp Physiol A 186:1095-1106.

Ebermann I, Scholl HP, Charbel Issa P, Becirovic E, Lamprecht J, Jurklies B, Millan JM, Aller E, Mitter D, Bolz H. 2007. A novel gene for Usher syndrome type 2: mutations in the long isoform of whirlin are associated with retinitis pigmentosa and sensorineural hearing loss. Hum Genet 121:203-211.

Edwards DC, Sanders LC, Bokoch GM, Gill GN. 1999. Activation of LIM-kinase by Pak1 couples Rac/Cdc42 GTPase signalling to actin cytoskeletal dynamics. Nat Cell Biol 1:253-259.

El Sayegh TY, Arora PD, Ling K, Laschinger C, Janmey PA, Anderson RA, McCulloch CA. 2007. Phosphatidylinositol-4,5 bisphosphate produced by PIP5KIgamma regulates

gelsolin, actin assembly, and adhesion strength of N-cadherin junctions. Mol Biol Cell 18:3026-3038.

El-Amraoui A, Petit C. 2005. Usher I syndrome: unravelling the mechanisms that underlie the cohesion of the growing hair bundle in inner ear sensory cells. J Cell Sci 118:4593-4603.

Engström B, Flock Å, Borg E. 1983. Ultrastructural studies of stereocilia in noise-exposed rabbits. Hear Res 12:251-264.

Eshraghi AA, Wang J, Adil E, He J, Zine A, Bublik M, Bonny C, Puel JL, Balkany TJ, Van De Water TR. 2007. Blocking c-Jun-N-terminal kinase signalling can prevent hearing loss induced by both electrode insertion trauma and neomycin ototoxicity. Hear Res 226:168-177.

Eun DW, Ahn SH, You JS, Park JW, Lee EK, Lee HN, Kang GM, Lee JC, Choi WS, Seo DW, Han JW. 2007. PKCepsilon is essential for gelsolin expression by histone deacetylase inhibitor apicidin in human cervix cancer cells. Biochem Biophys Res Commun 354:769-775.

Fayard E, Tintignac LA, Baudry A, Hemmings BA. 2005. Protein kinase B/Akt at a glance. J Cell Sci 118:5675-5678.

Ferrandi C, Ballerio R, Gaillard P, Giachetti C, Carboni S, Vitte PA, Gotteland JP, Cirillo R. 2004. Inhibition of c-Jun N-terminal kinase decreases cardiomyocyte apoptosis and infarct size after myocardial ischemia and reperfusion in anaesthetized rats. Br J Pharmacol 142:953-960.

Fettiplace R, Hackney CM. 2006. The sensory and motor roles of auditory hair cells. Nat Rev Neurosci 7:19-29.

Fiévet B, Louvard D, Arpin M. 2007. ERM proteins in epithelial cell organization and functions. Biochim Biophys Acta 1773:653-660.

Fiévet BT, Gautreau A, Roy C, Del Maestro L, Mangeat P, Louvard D, Arpin M. 2004. Phosphoinositide binding and phosphorylation act sequentially in the activation mechanism of ezrin. J Cell Biol 164:653-659.

Fishman G, Vasquez V, Fishman M, Berger D. 1979. Visual loss and foveal lesions in Usher's syndrome. Br J Ophthalmol 63:484-488.

Flock Å, Cheung HC. 1977. Actin filaments in sensory hairs of inner ear receptor cells. J Cell Biol 75:339-343.

Forge A, Li L, Corwin JT, Nevill G. 1993. Ultrastructural evidence for hair cell regeneration in the mammalian inner ear. Science 259:1616-1619.

Forge A, Richardson G. 1993. Freeze fracture analysis of apical membranes in cochlear cultures: differences between basal and apical-coil outer hair cells and effects of neomycin. J Neurocytol 22:854-867.

Forge A, Souter M, Denman-Johnson K. 1997. Structural development of sensory cells in the ear. Semin Cell Dev Biol 8:225-237.

Fornoni A, Cobianchi L, Sanabria NY, Pileggi A, Molano RD, Ichii H, Rosero S, Inverardi L, Ricordi C, Pastori RL. 2007. The l-isoform but not d-isoforms of a JNK inhibitory peptide protects pancreatic β-cells. Biochem Biophys Res Commun 354:227-233.

Friedman LM, Dror AA, Avraham KB. 2007. Mouse models to study inner ear development and hereditary hearing loss. Int J Dev Biol 51:609-631.

Friedman TB, Sellers JR, Avraham KB. 1999. Unconventional myosins and the genetics of hearing loss. Am J Med Genet 89:147-157.

Furness DN, Mahendrasingam S, Ohashi M, Fettiplace R, Hackney CM. 2008. The dimensions and composition of stereociliary rootlets in mammalian cochlear hair cells:

comparison between high- and low-frequency cells and evidence for a connection to the lateral membrane. J Neurosci 28:6342-6353.

Furness DN, Richardson GP, Russell IJ. 1989. Stereociliary bundle morphology in organotypic cultures of the mouse cochlea. Hear Res 38:95-109.

Gale JE, Marcotti W, Kennedy HJ, Kros CJ, Richardson GP. 2001. FM1-43 dye behaves as a permeant blocker of the hair-cell mechanotransducer channel. J Neurosci 21:7013-7025.

Gale JE, Meyers JR, Periasamy A, Corwin JT. 2002. Survival of bundleless hair cells and subsequent bundle replacement in the bullfrog's saccule. J Neurobiol 50:81-92.

Gary R, Bretscher A. 1995. Ezrin self-association involves binding of an N-terminal domain to a normally masked C-terminal domain that includes the F-actin binding site. Mol Biol Cell 6:1061-1075.

Gibson F, Walsh J, Mburu P, Varela A, Brown KA, Antonio M, Beisel KW, Steel KP, Brown SD. 1995. A type VII myosin encoded by the mouse deafness gene shaker-1. Nature 374:62-64.

Gieni RS, Hendzel MJ. 2009. Actin dynamics and functions in the interphase nucleus: moving toward an understanding of nuclear polymeric actin. Biochem Cell Biol 87:283-306.

Glowatzki E, Cheng N, Hiel H, Yi E, Tanaka K, Ellis-Davies GC, Rothstein JD, Bergles DE. 2006. The glutamate-aspartate transporter GLAST mediates glutamate uptake at inner hair cell afferent synapses in the mammalian cochlea. J Neurosci 26:7659-7664.

Gil J, Almeida S, Oliveira CR, Rego AC. 2003. Cytosolic and mitochondrial ROS in staurosporine-induced retinal cell apoptosis. Free Radic Biol Med 35:1500-1514.

Glaser M, Wanaski S, Buser CA, Boguslavsky V, Rashidzada W, Morris A, Rebecchi M, Scarlata SF, Runnels LW, Prestwich GD, Chen J, Aderem A, Ahn J, McLaughlin S.

1996. Myristoylated alanine-rich C kinase substrate (MARCKS) produces reversible inhibition of phospholipase C by sequestering phosphatidylinositol 4,5-bisphosphate in lateral domains. J Biol Chem 271:26187-26193.

Gong TW, Karolyi IJ, Macdonald J, Beyer L, Raphael Y, Kohrman DC, Camper SA, Lomax MI. 2006. Age-related changes in cochlear gene expression in normal and shaker 2 mice. J Assoc Res Otolaryngol 7:317-328.

Goodyear RJ, Gale JE, Ranatunga KM, Kros CJ, Richardson GP. 2008. Aminoglycoside-induced phosphatidylserine externalization in sensory hair cells is regionally restricted, rapid, and reversible. J Neurosci 28:9939-9952.

Goodyear RJ, Legan PK, Wright MB, Marcotti W, Oganesian A, Coats SA, Booth CJ, Kros CJ, Seifert RA, Bowen-Pope DF, Richardson GP. 2003. A receptor-like inositol lipid phosphatase is required for the maturation of developing cochlear hair bundles. J Neurosci 23:9208-9219.

Goodyear RJ, Marcotti W, Kros CJ, Richardson GP. 2005. Development and properties of stereociliary link types in hair cells of the mouse cochlea. J Comp Neurol 485:75-85.

Gould TD, Manji HK. 2005. Glycogen synthase kinase-3: a putative molecular target for lithium mimetic drugs. Neuropsychopharmacology 30:1223-1237.

Griesinger CB, Richards CD, Ashmore JF. 2004. Apical endocytosis in outer hair cells of the mammalian cochlea. Eur J Neurosci 20:41-50.

Gubbels SP, Woessner DW, Mitchell JC, Ricci AJ, Brigande JV. 2008. Functional auditory hair cells produced in the mammalian cochlea by in utero gene transfer. Nature 455:537-541.

Guma M, Rius J, Duong-Polk KX, Haddad GG, Lindsey JD, Karin M. 2009. Genetic and pharmacological inhibition of JNK ameliorates hypoxia-induced retinopathy through interference with VEGF expression. Proc Natl Acad Sci U S A 106:8760-8765.

Gupta S, Barrett T, Whitmarsh AJ, Cavanagh J, Sluss HK, Derijard B, Davis RJ. 1996. Selective interaction of JNK protein kinase isoforms with transcription factors. Embo J 15:2760-2770.

Haas MA, Vickers JC, Dickson TC. 2007. Rho kinase activates ezrin-radixin-moesin (ERM) proteins and mediates their function in cortical neuron growth, morphology and motility in vitro. J Neurosci Res 85:34-46.

Haddon C, Jiang YJ, Smithers L, Lewis J. 1998. Delta-Notch signalling and the patterning of sensory cell differentiation in the zebrafish ear: evidence from the mind bomb mutant. Development 125:4637-4644.

Hall A. 2009. The cytoskeleton and cancer. Cancer Metastasis Rev 28:5-14.

Han JW, Ahn SH, Park SH, Wang SY, Bae GU, Seo DW, Kwon HK, Hong S, Lee HY, Lee YW, Lee HW. 2000. Apicidin, a histone deacetylase inhibitor, inhibits proliferation of tumor cells via induction of p21WAF1/Cip1 and gelsolin. Cancer Res 60:6068-6074.

Hannemann S, Madrid R, Stastna J, Kitzing T, Gasteier J, Schonichen A, Bouchet J, Jimenez A, Geyer M, Grosse R, Benichou S, Fackler OT. 2008. The Diaphanous-related Formin FHOD1 associates with ROCK1 and promotes Src-dependent plasma membrane blebbing. J Biol Chem 283:27891-27903.

Hao JJ, Liu Y, Kruhlak M, Debell KE, Rellahan BL, Shaw S. 2009. Phospholipase C-mediated hydrolysis of PIP2 releases ERM proteins from lymphocyte membrane. J Cell Biol 184:451-462.

Harris HE, Weeds AG. 1984. Plasma gelsolin caps and severs actin filaments. FEBS Lett 177:184-188.

Harris JA, Cheng AG, Cunningham LL, MacDonald G, Raible DW, Rubel EW. 2003. Neomycin-induced hair cell death and rapid regeneration in the lateral line of zebrafish (Danio rerio). J Assoc Res Otolaryngol 4:219-234.

Hartman BH, Basak O, Nelson BR, Taylor V, Bermingham-McDonogh O, Reh TA. 2009. Hes5 expression in the postnatal and adult mouse inner ear and the drug-damaged cochlea. J Assoc Res Otolaryngol 10:321-340.

Hernández PP, Olivari FA, Sarrazin AF, Sandoval PC, Allende ML. 2007. Regeneration in zebrafish lateral line neuromasts: expression of the neural progenitor cell marker sox2 and proliferation-dependent and-independent mechanisms of hair cell renewal. Dev Neurobiol 67:637-654.

Hertzano R, Shalit E, Rzadzinska AK, Dror AA, Song L, Ron U, Tan JT, Shitrit AS, Fuchs H, Hasson T, Ben-Tal N, Sweeney HL, de Angelis MH, Steel KP, Avraham KB. 2008. A Myo6 mutation destroys coordination between the myosin heads, revealing new functions of myosin VI in the stereocilia of mammalian inner ear hair cells. PLoS Genet 4:e1000207.

Hervé M, Maillere B, Mourier G, Texier C, Leroy S, Menez A. 1997. On the immunogenic properties of retro-inverso peptides. Total retro-inversion of T-cell epitopes causes a loss of binding to MHC II molecules. Mol Immunol 34:157-163.

Hildebrand JD, Soriano P. 1999. Shroom, a PDZ domain-containing actin-binding protein, is required for neural tube morphogenesis in mice. Cell 99:485-497.

Hirao M, Sato N, Kondo T, Yonemura S, Monden M, Sasaki T, Takai Y, Tsukita S. 1996. Regulation mechanism of ERM (ezrin/radixin/moesin) protein/plasma membrane association: possible involvement of phosphatidylinositol turnover and Rho-dependent signaling pathway. J Cell Biol 135:37-51.

Hirokawa N, Tilney LG. 1982. Interactions between actin filaments and between actin filaments and membranes in quick-frozen and deeply etched hair cells of the chick ear. J Cell Biol 95:249-261.

Hirt L, Badaut J, Thevenet J, Granziera C, Regli L, Maurer F, Bonny C, Bogousslavsky J. 2004. D-JNKI1, a cell-penetrating c-Jun-N-terminal kinase inhibitor, protects against cell death in severe cerebral ischemia. Stroke 35:1738-1743.

Hoben GM, Athanasiou KA. 2008. Use of staurosporine, an actin-modifying agent, to enhance fibrochondrocyte matrix gene expression and synthesis. Cell Tissue Res 334:469-476.

Husbands JM, Steinberg SA, Kurian R, Saunders JC. 1999. Tip-link integrity on chick tall hair cell stereocilia following intense sound exposure. Hear Res 135:135-145.

Irvine DR, Brown M, Kamke MR, Rubel EW. 2009. Effects of restricted basilar papillar lesions and hair cell regeneration on auditory forebrain frequency organization in adult European starlings. J Neurosci 29:6871-6882.

Itoh M. 1982. Preservation and visualization of actin-containing filaments in the apical zone of cochlear sensory cells. Hear Res 6:277-289.

Izumi Y, Kim S, Zhan Y, Namba M, Yasumoto H, Iwao H. 2000. Important role of angiotensin II-mediated c-Jun NH(2)-terminal kinase activation in cardiac hypertrophy in hypertensive rats. Hypertension 36:511-516.

Izumikawa M, Minoda R, Kawamoto K, Abrashkin KA, Swiderski DL, Dolan DF, Brough DE, Raphael Y. 2005. Auditory hair cell replacement and hearing improvement by Atoh1 gene therapy in deaf mammals. Nat Med 11:271-276.

Izzedine H, Tankere F, Launay-Vacher V, Deray G. 2004. Ear and kidney syndromes: molecular versus clinical approach. Kidney Int 65:369-385.

Jamesdaniel S, Ding D, Kermany MH, Jiang H, Salvi R, Coling D. 2009. Analysis of cochlear protein profiles of Wistar, Sprague-Dawley, and Fischer 344 rats with normal hearing function. J Proteome Res 8:3520-3528.

Janke M, Herrig A, Austermann J, Gerke V, Steinem C, Janshoff A. 2008. Actin binding of ezrin is activated by specific recognition of PIP2-functionalized lipid bilayers. Biochemistry 47:3762-3769.

Janmey PA, Stossel TP. 1989. Gelsolin-polyphosphoinositide interaction. Full expression of gelsolin-inhibiting function by polyphosphoinositides in vesicular form and inactivation by dilution, aggregation, or masking of the inositol head group. J Biol Chem 264:4825-4831.

Janosik T, Wahlstromb N, Bergman J. 2008. Recent progress in the chemistry and applications of indolocarbazoles. Tetrahedron 64:9159–9180.

Jones JE, Corwin JT. 1996. Regeneration of sensory cells after laser ablation in the lateral line system: hair cell lineage and macrophage behavior revealed by time-lapse video microscopy. J Neurosci 16:649-662.

Kaiser CL, Kamien AJ, Shah PA, Chapman BJ, Cotanche DA. 2009. 5-Ethynyl-2'-deoxyuridine labeling detects proliferating cells in the regenerating avian cochlea. Laryngoscope 119:1770-1775.

Kakehata S, Yamamoto T, Takasaka T, Akaike N. 1995. Suppression of a nonselective cation conductance by substance P in cochlear outer hair cells. Am J Physiol 269:C1185-1192.

Kaltenbach JA, Falzarano PR, Simpson TH. 1994. Postnatal development of the hamster cochlea. II. Growth and differentiation of stereocilia bundles. J Comp Neurol 350:187-198.

Kaneko T, Harasztosi C, Mack AF, Gummer AW. 2006. Membrane traffic in outer hair cells of the adult mammalian cochlea. Eur J Neurosci 23:2712-2722.

Kanzaki S, Beyer LA, Swiderski DL, Izumikawa M, Stover T, Kawamoto K, Raphael Y. 2006. p27(Kip1) deficiency causes organ of Corti pathology and hearing loss. Hear Res 214:28-36.

Kataoka Y, Ohmori H. 1996. Of known neurotransmitters, glutamate is the most likely to be released from chick cochlear hair cells. J Neurophysiol 76:1870-1879.

Kawamoto K, Ishimoto S, Minoda R, Brough DE, Raphael Y. 2003. Math1 gene transfer generates new cochlear hair cells in mature guinea pigs in vivo. J Neurosci 23:4395-4400.

Kawamoto K, Izumikawa M, Beyer LA, Atkin GM, Raphael Y. 2009. Spontaneous hair cell regeneration in the mouse utricle following gentamicin ototoxicity. Hear Res 247:17-26.

Kayali AG, Austin DA, Webster NJ. 2002. Rottlerin inhibits insulin-stimulated glucose transport in 3T3-L1 adipocytes by uncoupling mitochondrial oxidative phosphorylation. Endocrinology 143:3884-3896.

Kazmierczak P, Sakaguchi H, Tokita J, Wilson-Kubalek EM, Milligan RA, Muller U, Kachar B. 2007. Cadherin 23 and protocadherin 15 interact to form tip-link filaments in sensory hair cells. Nature 449:87-91.

Khan NS, Schwabl U, Trincker DE. 1982. Sensory transduction and neuronal transmission as related to ultrastructure and encoding of information in different labyrinthine receptor systems of vertebrates. Arch Otorhinolaryngol 236:27-39.

Khan SY, Ahmed ZM, Shabbir MI, Kitajiri S, Kalsoom S, Tasneem S, Shayiq S, Ramesh A, Srisailpathy S, Khan SN, Smith RJ, Riazuddin S, Friedman TB. 2007. Mutations of the RDX gene cause nonsyndromic hearing loss at the DFNB24 locus. Hum Mutat 28:417-423.

Kikkawa Y, Mburu P, Morse S, Kominami R, Townsend S, Brown SD. 2005. Mutant analysis reveals whirlin as a dynamic organizer in the growing hair cell stereocilium. Hum Mol Genet 14:391-400.

Kikkawa Y, Shitara H, Wakana S, Kohara Y, Takada T, Okamoto M, Taya C, Kamiya K, Yoshikawa Y, Tokano H, Kitamura K, Shimizu K, Wakabayashi Y, Shiroishi T, Kominami R, Yonekawa H. 2003. Mutations in a new scaffold protein Sans cause deafness in Jackson shaker mice. Hum Mol Genet 12:453-461.

Kim AS, Kakalis LT, Abdul-Manan N, Liu GA, Rosen MK. 2000. Autoinhibition and activation mechanisms of the Wiskott-Aldrich syndrome protein. Nature 404:151-158.

Kim K, McCully ME, Bhattacharya N, Butler B, Sept D, Cooper JA. 2007. Structure/function analysis of the interaction of phosphatidylinositol 4,5-bisphosphate with actin-capping protein: implications for how capping protein binds the actin filament. J Biol Chem 282:5871-5879.

Kinoshita T, Matsubara M, Ishiguro H, Okita K, Tada T. 2006. Structure of human Fyn kinase domain complexed with staurosporine. Biochem Biophys Res Commun 346:840-844.

Kitajiri S, Fukumoto K, Hata M, Sasaki H, Katsuno T, Nakagawa T, Ito J, Tsukita S. 2004. Radixin deficiency causes deafness associated with progressive degeneration of cochlear stereocilia. J Cell Biol 166:559-570.

Kloepfer HW, Laguaite JK. 1966. The hereditary syndrome of congenital deafness and retinitis pigmentosa. (Usher's syndrome). Laryngoscope 76:850-862.

Kotani H, Takaishi K, Sasaki T, Takai Y. 1997. Rho regulates association of both the ERM family and vinculin with the plasma membrane in MDCK cells. Oncogene 14:1705-1713.

Kuan CY, Yang DD, Samanta Roy DR, Davis RJ, Rakic P, Flavell RA. 1999. The Jnk1 and Jnk2 protein kinases are required for regional specific apoptosis during early brain development. Neuron 22:667-676.

Kunda P, Baum B. 2009. The actin cytoskeleton in spindle assembly and positioning. Trends Cell Biol 19:174-179.

Kurian R, Krupp NL, Saunders JC. 2003. Tip link loss and recovery on chick short hair cells following intense exposure to sound. Hear Res 181:40-50.

Kurosu T, Tsuji K, Kida A, Koyama T, Yamamoto M, Miura O. 2007. Rottlerin synergistically enhances imatinib-induced apoptosis of BCR/ABL-expressing cells through its mitochondrial uncoupling effect independent of protein kinase C-delta. Oncogene 26:2975-2987.

Lan M, Kojima T, Murata M, Osanai M, Takano K, Chiba H, Sawada N. 2006. Phosphorylation of ezrin enhances microvillus length via a p38 MAP-kinase pathway in an immortalized mouse hepatic cell line. Exp Cell Res 312:111-120.

Lang F, Vallon V, Knipper M, Wangemann P. 2007. Functional significance of channels and transporters expressed in the inner ear and kidney. Am J Physiol Cell Physiol 293:C1187-1208.

Lebrand C, Dent EW, Strasser GA, Lanier LM, Krause M, Svitkina TM, Borisy GG, Gertler FB. 2004. Critical role of Ena/VASP proteins for filopodia formation in neurons and in function downstream of netrin-1. Neuron 42:37-49.

LeClaire LL, 3rd, Baumgartner M, Iwasa JH, Mullins RD, Barber DL. 2008. Phosphorylation of the Arp2/3 complex is necessary to nucleate actin filaments. J Cell Biol 182:647-654.

Lefèvre G, Michel V, Weil D, Lepelletier L, Bizard E, Wolfrum U, Hardelin JP, Petit C. 2008. A core cochlear phenotype in USH1 mouse mutants implicates fibrous links of the hair bundle in its cohesion, orientation and differential growth. Development 135:1427-1437.

Legendre K, Safieddine S, Kussel-Andermann P, Petit C, El-Amraoui A. 2008. alphaII-betaV spectrin bridges the plasma membrane and cortical lattice in the lateral wall of the auditory outer hair cells. J Cell Sci 121:3347-3356.

Leitges M, Elis W, Gimborn K, Huber M. 2001. Rottlerin-independent attenuation of pervanadate-induced tyrosine phosphorylation events by protein kinase C-delta in hemopoietic cells. Lab Invest 81:1087-1095.

Lenoir M, Daudet N, Humbert G, Renard N, Gallego M, Pujol R, Eybalin M, Vago P. 1999. Morphological and molecular changes in the inner hair cell region of the rat cochlea after amikacin treatment. J Neurocytol 28:925-937.

Li H, Liu H, Balt S, Mann S, Corrales CE, Heller S. 2004. Correlation of expression of the actin filament-bundling protein espin with stereociliary bundle formation in the developing inner ear. J Comp Neurol 468:125-134.

Li L, Forge A. 1997. Morphological evidence for supporting cell to hair cell conversion in the mammalian utricular macula. Int J Dev Neurosci 15:433-446.

Liberman MC, Dodds LW. 1987. Acute ultrastructural changes in acoustic trauma: serial-section reconstruction of stereocilia and cuticular plates. Hear Res 26:45-64.

Liberman MC. 1987. Chronic ultrastructural changes in acoustic trauma: serial-section reconstruction of stereocilia and cuticular plates. Hear Res 26:65-88.

Lim DJ. 1980. Cochlear anatomy related to cochlear micromechanics. A review. J Acoust Soc Am 67:1686-1695.

Lin HW, Schneider ME, Kachar B. 2005. When size matters: the dynamic regulation of stereocilia lengths. Curr Opin Cell Biol 17:55-61.

Lin KM, Wenegieme E, Lu PJ, Chen CS, Yin HL. 1997. Gelsolin binding to phosphatidylinositol 4,5-bisphosphate is modulated by calcium and pH. J Biol Chem 272:20443-20450.

Lin YC, Redmond L. 2008. CaMKIIbeta binding to stable F-actin in vivo regulates F-actin filament stability. Proc Natl Acad Sci U S A 105:15791-15796.

Liu AL, Wang XW, Liu AH, Su XW, Jiang WJ, Qiu PX, Yan GM. 2009. JNK and p38 were involved in hypoxia and reoxygenation-induced apoptosis of cultured rat cerebellar granule neurons. Exp Toxicol Pathol 61:137-143.

Loomis PA, Zheng L, Sekerkova G, Changyaleket B, Mugnaini E, Bartles JR. 2003. Espin cross-links cause the elongation of microvillus-type parallel actin bundles in vivo. J Cell Biol 163:1045-1055.

Lopez-Gonzalez MA, Delgado F, Lucas M. 1999. Aminoglycosides activate oxygen metabolites production in the cochlea of mature and developing rats. Hear Res 136:165-168.

Louvet-Vallée S. 2000. ERM proteins: from cellular architecture to cell signalling. Biol Cell 92:305-316.

Löwenheim H, Furness DN, Kil J, Zinn C, Gultig K, Fero ML, Frost D, Gummer AW, Roberts JM, Rubel EW, Hackney CM, Zenner HP. 1999a. Gene disruption of p27(Kip1) allows cell proliferation in the postnatal and adult organ of corti. Proc Natl Acad Sci U S A 96:4084-4088.

Löwenheim H, Kil J, Gultig K, Zenner HP. 1999b. Determination of hair cell degeneration and hair cell death in neomycin treated cultures of the neonatal rat cochlea. Hear Res 128:16-26.

Ma EY, Rubel EW, Raible DW. 2008. Notch signaling regulates the extent of hair cell regeneration in the zebrafish lateral line. J Neurosci 28:2261-2273.

Machesky LM, Insall RH. 1998. Scar1 and the related Wiskott-Aldrich syndrome protein, WASP, regulate the actin cytoskeleton through the Arp2/3 complex. Curr Biol 8:1347-1356.

Maciver SK, Hussey PJ. 2002. The ADF/cofilin family: actin-remodeling proteins. Genome Biol 3:reviews3007.

Mahendrasingam S, Furness DN, Hackney CM. 1998. Ultrastructural localisation of spectrin in sensory and supporting cells of guinea-pig organ of Corti. Hear Res 126:151-160.

Marcotti W, van Netten SM, Kros CJ. 2005. The aminoglycoside antibiotic dihydrostreptomycin rapidly enters mouse outer hair cells through the mechano-electrical transducer channels. J Physiol 567:505-521.

Marean GC, Burt JM, Beecher MD, Rubel EW. 1998. Auditory perception following hair cell regeneration in European starling (Sturnus vulgaris): frequency and temporal resolution. J Acoust Soc Am 103:3567-3580.

Maroney AC, Glicksman MA, Basma AN, Walton KM, Knight E, Jr., Murphy CA, Bartlett BA, Finn JP, Angeles T, Matsuda Y, Neff NT, Dionne CA. 1998. Motoneuron apoptosis is blocked by CEP-1347 (KT 7515), a novel inhibitor of the JNK signaling pathway. J Neurosci 18:104-111.

Matsui T, Maeda M, Doi Y, Yonemura S, Amano M, Kaibuchi K, Tsukita S. 1998. Rho-kinase phosphorylates COOH-terminal threonines of ezrin/radixin/moesin (ERM) proteins and regulates their head-to-tail association. J Cell Biol 140:647-657.

Matsui T, Yonemura S, Tsukita S. 1999. Activation of ERM proteins in vivo by Rho involves phosphatidyl-inositol 4-phosphate 5-kinase and not ROCK kinases. Curr Biol 9:1259-1262.

McGee J, Goodyear RJ, McMillan DR, Stauffer EA, Holt JR, Locke KG, Birch DG, Legan PK, White PC, Walsh EJ, Richardson GP. 2006. The very large G-protein-coupled receptor VLGR1: a component of the ankle link complex required for the normal development of auditory hair bundles. J Neurosci 26:6543-6553.

McGough A, Chiu W. 1999. ADF/cofilin weakens lateral contacts in the actin filament. J Mol Biol 291:513-519.

McLaughlin PJ, Gooch JT, Mannherz HG, Weeds AG. 1993. Structure of gelsolin segment 1-actin complex and the mechanism of filament severing. Nature 364:685-692.

McWilliams ML, Chen GD, Fechter LD. 2000. Characterization of the ototoxicity of difluoromethylornithine and its enantiomers. Toxicol Sci 56:124-132.

Meggio F, Donella Deana A, Ruzzene M, Brunati AM, Cesaro L, Guerra B, Meyer T, Mett H, Fabbro D, Furet P, et al. 1995. Different susceptibility of protein kinases to staurosporine inhibition. Kinetic studies and molecular bases for the resistance of protein kinase CK2. Eur J Biochem 234:317-322.

Meyer J, Furness DN, Zenner HP, Hackney CM, Gummer AW. 1998. Evidence for opening of hair-cell transducer channels after tip-link loss. J Neurosci 18:6748-6756.

Meyer J, Mack AF, Gummer AW. 2001. Pronounced infracuticular endocytosis in mammalian outer hair cells. Hear Res 161:10-22.

Meyer J, Preyer S, Hofmann SI, Gummer AW. 2005. Tonic mechanosensitivity of outer hair cells after loss of tip links. Hear Res 202:97-113.

Meyers JR, MacDonald RB, Duggan A, Lenzi D, Standaert DG, Corwin JT, Corey DP. 2003. Lighting up the senses: FM1-43 loading of sensory cells through nonselective ion channels. J Neurosci 23:4054-4065.

Michel V, Goodyear RJ, Weil D, Marcotti W, Perfettini I, Wolfrum U, Kros CJ, Richardson GP, Petit C. 2005. Cadherin 23 is a component of the transient lateral links in the developing hair bundles of cochlear sensory cells. Dev Biol 280:281-294.

Miki H, Takenawa T. 2003. Regulation of actin dynamics by WASP family proteins. J Biochem 134:309-313.

Moephuli SR, Klein NW, Baldwin MT, Krider HM. 1997. Effects of methionine on the cytoplasmic distribution of actin and tubulin during neural tube closure in rat embryos. Proc Natl Acad Sci U S A 94:543-548.

Mogensen MM, Rzadzinska A, Steel KP. 2007. The deaf mouse mutant whirler suggests a role for whirlin in actin filament dynamics and stereocilia development. Cell Motil Cytoskeleton 64:496-508.

Mookherjee P, Quintanilla R, Roh MS, Zmijewska AA, Jope RS, Johnson GV. 2007. Mitochondrial-targeted active Akt protects SH-SY5Y neuroblastoma cells from staurosporine-induced apoptotic cell death. J Cell Biochem 102:196-210.

Morriss-Kay G, Tuckett F. 1985. The role of microfilaments in cranial neurulation in rat embryos: effects of short-term exposure to cytochalasin D. J Embryol Exp Morphol 88:333-348.

Mu MY, Chardin S, Avan P, Romand R. 1997. Ontogenesis of rat cochlea. A quantitative study of the organ of Corti. Brain Res Dev Brain Res 99:29-37.

Müller M, Smolders JW. 1998. Hair cell regeneration after local application of gentamicin at the round window of the cochlea in the pigeon. Hear Res 120:25-36.

Muller U. 2008. Cadherins and mechanotransduction by hair cells. Curr Opin Cell Biol 20:557-566.

Mustapha M, Beyer LA, Izumikawa M, Swiderski DL, Dolan DF, Raphael Y, Camper SA. 2007. Whirler mutant hair cells have less severe pathology than shaker 2 or double mutants. J Assoc Res Otolaryngol 8:329-337.

Nakamura N, Oshiro N, Fukata Y, Amano M, Fukata M, Kuroda S, Matsuura Y, Leung T, Lim L, Kaibuchi K. 2000. Phosphorylation of ERM proteins at filopodia induced by Cdc42. Genes Cells 5:571-581.

Nakano H, Ōmura S. 2009. Chemical biology of natural indolocarbazole products: 30 years since the discovery of staurosporine. J Antibiot (Tokyo) 62:17-26.

Naoz M, Manor U, Sakaguchi H, Kachar B, Gov NS. 2008. Protein localization by actin treadmilling and molecular motors regulates stereocilia shape and treadmilling rate. Biophys J 95:5706-5718.

Naydenov NG, Hopkins AM, Ivanov AI. 2009. c-Jun N-terminal kinase mediates disassembly of apical junctions in model intestinal epithelia. Cell Cycle 8:2110-2121.

Neuhaus JM, Wanger M, Keiser T, Wegner A. 1983. Treadmilling of actin. J Muscle Res Cell Motil 4:507-527.

Nishikawa S, Sasaki F. 1996. Internalization of styryl dye FM1-43 in the hair cells of lateral line organs in Xenopus larvae. J Histochem Cytochem 44:733-741.

Nomachi A, Nishita M, Inaba D, Enomoto M, Hamasaki M, Minami Y. 2008. Receptor tyrosine kinase Ror2 mediates Wnt5a-induced polarized cell migration by activating c-Jun N-terminal kinase via actin-binding protein filamin A. J Biol Chem 283:27973-27981.

Nunnally MH, Powell LD, Craig SW. 1981. Reconstitution and regulation of actin gel-sol transformation with purified filamin and villin. J Biol Chem 256:2083-2086.

Ohashi K, Nagata K, Maekawa M, Ishizaki T, Narumiya S, Mizuno K. 2000. Rho-associated kinase ROCK activates LIM-kinase 1 by phosphorylation at threonine 508 within the activation loop. J Biol Chem 275:3577-3582.

Okamoto K, Narayanan R, Lee SH, Murata K, Hayashi Y. 2007. The role of CaMKII as an F-actin-bundling protein crucial for maintenance of dendritic spine structure. Proc Natl Acad Sci U S A 104:6418-6423.

Olano C, Mendez C, Salas JA. 2009. Antitumor compounds from actinomycetes: from gene clusters to new derivatives by combinatorial biosynthesis. Nat Prod Rep 26:628-660.

Omura S, Iwai Y, Hirano A, Nakagawa A, Awaya J, Tsuchya H, Takahashi Y, Masuma R. 1977. A new alkaloid AM-2282 OF Streptomyces origin. Taxonomy, fermentation, isolation and preliminary characterization. J Antibiot (Tokyo) 30:275-282.

Ono K, Nakagawa T, Kojima K, Matsumoto M, Kawauchi T, Hoshino M, Ito J. 2009. Silencing p27 reverses post-mitotic state of supporting cells in neonatal mouse cochleae. Mol Cell Neurosci.

Osborne MP, Comis SD, Pickles JO. 1984. Morphology and cross-linkage of stereocilia in the guinea-pig labyrinth examined without the use of osmium as a fixative. Cell Tissue Res 237:43-48.

Paavilainen VO, Oksanen E, Goldman A, Lappalainen P. 2008. Structure of the actin-depolymerizing factor homology domain in complex with actin. J Cell Biol 182:51-59.

Pakkanen R, Hedman K, Turunen O, Wahlstrom T, Vaheri A. 1987. Microvillus-specific Mr 75,000 plasma membrane protein of human choriocarcinoma cells. J Histochem Cytochem 35:809-816.

Pan L, Yan J, Wu L, Zhang M. 2009. Assembling stable hair cell tip link complex via multidentate interactions between harmonin and cadherin 23. Proc Natl Acad Sci U S A 106:5575-5580.

Papayannopoulos V, Co C, Prehoda KE, Snapper S, Taunton J, Lim WA. 2005. A polybasic motif allows N-WASP to act as a sensor of PIP(2) density. Mol Cell 17:181-191.

Parrini MC, Camonis J, Matsuda M, de Gunzburg J. 2009. Dissecting activation of the PAK1 kinase at protrusions in living cells. J Biol Chem 284:24133-24143.

Pasic L, Kotova T, Schafer DA. 2008. Ena/VASP proteins capture actin filament barbed ends. J Biol Chem 283:9814-9819.

Pataky F, Pironkova R, Hudspeth AJ. 2004. Radixin is a constituent of stereocilia in hair cells. Proc Natl Acad Sci U S A 101:2601-2606.

Pérez LM, Milkiewicz P, Ahmed-Choudhury J, Elias E, Ochoa JE, Sanchez Pozzi EJ, Coleman R, Roma MG. 2006. Oxidative stress induces actin-cytoskeletal and tight-junctional alterations in hepatocytes by a Ca2+ -dependent, PKC-mediated mechanism: protective effect of PKA. Free Radic Biol Med 40:2005-2017.

Petit C. 2001. Usher syndrome: from genetics to pathogenesis. Annu Rev Genomics Hum Genet 2:271-297.

Pickles JO, Comis SD, Osborne MP. 1984. Cross-links between stereocilia in the guinea pig organ of Corti, and their possible relation to sensory transduction. Hear Res 15:103-112.

Pickles JO, Osborne MP, Comis SD. 1987. Vulnerability of tip links between stereocilia to acoustic trauma in the guinea pig. Hear Res 25:173-183.

Pirvola U, Xing-Qun L, Virkkala J, Saarma M, Murakata C, Camoratto AM, Walton KM, Ylikoski J. 2000. Rescue of hearing, auditory hair cells, and neurons by CEP-1347/KT7515, an inhibitor of c-Jun N-terminal kinase activation. J Neurosci 20:43-50.

Plontke SK, Mynatt R, Gill RM, Borgmann S, Salt AN. 2007. Concentration gradient along the scala tympani after local application of gentamicin to the round window membrane. Laryngoscope 117:1191-1198.

Pocha SM, Cory GO. 2009. WAVE2 is regulated by multiple phosphorylation events within its VCA domain. Cell Motil Cytoskeleton 66:36-47.

Potin S, Bertoglio J, Breard J. 2007. Involvement of a Rho-ROCK-JNK pathway in arsenic trioxide-induced apoptosis in chronic myelogenous leukemia cells. FEBS Lett 581:118-124.

Prade L, Engh RA, Girod A, Kinzel V, Huber R, Bossemeyer D. 1997. Staurosporine-induced conformational changes of cAMP-dependent protein kinase catalytic subunit explain inhibitory potential. Structure 5:1627-1637.

Prasain N, Stevens T. 2009. The actin cytoskeleton in endothelial cell phenotypes. Microvasc Res 77:53-63.

Preyer S, Hemmert W, Zenner HP, Gummer AW. 1995. Abolition of the receptor potential response of isolated mammalian outer hair cells by hair-bundle treatment with elastase: a test of the tip-link hypothesis. Hear Res 89:187-193.

Purves D (ed). 2007 (4th edition). Neuroscience. Sinauer Associates Inc, USA. ISBN 978-0-87893-697-7

Puschner B, Schacht J. 1997. Calmodulin-dependent protein kinases mediate calcium-induced slow motility of mammalian outer hair cells. Hear Res 110:251-258.

Quint E, Furness DN, Hackney CM. 1998. The effect of explantation and neomycin on hair cells and supporting cells in organotypic cultures of the adult guinea-pig utricle. Hear Res 118:157-167.

Reiners J, van Wijk E, Marker T, Zimmermann U, Jurgens K, te Brinke H, Overlack N, Roepman R, Knipper M, Kremer H, Wolfrum U. 2005. Scaffold protein harmonin (USH1C) provides molecular links between Usher syndrome type 1 and type 2. Hum Mol Genet 14:3933-3943.

Repici M, Mare L, Colombo A, Ploia C, Sclip A, Bonny C, Nicod P, Salmona M, Borsello T. 2009. c-Jun N-terminal kinase binding domain-dependent phosphorylation of mitogen-activated protein kinase kinase 4 and mitogen-activated protein kinase kinase 7 and balancing cross-talk between c-Jun N-terminal kinase and extracellular signal-regulated kinase pathways in cortical neurons. Neuroscience 159:94-103.

Represa JJ, Miner C, Barbosa E, Giraldez F. 1988. Bombesin and other growth factors activate cell proliferation in chick embryo otic vesicles in culture. Development 103:87-96.

Reynolds ES. 1963. The use of lead citrate at high pH as an electron-opaque stain in electron microscopy. J Cell Biol 17:208-212.

Rincón M, Davis RJ. 2009. Regulation of the immune response by stress-activated protein kinases. Immunol Rev 228:212-224.

Roffey J, Rosse C, Linch M, Hibbert A, McDonald NQ, Parker PJ. 2009. Protein kinase C intervention: the state of play. Curr Opin Cell Biol 21:268-279.

Romand R, Chardin S. 1999. Effects of growth factors on the hair cells after ototoxic treatment of the neonatal mammalian cochlea in vitro. Brain Res 825:46-58.

Rose R, Weyand M, Lammers M, Ishizaki T, Ahmadian MR, Wittinghofer A. 2005. Structural and mechanistic insights into the interaction between Rho and mammalian Dia. Nature 435:513-518.

Rosenberg T, Haim M, Hauch AM, Parving A. 1997. The prevalence of Usher syndrome and other retinal dystrophy-hearing impairment associations. Clin Genet 51:314-321.

Russell IJ, Richardson GP. 1987. The morphology and physiology of hair cells in organotypic cultures of the mouse cochlea. Hear Res 31:9-24.

Rybak LP, Whitworth C. 1987. Ototoxicity of indacrinone is stereospecific. Hear Res 31:169-174.

Rybak LP, Whitworth C, Scott V. 1991. Comparative acute ototoxicity of loop diuretic compounds. Eur Arch Otorhinolaryngol 248:353-357.

Rzadzinska AK, Schneider ME, Davies C, Riordan GP, Kachar B. 2004. An actin molecular treadmill and myosins maintain stereocilia functional architecture and self-renewal. J Cell Biol 164:887-897.

Rzadzinska A, Schneider M, Noben-Trauth K, Bartles JR, Kachar B. 2005. Balanced levels of Espin are critical for stereociliary growth and length maintenance. Cell Motil Cytoskeleton 62:157-165.

Saihan Z, Webster AR, Luxon L, Bitner-Glindzicz M. 2009. Update on Usher syndrome. Curr Opin Neurol 22:19-27.

Sakaguchi H, Tokita J, Naoz M, Bowen-Pope D, Gov NS, Kachar B. 2008. Dynamic compartmentalization of protein tyrosine phosphatase receptor Q at the proximal end of stereocilia: implication of myosin VI-based transport. Cell Motil Cytoskeleton 65:528-538.

Sakamoto N, Uemura H, Hara Y, Saito T, Masuda Y, Nakaya H. 1998. Bradykinin B2-receptor-mediated modulation of membrane currents in guinea-pig cardiomyocytes. Br J Pharmacol 125:283-292.

Salles FT, Merritt RC, Jr., Manor U, Dougherty GW, Sousa AD, Moore JE, Yengo CM, Dose AC, Kachar B. 2009. Myosin IIIa boosts elongation of stereocilia by transporting espin 1 to the plus ends of actin filaments. Nat Cell Biol 11:443-450.

Sánchez C, Méndez C, Salas JA. 2006. Engineering biosynthetic pathways to generate antitumor indolocarbazole derivatives. J Ind Microbiol Biotechnol 33:560-568.

Sans A, Atger P, Cavadore C, Cavadore JC. 1989. Immunocytochemical localization of myosin, tropomyosin and actin in vestibular hair cells of human fetuses and cats. Hear Res 40:117-125.

Saotome I, Curto M, McClatchey AI. 2004. Ezrin is essential for epithelial organization and villus morphogenesis in the developing intestine. Dev Cell 6:855-864.

Schafer DA, Jennings PB, Cooper JA. 1996. Dynamics of capping protein and actin assembly in vitro: uncapping barbed ends by polyphosphoinositides. J Cell Biol 135:169-179.

Schneider ME, Belyantseva IA, Azevedo RB, Kachar B. 2002. Rapid renewal of auditory hair bundles. Nature 418:837-838.

Schneider ME, Dose AC, Salles FT, Chang W, Erickson FL, Burnside B, Kachar B. 2006. A new compartment at stereocilia tips defined by spatial and temporal patterns of myosin IIIa expression. J Neurosci 26:10243-10252.

Schuck JB, Smith ME. 2009. Cell proliferation follows acoustically-induced hair cell bundle loss in the zebrafish saccule. Hear Res 253:67-76.

Schwartz M. 2004. Rho signalling at a glance. J Cell Sci 117:5457-5458.

Sekerková G, Zheng L, Loomis PA, Changyaleket B, Whitlon DS, Mugnaini E, Bartles JR. 2004. Espins are multifunctional actin cytoskeletal regulatory proteins in the microvilli of chemosensory and mechanosensory cells. J Neurosci 24:5445-5456.

Sekerková G, Zheng L, Mugnaini E, Bartles JR. 2006a. Differential expression of espin isoforms during epithelial morphogenesis, stereociliogenesis and postnatal maturation in the developing inner ear. Dev Biol 291:83-95.

Sekerková G, Zheng L, Loomis PA, Mugnaini E, Bartles JR. 2006b. Espins and the actin cytoskeleton of hair cell stereocilia and sensory cell microvilli. Cell Mol Life Sci 63:2329-2341.

Self T, Sobe T, Copeland NG, Jenkins NA, Avraham KB, Steel KP. 1999. Role of myosin VI in the differentiation of cochlear hair cells. Dev Biol 214:331-341.

Sells MA, Knaus UG, Bagrodia S, Ambrose DM, Bokoch GM, Chernoff J. 1997. Human p21-activated kinase (Pak1) regulates actin organization in mammalian cells. Curr Biol 7:202-210.

Seth A, Otomo C, Rosen MK. 2006. Autoinhibition regulates cellular localization and actin assembly activity of the diaphanous-related formins FRLalpha and mDia1. J Cell Biol 174:701-713.

Shen J, Harada N, Nakazawa H, Yamashita T. 2005. Involvement of the nitric oxide-cyclic GMP pathway and neuronal nitric oxide synthase in ATP-induced Ca2+ signalling in cochlear inner hair cells. Eur J Neurosci 21:2912-2922.

Shepherd GM, Barres BA, Corey DP. 1989. "Bundle blot" purification and initial protein characterization of hair cell stereocilia. Proc Natl Acad Sci U S A 86:4973-4977.

Shim K. 2006. The auditory sensory epithelium: the instrument of sound perception. Int J Biochem Cell Biol 38:1827-1833.

Shinozuka Y, Okada M, Yasuda N, Yokoyama KK. 2003. Staurosporine stimulates insulin gene expression via CRE dependent manner. Nucleic Acids Res Suppl:301-302.

Shou J, Zheng JL, Gao WQ. 2003. Robust generation of new hair cells in the mature mammalian inner ear by adenoviral expression of Hath1. Mol Cell Neurosci 23:169-179.

Si F, Brodie H, Gillespie PG, Vazquez AE, Yamoah EN. 2003. Developmental assembly of transduction apparatus in chick basilar papilla. J Neurosci 23:10815-10826.

Siemens J, Lillo C, Dumont RA, Reynolds A, Williams DS, Gillespie PG, Muller U. 2004. Cadherin 23 is a component of the tip link in hair-cell stereocilia. Nature 428:950-955.

Silacci P, Mazzolai L, Gauci C, Stergiopulos N, Yin HL, Hayoz D. 2004. Gelsolin superfamily proteins: key regulators of cellular functions. Cell Mol Life Sci 61:2614-2623.

Slepecky N, Chamberlain SC. 1982. Distribution and polarity of actin in the sensory hair cells of the chinchilla cochlea. Cell Tissue Res 224:15-24.

Slepecky N, Chamberlain SC. 1985. Immunoelectron microscopic and immunofluorescent localization of cytoskeletal and muscle-like contractile proteins in inner ear sensory hair cells. Hear Res 20:245-260.

Sliwinska-Kowalska M, Rzadzinska A, Rajkowska E, Malczyk M. 2005. Expression of bFGF and NGF and their receptors in chick's auditory organ following overexposure to noise. Hear Res 210:93-103.

Smith CD, Mooberry SL. 1992. The protein kinase inhibitor, staurosporine, does not inhibit phosphoinositide kinases. Biochem Int 26:679-685.

Smith SW. 2009. Chiral toxicology: it's the same thing...only different. Toxicol Sci 110:4-30.

Sobkowicz HM, August BK, Slapnick SM. 1992. Epithelial repair following mechanical injury of the developing organ of Corti in culture: an electron microscopic and autoradiographic study. Exp Neurol 115:44-49.

Sobkowicz HM, August BK, Slapnick SM. 1997. Cellular interactions as a response to injury in the organ of Corti in culture. Int J Dev Neurosci 15:463-485.

Sobkowicz HM, Slapnick SM, August BK. 1995. The kinocilium of auditory hair cells and evidence for its morphogenetic role during the regeneration of stereocilia and cuticular plates. J Neurocytol 24:633-653.

Söllner C, Rauch GJ, Siemens J, Geisler R, Schuster SC, Muller U, Nicolson T. 2004. Mutations in cadherin 23 affect tip links in zebrafish sensory hair cells. Nature 428:955-959.

Soltoff SP. 2001. Rottlerin is a mitochondrial uncoupler that decreases cellular ATP levels and indirectly blocks protein kinase Cdelta tyrosine phosphorylation. J Biol Chem 276:37986-37992.

Spandau UH, Rohrschneider K. 2002. Prevalence and geographical distribution of Usher syndrome in Germany. Graefes Arch Clin Exp Ophthalmol 240:495-498.

Steyger PS, Burton M, Hawkins JR, Schuff NR, Baird RA. 1997. Calbindin and parvalbumin are early markers of non-mitotically regenerating hair cells in the bullfrog vestibular otolith organs. Int J Dev Neurosci 15:417-432.

Stoschitzky K, Zernig G, Lindner W. 1998. Racemic beta-blockers – fixed combinations of different drugs. Journal of Clinical and Basic Cardiology 1:14-18.

Stryer L. 1995. Biochemistry. Freeman. ISBN 0-7167-2009-4

Stepczynska A, Lauber K, Engels IH, Janssen O, Kabelitz D, Wesselborg S, Schulze-Osthoff K. 2001. Staurosporine and conventional anticancer drugs induce overlapping, yet distinct pathways of apoptosis and caspase activation. Oncogene 20:1193-1202.

Suetsugu S, Miki H, Takenawa T. 1998. The essential role of profilin in the assembly of actin for microspike formation. Embo J 17:6516-6526.

Sweeney HL, Houdusse A. 2007. What can myosin VI do in cells? Curr Opin Cell Biol 19:57-66.

Sziklai I, Szonyi M, Dallos P. 2001. Phosphorylation mediates the influence of acetylcholine upon outer hair cell electromotility. Acta Otolaryngol 121:153-156.

Takashima S. 2009. Phosphorylation of myosin regulatory light chain by myosin light chain kinase, and muscle contraction. Circ J 73:208-213.

Takumida M. 2001. Functional morphology of the crista ampullaris: with special interests in sensory hairs and cupula: a review. Biol Sci Space 15:356-358.

Tamaoki T, Nomoto H, Takahashi I, Kato Y, Morimoto M, Tomita F. 1986. Staurosporine, a potent inhibitor of phospholipid/Ca++dependent protein kinase. Biochem Biophys Res Commun 135:397-402.

Taura A, Kojima K, Ito J, Ohmori H. 2006. Recovery of hair cell function after damage induced by gentamicin in organ culture of rat vestibular maculae. Brain Res 1098:33-48.

Taylor RR, Forge A. 2005. Hair cell regeneration in sensory epithelia from the inner ear of a urodele amphibian. J Comp Neurol 484:105-120.

Taylor RR, Nevill G, Forge A. 2008. Rapid hair cell loss: a mouse model for cochlear lesions. J Assoc Res Otolaryngol 9:44-64.

Taylor WC. 1965. Deformity of Ears and Kidneys. Can Med Assoc J 93:107-110.

Tilney LG, Cotanche DA, Tilney MS. 1992a. Actin filaments, stereocilia and hair cells of the bird cochlea. VI. How the number and arrangement of stereocilia are determined. Development 116:213-226.

Tilney LG, DeRosier DJ. 1986. Actin filaments, stereocilia, and hair cells of the bird cochlea. IV. How the actin filaments become organized in developing stereocilia and in the cuticular plate. Dev Biol 116:119-129.

Tilney LG, Derosier DJ, Mulroy MJ. 1980. The organization of actin filaments in the stereocilia of cochlear hair cells. J Cell Biol 86:244-259.

Tilney LG, Saunders JC. 1983. Actin filaments, stereocilia, and hair cells of the bird cochlea. I. Length, number, width, and distribution of stereocilia of each hair cell are related to the position of the hair cell on the cochlea. J Cell Biol 96:807-821.

Tilney LG, Tilney MS, Cotanche DA. 1988. Actin filaments, stereocilia, and hair cells of the bird cochlea. V. How the staircase pattern of stereociliary lengths is generated. J Cell Biol 106:355-365.

Tilney LG, Tilney MS, DeRosier DJ. 1992b. Actin filaments, stereocilia, and hair cells: how cells count and measure. Annu Rev Cell Biol 8:257-274.

Tilney LG, Tilney MS, Saunders JS, DeRosier DJ. 1986. Actin filaments, stereocilia, and hair cells of the bird cochlea. III. The development and differentiation of hair cells and stereocilia. Dev Biol 116:100-118.

Tischler AS, Ruzicka LA, Dobner PR. 1991. A protein kinase inhibitor, staurosporine, mimics nerve growth factor induction of neurotensin/neuromedin N gene expression. J Biol Chem 266:1141-1146.

Tomasevic N, Jia Z, Russell A, Fujii T, Hartman JJ, Clancy S, Wang M, Beraud C, Wood KW, Sakowicz R. 2007. Differential regulation of WASP and N-WASP by Cdc42, Rac1, Nck, and PI(4,5)P2. Biochemistry 46:3494-3502.

Tournier C, Hess P, Yang DD, Xu J, Turner TK, Nimnual A, Bar-Sagi D, Jones SN, Flavell RA, Davis RJ. 2000. Requirement of JNK for stress-induced activation of the cytochrome c-mediated death pathway. Science 288:870-874.

Tsuprun V, Santi P. 2002. Structure of outer hair cell stereocilia side and attachment links in the chinchilla cochlea. J Histochem Cytochem 50:493-502.

Tsuprun V, Santi P. 1998. Structure of outer hair cell stereocilia links in the chinchilla. J Neurocytol 27:517-528.

Tsuprun V, Schachern PA, Cureoglu S, Paparella M. 2003. Structure of the stereocilia side links and morphology of auditory hair bundle in relation to noise exposure in the chinchilla. J Neurocytol 32:1117-1128.

Udovichenko IP, Gibbs D, Williams DS. 2002. Actin-based motor properties of native myosin VIIa. J Cell Sci 115:445-450.

van Wijk E, van der Zwaag B, Peters T, Zimmermann U, Te Brinke H, Kersten FF, Marker T, Aller E, Hoefsloot LH, Cremers CW, Cremers FP, Wolfrum U, Knipper M, Roepman R, Kremer H. 2006. The DFNB31 gene product whirlin connects to the Usher protein network in the cochlea and retina by direct association with USH2A and VLGR1. Hum Mol Genet 15:751-765.

Vardouli L, Moustakas A, Stournaras C. 2005. LIM-kinase 2 and cofilin phosphorylation mediate actin cytoskeleton reorganization induced by transforming growth factor-beta. J Biol Chem 280:11448-11457.

Verpy E, Leibovici M, Zwaenepoel I, Liu XZ, Gal A, Salem N, Mansour A, Blanchard S, Kobayashi I, Keats BJ, Slim R, Petit C. 2000. A defect in harmonin, a PDZ domain-containing protein expressed in the inner ear sensory hair cells, underlies Usher syndrome type 1C. Nat Genet 26:51-55.

Verpy E, Weil D, Leibovici M, Goodyear RJ, Hamard G, Houdon C, Lèfevre GM, Hardelin JP, Richardson GP, Avan P, Petit C. 2008. Stereocilin-deficient mice reveal the origin of cochlear waveform distortions. Nature 456:255-258.

Walsh T, Walsh V, Vreugde S, Hertzano R, Shahin H, Haika S, Lee MK, Kanaan M, King MC, Avraham KB. 2002. From flies' eyes to our ears: mutations in a human class III myosin cause progressive nonsyndromic hearing loss DFNB30. Proc Natl Acad Sci U S A 99:7518-7523.

Wang J, Ladrech S, Pujol R, Brabet P, Van De Water TR, Puel JL. 2004. Caspase inhibitors, but not c-Jun NH_2-terminal kinase inhibitor treatment, prevent cisplatin-induced hearing loss. Cancer Res 64:9217-9224.

Wang J, Ruel J, Ladrech S, Bonny C, van de Water TR, Puel JL. 2007. Inhibition of the c-Jun N-terminal kinase-mediated mitochondrial cell death pathway restores auditory function in sound-exposed animals. Mol Pharmacol 71:654-666.

Wang J, Van De Water TR, Bonny C, de Ribaupierre F, Puel JL, Zine A. 2003. A peptide inhibitor of c-Jun N-terminal kinase protects against both aminoglycoside and acoustic trauma-induced auditory hair cell death and hearing loss. J Neurosci 23:8596-8607

Warchol ME, Lambert PR, Goldstein BJ, Forge A, Corwin JT. 1993. Regenerative proliferation in inner ear sensory epithelia from adult guinea pigs and humans. Science 259:1619-1622.

Wear MA, Cooper JA. 2004. Capping protein: new insights into mechanism and regulation. Trends Biochem Sci 29:418-428.

Wegner A. 1976. Head to tail polymerization of actin. J Mol Biol 108:139-150.

Weil D, Blanchard S, Kaplan J, Guilford P, Gibson F, Walsh J, Mburu P, Varela A, Levilliers J, Weston MD, et al. 1995. Defective myosin VIIA gene responsible for Usher syndrome type 1B. Nature 374:60-61.

Weil D, El-Amraoui A, Masmoudi S, Mustapha M, Kikkawa Y, Laine S, Delmaghani S, Adato A, Nadifi S, Zina ZB, Hamel C, Gal A, Ayadi H, Yonekawa H, Petit C. 2003. Usher syndrome type I G (USH1G) is caused by mutations in the gene encoding SANS, a protein that associates with the USH1C protein, harmonin. Hum Mol Genet 12:463-471.

Welch MD, DePace AH, Verma S, Iwamatsu A, Mitchison TJ. 1997. The human Arp2/3 complex is composed of evolutionarily conserved subunits and is localized to cellular regions of dynamic actin filament assembly. J Cell Biol 138:375-384.

Wells AL, Lin AW, Chen LQ, Safer D, Cain SM, Hasson T, Carragher BO, Milligan RA, Sweeney HL. 1999. Myosin VI is an actin-based motor that moves backwards. Nature 401:505-508.

Weston MD, Luijendijk MW, Humphrey KD, Moller C, Kimberling WJ. 2004. Mutations in the VLGR1 gene implicate G-protein signaling in the pathogenesis of Usher syndrome type II. Am J Hum Genet 74:357-366.

White PM, Doetzlhofer A, Lee YS, Groves AK, Segil N. 2006. Mammalian cochlear supporting cells can divide and trans-differentiate into hair cells. Nature 441:984-987.

Williams DS. 2008. Usher syndrome: animal models, retinal function of Usher proteins, and prospects for gene therapy. Vision Res 48:433-441.

Woolley SM, Rubel EW. 2002. Vocal memory and learning in adult Bengalese Finches with regenerated hair cells. J Neurosci 22:7774-7787.

Xia Y, Karin M. 2004. The control of cell motility and epithelial morphogenesis by Jun kinases. Trends Cell Biol 14:94-101.

Yamashita A, Maeda K, Maeda Y. 2003. Crystal structure of CapZ: structural basis for actin filament barbed end capping. Embo J 22:1529-1538.

Yamasoba T, Kondo K. 2006. Supporting cell proliferation after hair cell injury in mature guinea pig cochlea in vivo. Cell Tissue Res 325:23-31.

Yamauchi J, Hirasawa A, Miyamoto Y, Itoh H, Tsujimoto G. 2001. Beta2-adrenergic receptor/cyclic adenosine monophosphate (cAMP) leads to JNK activation through Rho family small GTPases. Biochem Biophys Res Commun 284:1199-1203.

Yamauchi T. 2005. Neuronal Ca2+/calmodulin-dependent protein kinase II--discovery, progress in a quarter of a century, and perspective: implication for learning and memory. Biol Pharm Bull 28:1342-1354.

Yamazaki D, Oikawa T, Takenawa T. 2007. Rac-WAVE-mediated actin reorganization is required for organization and maintenance of cell-cell adhesion. J Cell Sci 120:86-100.

Yang DD, Kuan CY, Whitmarsh AJ, Rincon M, Zheng TS, Davis RJ, Rakic P, Flavell RA. 1997. Absence of excitotoxicity-induced apoptosis in the hippocampus of mice lacking the Jnk3 gene. Nature 389:865-870.

Yarar D, To W, Abo A, Welch MD. 1999. The Wiskott-Aldrich syndrome protein directs actin-based motility by stimulating actin nucleation with the Arp2/3 complex. Curr Biol 9:555-558.

Yin HL, Iida K, Janmey PA. 1988. Identification of a polyphosphoinositide-modulated domain in gelsolin which binds to the sides of actin filaments. J Cell Biol 106:805-812.

Ylikoski J, Xing-Qun L, Virkkala J, Pirvola U. 2002. Blockade of c-Jun N-terminal kinase pathway attenuates gentamicin-induced cochlear and vestibular hair cell death. Hear Res 166:33-43.

Yonemura S, Matsui T, Tsukita S. 2002. Rho-dependent and -independent activation mechanisms of ezrin/radixin/moesin proteins: an essential role for polyphosphoinositides in vivo. J Cell Sci 115:2569-2580.

Zemans RL, Arndt PG. 2009. Tec kinases regulate actin assembly and cytokine expression in LPS-stimulated human neutrophils via JNK activation. Cell Immunol 258:90-97.

Zhang G, Yan G, Gurtu V, Spencer C, Kain SR. 1998. Caspase inhibition prevents staurosporine-induced apoptosis in CHO-K1 cells. Apoptosis 3:27-33.

Zhao H, Tian W, Cohen DM. 2002. Rottlerin inhibits tonicity-dependent expression and action of TonEBP in a PKCdelta-independent fashion. Am J Physiol Renal Physiol 282:F710-717.

Zheng L, Sekerkova G, Vranich K, Tilney LG, Mugnaini E, Bartles JR. 2000. The deaf jerker mouse has a mutation in the gene encoding the espin actin-bundling proteins of hair cell stereocilia and lacks espins. Cell 102:377-385.

Zheng JL, Frantz G, Lewis AK, Sliwkowski M, Gao WQ. 1999. Heregulin enhances regenerative proliferation in postnatal rat utricular sensory epithelium after ototoxic damage. J Neurocytol 28:901-912.

Zheng JL, Gao WQ. 1997. Analysis of rat vestibular hair cell development and regeneration using calretinin as an early marker. J Neurosci 17:8270-8282.

Zheng JL, Helbig C, Gao WQ. 1997. Induction of cell proliferation by fibroblast and insulin-like growth factors in pure rat inner ear epithelial cell cultures. J Neurosci 17:216-226.

Zheng JL, Keller G, Gao WQ. 1999. Immunocytochemical and morphological evidence for intracellular self-repair as an important contributor to mammalian hair cell recovery. J Neurosci 19:2161-2170.

Zheng JL, Shou J, Guillemot F, Kageyama R, Gao WQ. 2000. Hes1 is a negative regulator of inner ear hair cell differentiation. Development 127:4551-4560.

Zine A, de Ribaupierre F. 1998. Replacement of mammalian auditory hair cells. Neuroreport 9:263-268.

Zine A, Hafidi A, Romand R. 1995. Fimbrin expression in the developing rat cochlea. Hear Res 87:165-169.

Zine A, Romand R. 1996. Development of the auditory receptors of the rat: a SEM study. Brain Res 721:49-58.